Fall 2020

The Effect of Cold Pool Variability on Zooplankton Dynamics of the Eastern Bering Sea Shelf

JENNIFER JOHNSON
University of New Hampshire, Durham

The Effect of Cold Pool Variability on Zooplankton Dynamics of the Eastern Bering Sea Shelf

By

Jennifer J'Lai Johnson
BSc, Virginia Polytechnic Institute and State University, 2014

THESIS

Submitted to the University of New Hampshire
in Partial Fulfillment of
the Requirements for the Degree of

Master of Science
In
Oceanography

September, 2020

This thesis/dissertation was examined and approved in partial fulfillment of the requirements for the degree of Master of Science in Oceanography by:

Thesis Director, Dr. Jennifer L. Miksis-Olds, Research Professor Center for Acoustics Research and Education

Dr. Thomas C. Lippmann, Associate Professor Earth Sciences

Dr. J. Michael Jech, Research Fisheries Biologist National Oceanic and Atmospheric Administration Northeast Fisheries Science Center

Dr. James M. Pringle, Professor Earth Sciences-Joint Positions

Dr. Kerri D. Seger, Affiliate Research Professor Center for Acoustics Research and Education

On July 31, 2020

Approval signatures are on file with the University of New Hampshire Graduate School.

TABLE OF CONTENTS

ACKNOWLEDGEMENTS

I would like to thank my advisor Jennifer Miksis-Olds and thesis committee for their counsel, enthusiasm, and patience. I am appreciative of the writing skills I have gained from the guidance of Jennifer Miksis-Olds and the opportunity to work on this project. I am grateful for the continued mentoring from J. Michael Jech and the self-confidence that has resulted from his teachings in the realm of fisheries acoustics. I am privileged to have been a pupil of Thomas Lippmann, who opened a world of possibilities to me through time series, but above all else was encouraging and brought a surplus of positivity. The committee's willingness to share their knowledge and expertise has helped me develop as a critical thinker and assisted in building the foundation of a growing scientist.

I would like to acknowledge the Office of Naval Research and the North Pacific Research Board for providing the funding necessary to complete this work.

Finally, I would like to thank my unbelievably kind and diverse classmates and professors at UNH. A special recognition is given to my office mates in the Jere A. Chase Laboratory for the laughter I experienced daily. Thank you to all who made this thesis possible.

LIST OF FIGURES

LIST OF TABLES

ABSTRACT

Interannual variability of ocean temperatures and sea ice extent has been observed on the eastern Bering Sea (EBS) shelf, where annual conditions have resulted in regional "Cold" or "Warm" years. Consecutive years of Cold or Warm year characterization has resulted in regime states within the past two decades. A characteristic feature of the EBS is a subsurface layer linked to seasonal sea ice (SSI) and defined by bottom temperatures less than 2°C, termed the Cold Pool. Cold Pool variability is tied to the dynamics of fish distribution in the Arctic and subarctic ecotones. Water column, multifrequency acoustic backscatter data were collected remotely using upward looking echosounders along the EBS shelf from 2008-2018. Acoustic data were coupled with additional bottom temperature, regional SSI, and local SSI data from the Cold regime between 2006-2013 and the Warm regime from 2014-2018 to assess the relationship between zooplankton communities and Cold Pool variation. Water column averaged area backscatter was two orders of magnitude greater during the Cold regime than during the Warm regime coupled with early ice edge receding. Multifrequency acoustic analysis indicated a shift in the Warm regime zooplankton communities from larger to smaller bodied species on the EBS shelf resulting in a change in the average acoustic abundance. Cold Pool proxy regional SSI was a better predictor variable for zooplankton abundance than bottom temperature in the Cold regime, while Warm regime bottom temperature and regional SSI were equal in predictive power and resulted in improved predictive model performance. Although the predictive models did not capture the dynamics of the regime shift in 2013, the Cold regime exhibited increased stochasticity in bottom temperature, SSI, and acoustic backscatter prior to the shift. Regime shift early warning signals from further mining of acoustic and environmental data warrant

exploration for comprehensive management practices in the Bering Sea and neighboring Arctic ecosystems.

CHAPTER 1: INTRODUCTION

The Bering Sea is responsive to climate change based on decadal variability driven by meteorological and atmospheric coupling with the Arctic of 3-7 year cyclical durations. Arctic coupling results in Bering Sea seasonal sea ice (SSI) coverage and water column temperature variation (Hunt, 2001; Stabeno et al., 2012). Prior to 2000, annually altering Warm and Cold years dominated the Southeast Bering Sea (SEBS), with the presence of sea ice in March and April determining the Warm or Cold year characterization (Stabeno et al., 2017). Since then, the SEBS has experienced groups of consecutive years with similar conditions categorized as climatic regimes. These multi-year cyclical periodicities are referred to as Warm and Cold regimes (Brown et al., 2012). Extensive sea ice and cold ocean temperatures during 2006-2013 was categorized as a Cold regime, or a group of Cold years, while 2001-2005 and 2014-2019 which had less extensive sea ice and warmer ocean temperatures were categorized as Warm regimes (Stabeno and Bell, 2019) (Figure 1). Since regimes now last for more than a year, interannual variability within a regime occurs and is defined by sea ice extent, temperature, and distribution of species (Stabeno et al., 2012, Stauffer et al., 2015).

The Bering Sea is undergoing rapid changes. A characteristic feature of the eastern Bering Sea, linked to changes in SSI, is a subsurface layer defined by waters less than 2°C that is referred to as the "Cold Pool." Because variability in Cold Pool temperature and extent is tied to comprehensively understanding the effects and implications of climate variability on community structure and dynamics of fishes in the Arctic and subarctic ecotones, it has been a feature of considerable interest since the 1930s. As a distinct water mass, the Cold Pool influences the distribution of endemic species that exhibit narrow thermal tolerances within the Bering Sea. Following the 2018 most extreme Warm year winter with the lowest winter-maximum areal sea

ice coverage ever observed, there was no Cold Pool in the SEBS (Stabeno and Bell, 2019). The lack of a Cold Pool has had repercussions on the ecosystem that have yet to be fully understood. The absence of a Cold Pool in 2018 was followed by another year in which the ice in November and December 2019 was 1/3 of the historical average, and sea surface temperatures were warmer than normal in the Bering, Chukchi, and Beaufort Seas (Thoman and Walsh, 2019). Therefore, Cold Pool importance on ecosystems and marine resources are highlighted in this study.

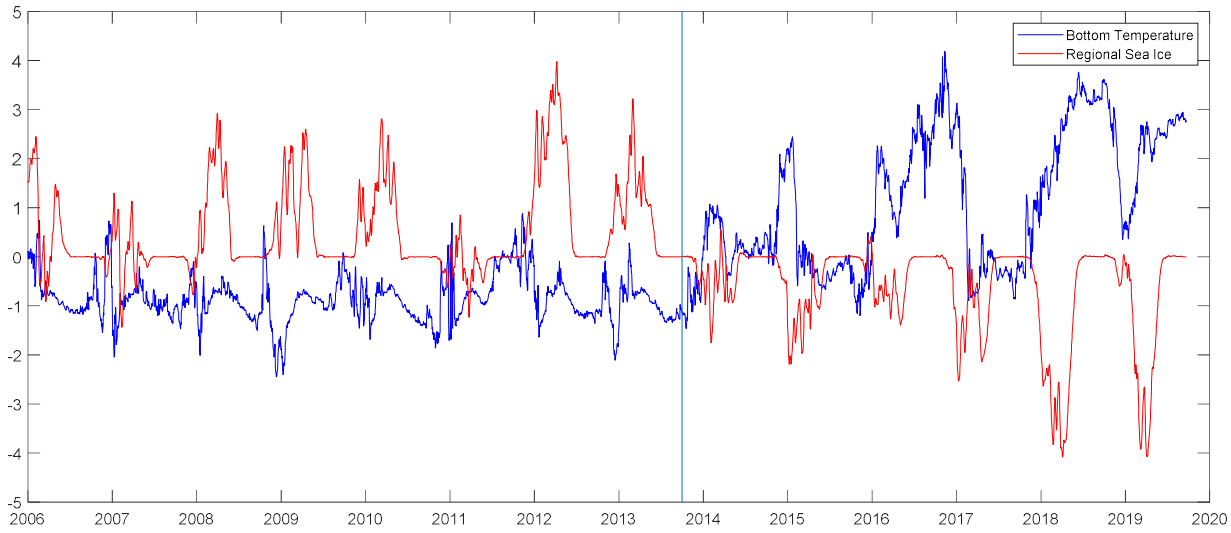

Figure 1. Bering Sea bottom temperature (site M5 59 54.285N, 171 42.285W) (blue curve) and regional seasonal sea ice (https://nsidc.org/) anomalies (red curve) 2006-2020 with the vertical light-blue line depicting demarcation of Cold to Warm years October 1, 2013.

1.1 Eastern Bering Sea Physical Oceanography

The Eastern Bering Sea is divided into three shelf domains: Coastal, Middle, and Outer Shelves. Characteristic water masses and hydrographic variability in each domain results in cross-shelf oceanographic variability. The mid-shelf region (Middle domain) lies along the 70m isobath and has the greatest variability in water column oceanographic structure (Eisner, 2014). Along-slope lack of variability within the Middle domain is generally perpetuated by weak surface currents (on average <2.0 cm/s) and relatively weaker deeper currents (Stabeno et al., 2012). During the fall, the Middle Shelf domain undergoes full water column mixing. During Warm years, fall surface and at-depth currents are westward, while during Cold years the near-bottom current flow is northward. Notably, near-bottom currents are substantially weaker than the near-surface currents and have more baroclinicity in Cold years than Warm years (Stabeno et al., 2012). The mechanisms that control current flow are not well known, but are likely mediated by flow-topography interactions, slope current instabilities, and tides (Danielson et al., 2011). Atmospheric (wind) forcing accounts for minimal current fluctuation and increased wind variability has occurred more frequently since 2016. While wind fluctuation does not significantly affect currents, sea ice advancement over the shelf is dependent on atmospheric forcing (Stabeno and Bell, 2019).

Southward advection of polynyas, or coastal ice formations, result from northerly winds blowing over the EBS shelf that cause water-column cooling (Stabeno and Bell, 2019). The formation of sea ice in winter on the shallow Bering Sea shelf locks up freshwater input from land sources and leaves behind very saline water beneath the ice. The salty water remains liquid when temperatures range from below-freezing to an average minimum of -1.7˚C. The stability and persistence of this cold water is what remains the following summer season. Due to strong

spring stratification, the colder bottom layer of the Middle Shelf is isolated from the surface water (Stabeno et al. 2002). This stratified bottom layer is the Cold Pool, and it has historically persisted through the summer season (Maeda, 1977) varying in extent and duration (Stabeno et al., 2012) (Figure 2).

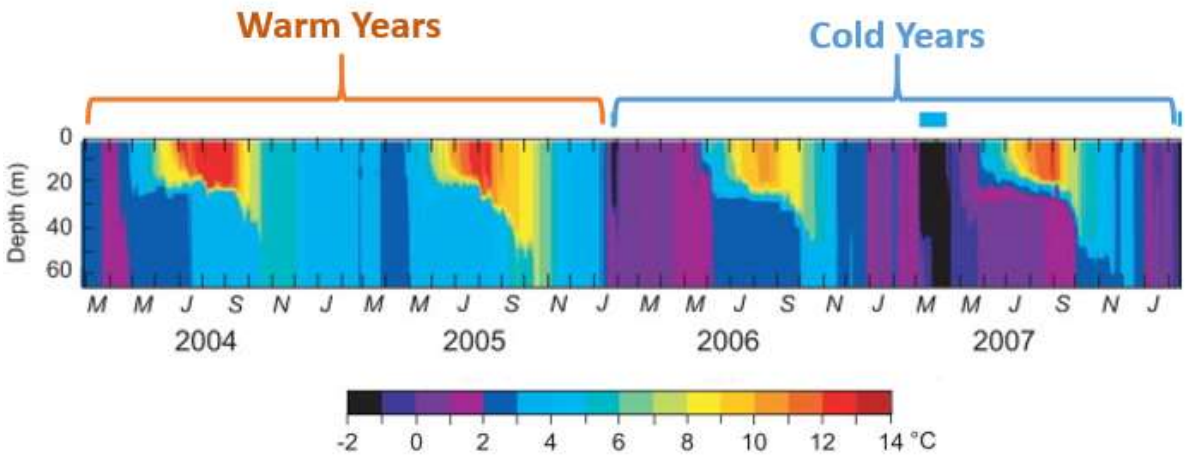

Figure 2. Annual evolution of water column temperature on the Bering Sea shelf 70m isobath (site M2 56 51.989N, 164 3.002W) by Warm and Cold years modified after Stabeno et al. (2012).

1.1.1 Cold Pools

A persistent Cold Pool is not unique to the Bering Sea. Isolated dense, colder bodies of water have been observed in various regions of the world. These characteristic oceanographic features are important indicators of salinity and temperature, and they drive nutrient water column distribution. Cold Pools have been observed in the Mid-Atlantic Bight (MAB), the Adriatic Sea, along the European shelf, and in the Yellow Sea (Houghton et al., 1982, Henderschott and Rizzoli, 1976, Horsburgh et al., 2000, Hu et al., 1991, respectively). The degree of our understanding is varied among different Cold Pools, for example a distinction between the MAB and the Bering Sea Cold Pool is the difference in comprehensive understanding for each system. The MAB Cold Pool is well documented and oceanographic models have been created for annual spatial and temporal dynamics (Chen et al., 2018). The

Bering Sea Cold Pool is less well documented, and historic bottom temperature data series in the EBS used to estimate Cold Pool volume are primarily from ground fish trawl surveys conducted by the Alaska Fisheries Science Center (AFSC). The areal extent of the Bering Sea Cold Pool is calculated based on the area (km^2) over which bottom temperatures are <2°C, and the Bering Sea Cold Pool Index is a standardized estimate of the fraction of surveyed area covered by this <2°C bottom water.

In comparison to the Bering Sea Cold Pool, the MAB Cold Pool has a warmer temperature threshold (<10˚C) and higher salinity. It also varies spatially and temporally due to surface water heating and strong southern advection. The hydrography of the bottom of the MAB is narrow, with low salinity intrusions occurring from the continental shelf and slope (Chen, 2018). Rapid de-stratification and seasonal disappearance of the MAB Cold Pool due to tropical and extratropical storms have resulted in increased regional fish movement (Secor et al., 2018).

Compared to the MAB Cold Pool dynamics, fresh water from melted sea ice in the Bering Sea acts as an insulator, preventing heat advection to the bottom layer. This results in the Bering Sea Cold Pool formation on the hydrographically flat sea shelf, approximately 70m deep. In the SEBS, Cold Pool formation is primarily driven by decreased water temperature due to sea ice, and the dissipation is driven by decreased salinity and increased temperature from de-stratification caused by fall winds and storms. In the Northeast Bering Sea (NEBS), Cold Pool formation relies on both temperature and salinity, therefore implying that the SEBS is more sensitive to the timing of the fall cooling when formation is beginning (Ladd and Stabeno, 2012). Because the Bering Sea Cold Pool exhibits minimal migration due to the weak currents, it is overall more geographically stationary and sustaining than the MAB Cold Pool, but less understood (Stabeno et al., 2012).

1.1.2 Bering Sea Cold Pool Variability

Although the presence of the Bering Sea Cold Pool is relatively stationary and sustaining, annual variability in the Cold Pool is linked to previous winter sea ice. With current climatic shifts and warming of the Arctic, the Cold Pool's extent, average temperature, and location are highly variable (Wyllie and Wooster, 2002) (Figure 3). The Cold Pool has been observed to be more extensive after more expansive southern latitudinal ice extent from the previous winter (Wyllie and Wooster, 1998). The winter ice extent varies across long time scales and is related to the position and intensity of the Aleutian Low-Pressure System. Historically, the southernmost sea ice extent occurs in February or March (Wyllie and Wooster, 1998), but has been observed as late as May (Stabeno, Farley et al., 2012). The timing of the seasonal ice extent is indicative of summertime shelf conditions. Atmospheric forcing and ocean temperatures are primarily responsible for the advance in southern sea ice extent. Northerly winds cool the water column and drive the ice edge southward across the shelf, whereas warm ocean water opposes the advancement of the ice. The persistence of northerly winds eventually forces sea ice southward (Stabeno and Bell, 2019). Thickness of the sea ice influences SSI extent temporally, affecting the timing of peak extent and melt duration.

The Cold Pool can have two components. Interannual sea ice distribution has resulted in the Cold Pool often consisting of a southeastern Cold Pool component centered at approximately 57°N and a northern Cold Pool component extending northward from 58°N. The northern Cold Pool component is based on extensive ice cover and is separated from the southeastern Cold Pool by an intermediate zone that consists of warmer water with weaker stratification. While some evidence exists that indicates the northern Cold Pool is isolated from the southern Cold Pool, little is known about this variability and the mechanisms of isolation (Stabeno et al., 2002).

Under projected climate warming conditions, the northern and southeastern Cold Pool components are forecasted to differ in physical characteristics, with bottom temperatures of the northern shelf predicted to remain cold (Stabeno et al., 2012). Stabeno et al. (2012) projected that the northern shelf temperature will remain consistent and be colder than what is presently observed on the southern shelf, with the north-south transition at approximately 60°N.

Stabeno et al. (2012) assessed the importance of the Cold Pool and sea ice for determining habitat suitability for species within the region under these same projected climatic conditions. Because a temperature delineation between the north and south shelf is expected to continue, a simple northward shift of the southern shelf ecosystem will not likely occur in the future. Because of the dichotomy of physical and biological conditions that currently exist between the north and south, significant changes to the Bering Sea shelf ecosystem as a whole are predicted. While warming of the southern region occurs, the northern region is predicted to remain cold but modified by the ecosystem changes in the southern shelf.

Current Bering Sea conditions have established cross-shelf variability that separates oceanic and shelf zooplankton communities by the 32.4 isohaline boundary (Coyle et al., 2008). During Cold years, the separating front is confined to the shelf break by the Cold Pool. During Warm years, when the Cold Pool is absent or less developed, the separating front penetrates much further inshore (Coyle et al., 2008). Eisner et al. (2014), described the spatial variations in large and small zooplankton community composition along-shelf between the north and southeastern Bering Sea in the Outer domain (shelf) during Warm and Cold regimes and compared them to the Inner and Middle domains. There was significant variability in key taxa abundance and total biomass between assemblages in the north and south. Eisner et al. (2014) hypothesized that large zooplankton taxa have a direct or indirect relationship (dependent on

taxa) to bottom temperature and a direct relationship to sea ice extent, whereas small zooplankton taxa have a direct relationship to surface and bottom temperatures.

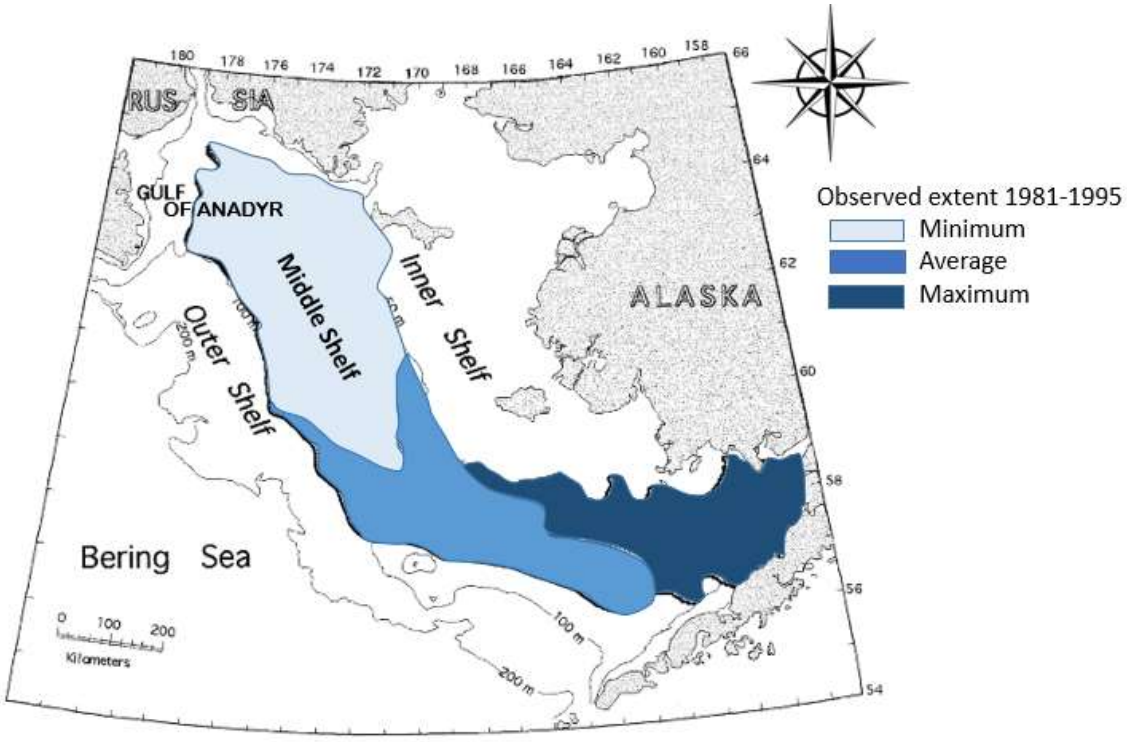

Figure 3. Bering Sea shelf and shelf domains with Cold Pool bottom temperature extent 1981-1995 modified after Wyllie and Wooster (1998).

1.1.3 Eastern Bering Sea Shelf Delineated Regions

The EBS is divided into Marine Region designations based on oceanographic/hydrographic and fisheries characteristics (Ortiz et al., 2012, Harvey and Sigler, 2013). Designated regions have been further grouped by Eisner et al. (2014) in each shelf domain—South Inner (<50m bathymetry), South Middle (50-100m), South Outer (100-200m), North Inner (<~40m), and North Middle (<~40-100m) (Figure 4) and by Baker and Hollowed (2014) as ecoregions – Inner Shelf, Middle/inner (south), Southern, Northern, Middle/outer (north), and Shelf break (Figure 5), for identifying key biological features and ecological

processes that define areas and govern their dynamics. Baker and Hollowed (2014) found that depth was the strongest explanatory physical predictor of species abundance among the environmental gradients they identified.

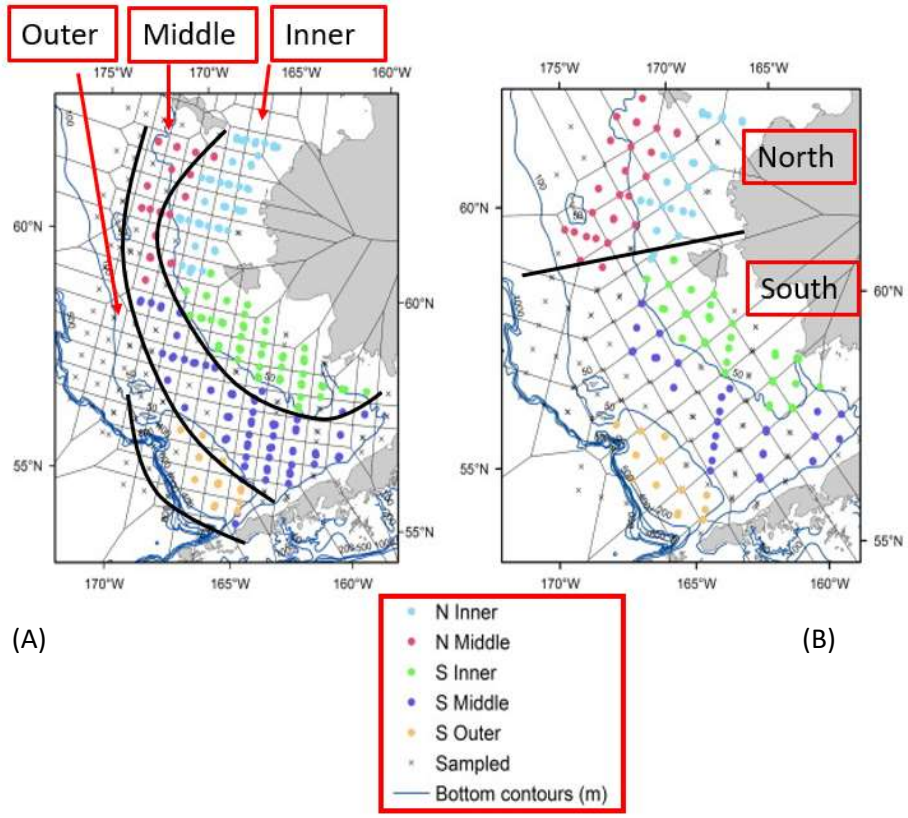

Figure 4. Bering Sea shelf major oceanographic domains in red boxes, with colored dots representing zooplankton sample stations for (A) large zooplankton and (B) small zooplankton by domain in Warm years (2003-2005) and Cold years (2006-2009) modified after Eisner et al. (2014).

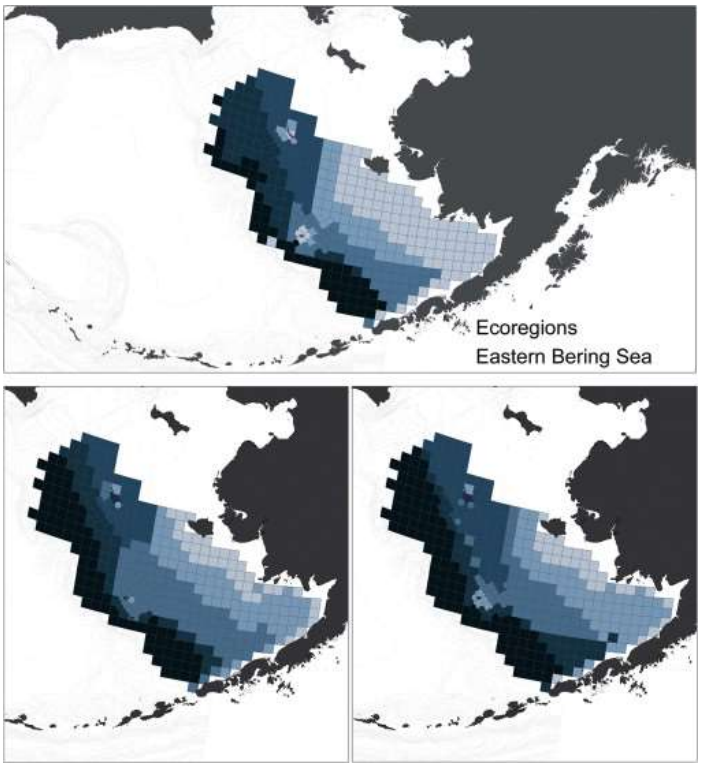

Figure 5. Delineation of ecoregions based on clustering survey stations to represent distinct biological communities. Ecoregions are displayed for the entire time series (top) as well for Warm years (2001-2005, bottom left) and Cold years (2006-2010, bottom right) (Baker and Hollowed, 2014).

1.2 Eastern Bering Sea Biological Communities

1.2.1 Zooplankton Communities

Within each ecoregion, EBS zooplankton communities are comprised of two distinct communities of herbivorous zooplankton, separated by an oceanographic front during spring conditions, that both rely heavily on the sea ice algae. Isolation of the Middle shelf and Outer shelf is demarcated by a front defined by persistent salinity and lack of cross-shelf advection. Offshore, large oceanographic zooplankton*, Neocalanus plumchrus*, dominate the Outer shelf domain and slope, while the Middle domain is dominated by an inshore zooplankton community of the euphausiid *Thysanoessa raschii* in April and May. Large copepods, *Calanus marshallae,* peak in late May and early June, and populations of adult small copepods, *Oithona*

similis and *Pseudocalanus spp,* are prevalent in June (Vidal and Smith, 1985). Following the spring bloom of phytoplankton dominated by *Chrysophyceae*, Outer shelf zooplankton communities develop in early spring and attain maximum biomass and growth rates by late spring, then begin downward migration. The Middle domain zooplankton community exhibits a delayed response to the spring phytoplankton bloom dominated by diatoms, which occurs earlier and attains higher levels of phytoplankton concentration than the Outer shelf bloom. Percent ice cover influences whether and when ice-associated blooms occur. If sea ice is present, the mid-spring bloom timing is related to the nearby ice edge; if sea ice is absent or retreats before mid-March, a later spring bloom occurs in May or early June. In Cold years on the Middle domain during the early spring (April –May), biomass remains relatively unchanged (90% *T. raschii* : 10% *C. marshallae*) and increases substantially after the spring bloom by late May and early June when it becomes more evenly split (50% *T. raschii* : 50% *C. marshallae*). Warm years have earlier spring blooms and the biomass is dominated by small-bodied taxa of the *Pseudocalanus spp.* (Kimmel et al., 2017).

1.2.2 Zooplankton and Environmental Variability

Because *T.raschii* and *Calanus spp*. are estimated to be approximately 90% of Middle domain zooplankton biomass, studies have been focused on these groups (Smith and Vidal 1986, Coyle et al., 2008). *T. raschii* are associated with colder, less saline waters in the Bering Sea (Fukuchi, 1977). Overwintering partially on stored lipid, the *T. raschii* euphausiid populations are thought to rely on omnivorous feeding throughout the year. Smith (1991) observed during Warm years with abundant food that growth rates increase, resulting in larger sized individuals and less overall euphausiid biomass. Favorable euphausiid recruitment is extended based on possible mechanisms of reduced metabolism coupled with better feeding

conditions associated with spring-time ice cover and sustained phytoplankton food production in colder years.

Calanus spp. also have more productive recruitment in cold, icy years with an earlier spring bloom and reduced predation pressure during ice retreat while in critical copepodite states (specifically when metamorphosizing from nauplii to copepodites) (Ressler et al., 2014). Eisner et al. (2014) observed that most small zooplankton taxa decrease in abundance with decreasing temperatures in the Middle domain from Warm to Cold years. Total zooplankton biomass was highest in the coldest years (2008-2009) of the sample period (2003-2009) in the southern Bering Sea due to increases in large zooplankton biomass.

Whether copepod metabolism, reproduction, and awakening from winter diapause aligns with the spring bloom depends on average bottom temperatures and sea ice. *Calanus spp.* may benefit from strong recruitment during years when ice reaches maximum extent after March 15 with early retreat. Bair and Napp (2003) hypothesized that recruitment of *Calanus spp.* was dependent on early spring phytoplankton blooms and cold winters for winter survival and reduced metabolic rates. Copepod nauplii are most abundant over the Middle shelf in late May and early June, following the seasonal increase of sea surface temperatures. The Bair and Napp (2003) hypothesis was expanded by Sigler et al. (2014) by presenting three scenarios for the development of *Calanus* spp. during Warm and Cold years.

The first scenario, "*Cold years with early ice retreat"*, results in increased egg production rates of early spawners and metamorphosis benefits from early ice retreat followed by spring bloom production. Copepod lipid production is primarily dependent on summer phytoplankton and microzooplankton, thus early spring bloom production results in winter lipid storage levels reached earlier in the season to facilitate early overwintering. Early overwintering copepods miss

the advantages of the fall bloom. However, overwintering respiration rates are lower in colder temperatures which leads to increased winter survival.

The second scenario, "*Cold years with late ice retreat"*, results in all spawners, including early and late spawners, benefiting from the under-ice algae and open water spring bloom. Cold year metamorphosis likely develops post spring bloom, depending on summer primary and microzooplankton lipid production. Differing from the first scenario, later overwintering occurs with individuals taking advantage of the fall bloom for additional lipids and low respiration rates due to cold bottom temperatures. This second scenario results in the strongest copepod winter survival.

The third scenario, "*Warm, ice-depleted years"*, results in reduced egg production from the absence or short duration of ice and ice algae presence. When the open water spring bloom is late, it is mismatched with the metamorphosis of late spawners. Diapause is then delayed until after the fall bloom, and warm temperatures cause increased respiration rates. Since lipid storage is dependent on combined primary and microzooplankton populations, reserves are exhausted during these Warm year winters when the duration of diapause is delayed. Low reproductive input by early spawners and increased predation metabolism also occur in this third (Warm) scenario. In these three ways, Cold and Warm years impact copepod recruitment.

With lower trophic level recruitment varying based on annual environmental conditions, acoustical surveys have been conducted for assessing the status and trends of euphausiid and copepod stock in the Bering Sea during both Cold and Warm years. Information gained from the acoustical surveys of zooplankton have been linked to walleye pollock (*Gadus chalcogrammus)* abundance. Results have shown that euphausiid biomass increased between 2004 and 2009 (during Cold years), while pollock stock declined after a series of Cold years with poor pollock

recruitment (Ressler et al., 2012). Ressler et al. (2014) investigated predation by pollock as a significant top-down control on euphausiid biomass from 2004-2012 by comparing predictive models. Using acoustical methods and net pairing, Ressler et al. (2014), tested the hypothesis that top-down mechanisms of zooplankton abundance were driven by pollock biomass, and bottom-up mechanisms were driven by bottom and surface temperatures. Results indicated that pollock biomass had a nominal effect on the predictive models while bottom temperature and location (lat/long) explained ~40% of euphausiid biomass on the shelf. In contrast, Hunt et al. (2016) observed that euphausiids in the Bering Sea exhibited both a top-down predation effect and had a strong negative relationship with bottom-up mechanisms from water temperature during 2004-2012. The differences between the studies may relate to variation in spatial and temporal scales used to assess the predator or euphausiid biomass in the analyses.

1.2.3 Ecological Implications

The dynamics and mechanisms of the EBS shelf ecosystem are complex, and the interrelatedness of physical and biological processes is not fully understood. The Bering Sea Middle shelf is considered a highly productive "green belt" of resources for higher trophic levels (Okkonen et al., 2004). The mid-shelf or Middle domain is inhabited by commercially and ecologically important species such as subarctic walleye pollock and Arctic cod *(Boreogadus saida).* Both species have significant ecosystem roles as prey for larger species, so they directly tie their predators to zooplankton community composition via energy transfer. This makes the phenology of zooplankton community composition during Warm and Cold years pertinent to the fishing industry.

Walleye pollock spawning is low in spatial and temporal variability regardless of environmental conditions that leads to high site fidelity in the spring during February- May

(Brodeur et al., 2000). Bering Sea zooplankton community composition influences energy accumulation for the winter survival of juvenile fish, growth, and gonad development (Coyle et al., 2011). The timing of shifts in abundance of key zooplankton taxa and size classes is important for sustainability of fishes in this region and minimizing the chance of a match-mismatch in prey abundance. The match-mismatch hypothesis (MMH), first described by Cushing (1990), explains recruitment variation of a population by relating its phenology and immediate lower trophic level phenology. MMH can occur spatially and temporally. The spatiotemporal dynamics of fish egg hatching and larval consumption with optimal zooplankton abundance, community size classes, and lipid content, is an important energy driver, and can result in long-term changes (Hunt, 2010).

1.2.4 Ecosystem Dynamics and the Cold Pool

Proposed by Hunt et al. (2002), the Oscillating Control Hypothesis (OCH) predicts that pelagic ecosystems in the southeastern Bering Sea alternate between bottom-up control in Cold regimes and top-down control in Warm regimes. The OCH outlines the importance of the a) timing of ice retreat, b) water temperatures during the spring bloom, and c) relationship between zooplankton and forage fish, for large predatory fish population sustainability. While the ecosystem varies between Warm and Cold regimes, there is also interannual variability within a regime. Primary phytoplankton and secondary zooplankton community composition vary within a cold regime, where phytoplankton bloom timing stimulates different populations of secondary producers (Stauffer et al., 2015). Variation of zooplankton community size class composition has been observed to occur within a Warm regime (Coyle et al., 2011).

Zooplankton abundance, size classes of life history stages, and composition of lipids influence fecundity and recruitment rates of managed fish species. Forage fish, or juvenile prey,

are not only prey for adult fish and higher trophic levels, but also are the survivors that enter the fishery as mature adults (Hunt et al., 2002). During Warm years, little seasonal sea ice forms and lipid-deficient copepods and euphausiids decrease energy transfer to higher trophic levels. Because these zooplankton are prey for both adult and juvenile fish, high juvenile mortality occurs (1) prior to winter when adults cannibalize them and (2) during winter from starvation. When zooplankton are lipid-deficient, fewer surviving age-1 fish grow and mature to join the stock (Figure 6-top panel). Comparatively, during Cold years when more seasonal sea ice forms, lipid-rich large copepods and euphausiids increase energy transfer to higher trophic levels. Fewer juvenile fish are cannibalized, and more juveniles survive the winter to join the stock, resulting in higher stock assemblages (Figure 6-bottom panel).

Long term Cold Pool variation due to environmental changes, such as the warming of global ocean temperatures via climate change, will directly affect stock abundance, survival of age-0 fish, and species distribution. Stomach analyses of age-0 pollock have indicated shifts from large to small copepods in their diets during Warm years as compared to Cold years. The Warm years, when small copepods are eaten more often, are accompanied by a stable water-column and warmer temperatures above the thermocline (Coyle et al., 2008). The Cold Pool acts as a thermal barrier, preventing warmer-water, large predatory, southern Bering species and northern Bering fatty forage fish such as Arctic cod and Smelt from entering critical habitat space of juvenile pollock and cod. In this way, the Cold Pool offers refuge to juvenile pollock and Arctic cod that have higher cold tolerances from adult cannibalistic behavior. While cannibalism of age-1 pollock predicts recruitment success, warmer temperatures increase spatial overlap between overwintering juvenile and adult pollock, resulting in increased spring cannibalism (DeRobertis and Cokelet 2012).

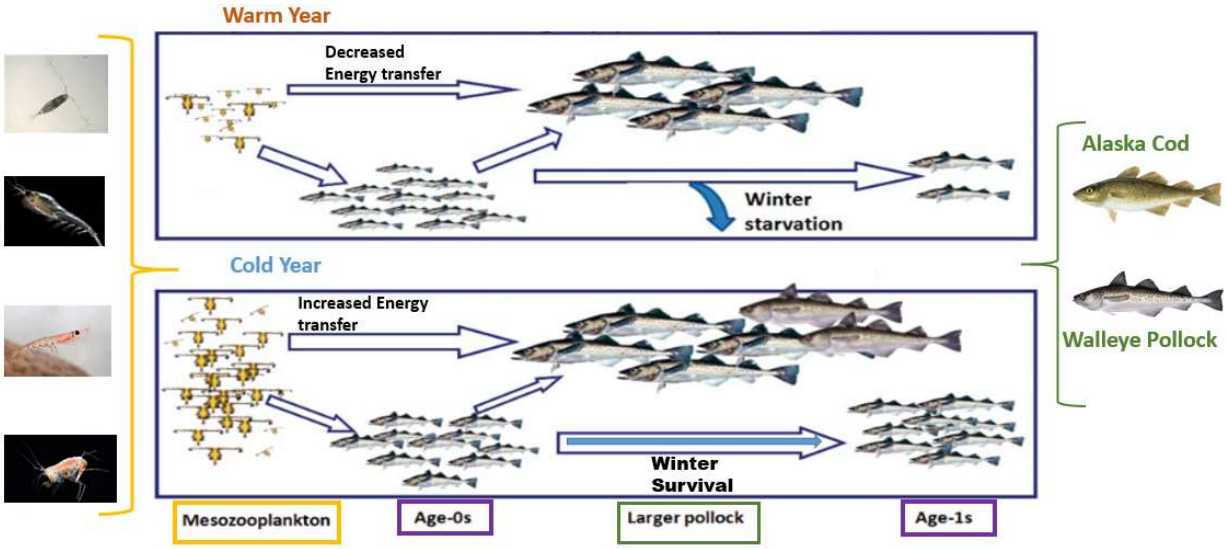

Figure 6. Schematic of Warm vs. Cold years in the Bering Sea and walleye pollock abundances modified after Coyle et al. (2011).

1.2.5 Bering Sea and Human Implications

Major economic impacts are directly tied to community composition of Bering Sea zooplankton communities that feed commercially important fish stocks. Zooplankton dynamics vary between climate regimes, Cold Pool variation, and are likely to have cascading effects on important managed commercial species (Coyle, 2011). Alaska walleye pollock is the largest landed species by mass globally and in the United States. Within the United States specifically, this fishery accounts for 29% of total value and 58% of total landings, which is approximately 2 million metric tons per year (NMFS NOAA 2016).

Cold Pool variation, which can be an indicator of environmental changes and habitat shifts, can impact this billion-dollar fishery, which accounts for the majority of the Bering Sea and Aleutian Island (BSAI) ground fish harvest (Ianelli et al., 2016). Adult pollock distribution is primarily governed by the Cold Pool shape (extent) and volume (De Robertis and Cokelet,

2012). Pollock aggregation depends on Cold Pool variation that can result in advantages or disadvantages for commercial catch-per-unit-effort (CPUE). In 2018 during the most extreme minimal Cold Pool extent, i.e., no observed thermal barrier, the majority of pollock assemblages occurred in the northern Bering Sea and resulted in the fishery relying more on northern shelf slow growing economically valuable benthic communities for consumption (Cornwall, 2019). The 2018 Cold Pool anomaly had major pelagic and benthic stock affects for 2019, as well as potential economic impacts to both U.S. and Russian marine resources.

The Bering Sea ecosystem and the surrounding human communities have a direct relationship due to the widespread use of the local marine resources. Native communities surrounding the Bering Sea process hundreds of kilograms of food per capita, benefiting local residents as an important source of nutrition and subsistence. High latitude communities rely on tourism that the fishery brings to the region and the economic structure it provides, especially within indigenous markets. The harvesting of fish, marine mammals, and seabirds from the region produces cultural, intellectual, and spiritual connections between the ecosystem and the local people (Haynie and Huntington, 2016). Thus, human interaction with the Bering Sea ecosystem is a bilateral relationship, where humans rely on the fisheries and marine mammals, but can directly impact these communities that they rely on. Climate acts as an independent variable that directly affects this ecosystem (Figure 7). Climate trends that are affecting the sea ice edge extent and water temperature determine the Cold Pool, species distributions, and abundance trends.

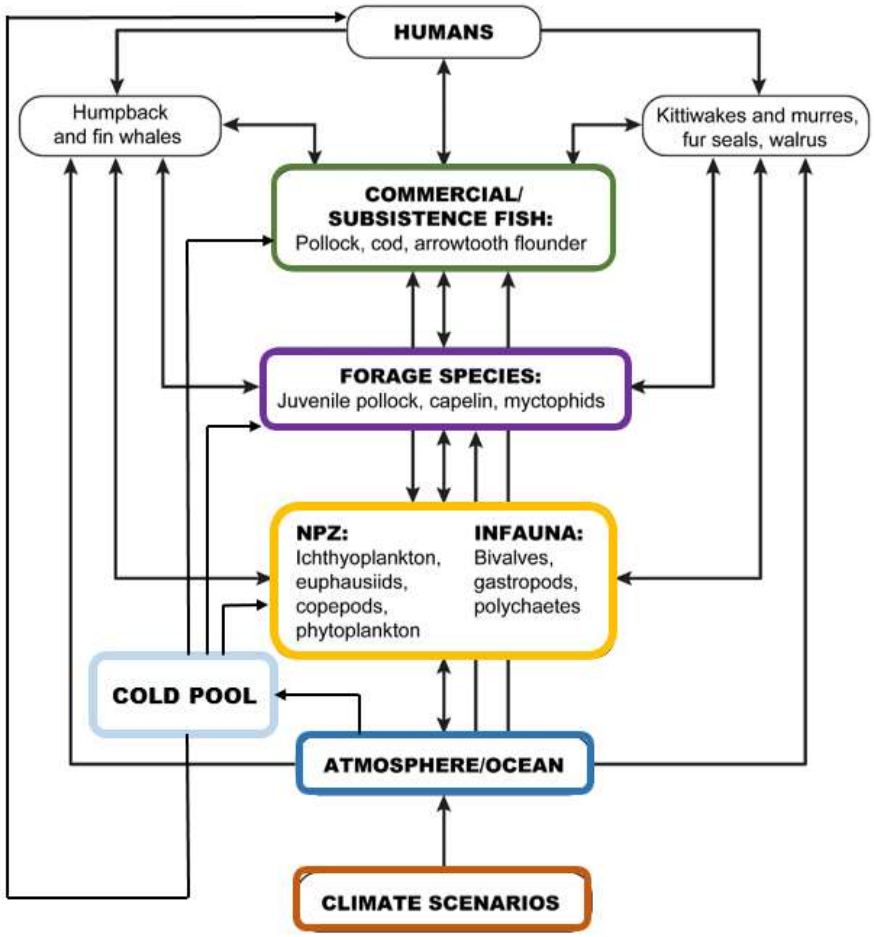

Figure 7. Schematic of direct relationships in the Bering Sea Ecosystem, highlighting the Cold Pool relationship modified after Haynie and Huntington (2016).

1.2 Sampling in the Eastern Bering Sea

1.3.1. Biological Sampling

Traditionally, sampling of Bering Sea zooplankton communities is largely conducted by shipboard biological net sampling. Although nets can sample over large spatial scales, they are essentially a point sample in time. Biological point sampling using nets has limitations in comprehensiveness due to the restrictions in the time of year sampling can take place, operational time of day, and biases due to net avoidance based on vessel speed and noise. Annual zooplankton net-based estimates are made during ice free conditions in the spring and

summer months, approximately April-September. Sampling under ice is necessary for full seasonal community dynamics to be captured. Scientific echosounders are tools that are noninvasive and can measure the presence of biological scatterers in the water column autonomously at high temporal and vertical spatial resolutions underwater and even under ice.

With the development of scientific echosounders, net sampling has been done in conjunction with acoustical sampling to verify species composition of target layers. Acoustic-net paired sampling provides a comprehensive view of the ecosystem and of the species and sizes present in the region. However, orders of magnitude of discrepancies are often observed between acoustical and net capture estimates, especially with euphausiid densities, usually resulting in acoustical estimates far greater than observed with net captures due to net avoidance (Coyle, 2000, Coyle and Punchuk, 2002, Warren and Wiebe, 2008). Acoustical and net capture estimates might be considered upper and lower bounds on euphausiid density (Warren and Wiebe, 2008).

De Robertis et al. (2010) developed a classification method for acoustically detecting biological groups in the Bering Sea during dedicated *in-situ* pollock trawl surveys, and data from acoustical assessments is now incorporated in the stock assessment (Trenkel et al., 2011). De Robertis et al. (2012) documented the distribution of pelagic organisms in open water areas of the EBS during ice-covered (spring) conditions. Using acoustical sampling, and comparisons from previous ground-truthed acoustical surveys, the study determined the continental shelf zooplankton to be dominated by euphausiids, more evenly distributed, and less restricted by water temperature and ice cover, when compared to fish. Substantial backscatter from macro-zooplankton suggests zooplankton populations overwinter on the EBS shelf.

1.3.2 Active Acoustic Sampling

Acoustical sampling techniques in the ocean are used to observe the environment, biology, and human interactions. Active acoustics is used for observing the ocean topography, currents and temperature, and abundance of marine life (Howe et al., 2019). Scientific echosounders are remote sensing tools that use sound to detect the distribution and density of fish and related biodiversity.

Using long-term acoustical data has advantages, but also comes with unique challenges. Sensors used for long-term monitoring programs on mooring platforms that are deployed remotely on annual or biannual cycles endure propagation variation due to the natural seasonal change, as well as electrical interference from nearby sensors also collecting data. In the case of acoustic sensors, seasonality can affect absorption and sound speed rates used in the processing of the received signal. The instruments can endure drift in the internal clocks and in the overall gain applied in deployment settings requiring routine calibrations. Older versions of equipment are limited in capabilities compared to state-of-the-art technology and software at present day; however, to preserve the power of long time-series data, lower resolution data from restrictive parameters of older sensors are maintained to ensure consistency. Finally, long time series are powerful for observing relative changes, but across multiple field seasons gaps in data arise, sensors malfunction, and documentation is subject to human error as projects pass from researcher to researcher. This study is not immune to these limitations and extensive data quality control methods were explored to maximize the accuracy and value of the data set.

Metrics for measuring variability of backscatter vertical distribution in the water column with remote acoustic sampling systems have been proposed in the acoustical community for widespread consistency. Acoustical water column metrics quantify measurements as succinct descriptors of vertical distribution, total abundance, mean density, occupied area, location,

spread, evenness, aggregation, and number of backscattering layers through time, which can address ecological questions on long time scales (Urmy et al., 2012). Examples of these metrics include:

- Center of Mass (*CM*) or average sample depths weighted by their volume backscatter strength (S_v)
- Inertia (*I*) or spread as the sum of squared distances from the CM
- Number of layers (N_{layers}) or layer structure using local scattering maxima in the vertical direction

Species classification using acoustics can be achieved using multi-frequency methods by utilizing several sonars with different single frequencies, or a single broadband sonar with a range of frequencies. The use of multiple frequencies within a single system have increased the ability of quantifying pelagic organisms in a noninvasive way. By plotting backscattered energy from one frequency against backscattered energy of other echosounder frequencies, frequency response curves of organisms can be obtained. There are several groups of organisms with distinct frequency response curves in the 10-200 kHz frequency band (Figure 8). The overall acoustic energy scattered from pelagic organisms is a function of abundance, species composition, and size distribution; thus, acoustic-net pair sampling corroboration is the standard for creating multi-frequency volume backscattering (S_v) response curves (Trenkel and Berger, 2013). Additionally, general signals can be further complicated by non-biological sources of scattering, such as turbulence layers or internal waves. Thus, the use of multifrequency techniques can discriminate biological from non-biological scatter (Benoit-Bird and Lawson, 2016).

Kang et al. (2002) developed an acoustical methodology of species identification by utilizing the difference of mean volume backscattering strengths among multiple frequencies, specifically echoes differentiated from walleye pollock and krill (*Euphausia pacifica*). Commonly referred to as "Delta-S_v" or "dB differencing", attaining changes of S_v by subtraction is a popular technique in distinguishing animal groups, such as fish and zooplankton or larger planktonic groups. Delta-S_v methods can be used for "acoustic inversion" or estimating biomass using the intensity level, or Target strength (TS), received by a species of interest.

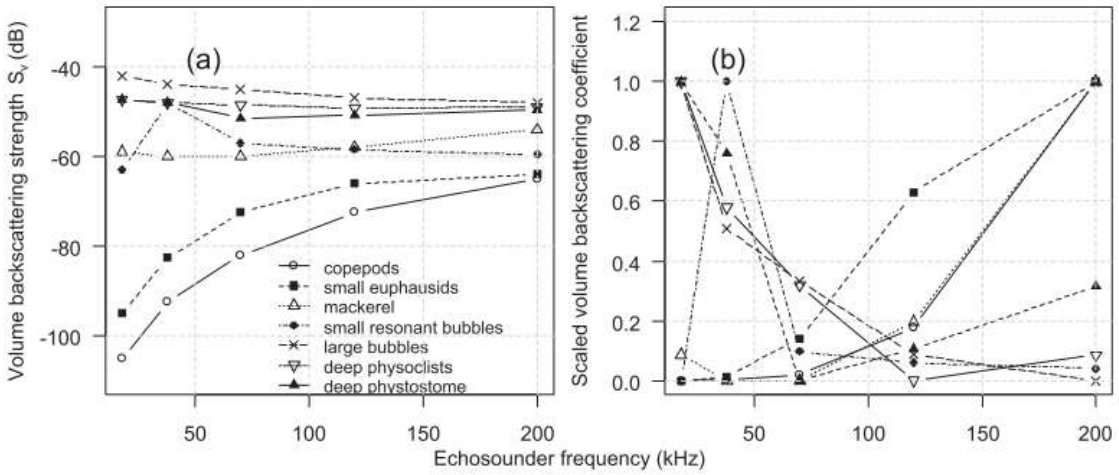

Figure 8. Fisheries acoustic frequency response curves of volume backscattering strength (Trenkel and Berger, 2013).

The signal or intensity received by scientific echosounders can be converted to S_v or TS values. TS is a logarithmic measure of the proportion of the incident intensity backscattered from the target measured in units of decibels (dB) relative to $1m^2$ (Equation 1) (Simmonds and MacLennan, 2002). Mean volume backscatter (S_v) is measured in dB re $1m^{-1}$ (Equation 2) and is a function of TS.

$$\boldsymbol{TS = \log_{10} p_{er} + 40 \log_{10} r + 2\alpha_a r - 10 \log_{10} \frac{p_{etg_o 2_\lambda 2}}{16\pi^2}} \qquad \text{Equation 1}$$

$$\boldsymbol{Sv = \sum TS - 10 \log_{10}(\frac{C_w \tau \varphi r^2}{2})} \qquad \text{Equation 2}$$

where:

TS= target strength (dB re 1 m^2)
S_v= volume backscattering strength (dB re 1 m^2 m^{-3})
P_{er}=received electric power (W)
r= distance from transducer to target or range (m)
C_w= Sound speed (m s^{-1})
α_a= absorption coefficient (dB m^{-1})
p_{et}=transmit electric power (W)
g_0=on-axis transducer gain
λ= acoustic wavelength (m)
τ= pulse duration (s)
ψ=equivalent two-way beam angle or a 3D measure of the beam width (steradians, sr)

Various scattering coefficients exist for estimating density and biomass from acoustic backscatter data. Scattering by an individual organism is expressed as a backscattering cross-section (σ_{bs}) which can be estimated based on organism TS (Equation 3). When a single organism type dominates the acoustic scattering volume (example: euphausiids), the number of targets can be estimated in a volume with Equation 4 or in an area with Equation 5.

$$\boldsymbol{TS = 10 \log_{10} \sigma_{bs}} \quad \text{Equation 3}$$

$$\boldsymbol{N = \frac{Sv}{\sigma_{bs}}} \quad \text{Equation 4}$$

$$\boldsymbol{ABC = 10^{\frac{Sv}{10}} * T} \quad \text{Equation 5}$$

where:

N= number organisms per unit volume (m^{-3})
σ_{bs}= average backscattering cross-section weighted by the distribution of organism lengths (m^2)
ABC= Area backscattering coefficient ($m^2 m^{-2}$)
T= mean thickness (m)

1.3.3 Eastern Bering Sea Zooplankton TS

Bering Sea zooplankton TS varies spatially and seasonally. Smith et al. (2010) measured the material properties for Bering Sea zooplankton communities including sound speed or "h", and density or "g", which are both based on lipid content and size. Their measurements showed significant variation in TS ranging up to 20 dB, suggesting that uncertainty could be reduced if material-property values specific to taxon, location, and time of year are studied. In addition to material properties, Demer and Conti (2006) observed TS to vary significantly with krill-orientation and distribution. Location appeared to be a significant influence on euphausiid TS in the Bering Sea. TS estimates varied by 19.5 dB for eastern Bering Sea euphausiids and 16.7 dB for western euphausiids. Smith and Ressler et al., (2013) observed Bering Sea euphausiid TS can range up to 30 dB based on length distributions (Figure 9).

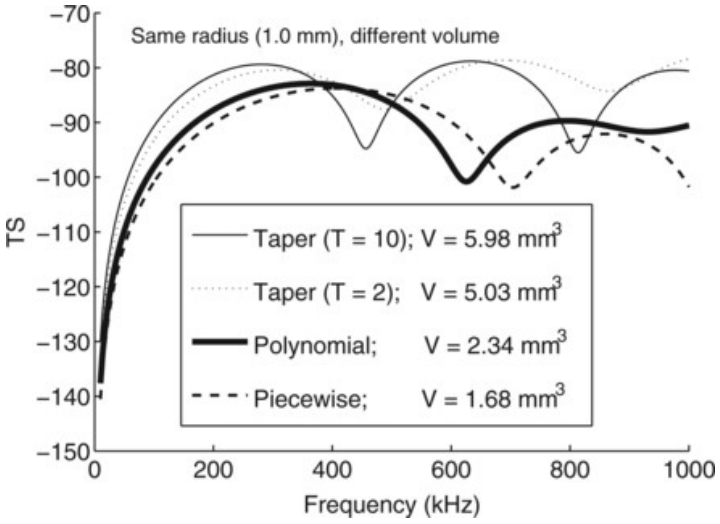

Figure 9. Target Strength (TS) (dB re 1 m^2) calculated as a function of frequency for individual Bering Sea euphausiids with measured mean length (L), density contrast (g), and sound speed contrast (h) values. Calculations were made for an animal with broadside incidence and polynomial shape. Constant radius (r = 1 mm) was used for each euphausiid shape, while the volume (V) varied among physical shape models from Smith et al. (2013).

TS is a function of shape, density, tilt, and other physical parameters, depending on the complexity of the organism being modelled. The Stochastic Distorted Wave Born

Approximation (SDWBA) physical model, a variant from the Distorted Wave Born Approximation Model (DWBA) (Chu et al., 1993, Stanton et al., 1993), is used to calculate species-specific TS-length relationships based on shape, volume, length, and animal vertical orientation (Demer and Conti, 2003 &2006). The DWBA and SDWBA analytical models have been shown to improve predictions of measured scattering levels for angles that are well away from normal incidence. Jech et al. (2015) found the SDWBA model compared to other analytical and numerical scattering models for marine aquatic organisms, was approximate for weak scatterers for all shapes, frequencies, and angles tested for TS values over the 12-400 kHz range. Small variations of input parameters, such as g and h, can significantly affect model frequency response results.

Estimates of g and h from ex-situ studies have been variable for euphausiid species in the Bering Sea, which creates difficulty in using this essential parameter that affects the SDWBA model results (Figure 10). While length distributions, g's, and h's have been documented during the Cold Years (2005-2012) (Smith et al., 2010, Smith et al., 2011, Smith et al., 2012, McQuinn et al., 2013) there is further need for Warm year (2014-present) investigation where lipid levels have been observed to be greatly reduced suggesting additional variability in essential model parameters.

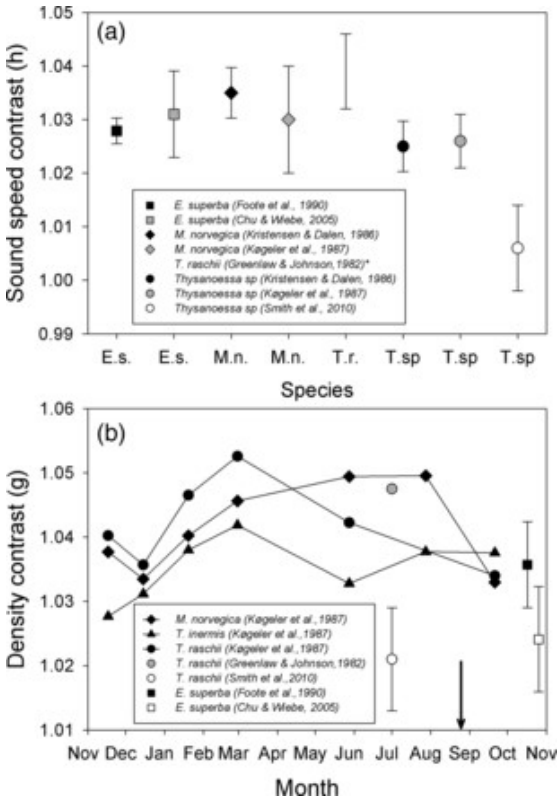

Figure 10. a) Sound-speed contrast (*h*); literature estimates of *h* showing species variability [mean and s.d., except for Greenlaw and Johnson (1982) where bars show value range] and (b) density contrast (*g*); literature estimates of *g* showing seasonal, geographic, and species variability (mean and s.d. where available). The arrow marks the period of data collection for the present study from McQuinn et al. (2013).

1.3.4 Ecosystem Based Acoustic Monitoring

Assessing and monitoring the abundance and biomass of zooplankton and commercially important fish is a necessary practice for ecosystem-based management (EBM) (Trenkel et al., 2011). EBM in the United States is systematic approach for management of marine and coastal resources with the goal of managing natural resources, habitat, and species in a sustainable manner, while maintaining human service resiliency (Dell'Apa et al., 2015). Limitations of EBM is the lack of knowledge of principles and best practices and implementation by managers. Using active acoustical measurements for biological monitoring of ecosystems has led to the development of robust ecosystem indicators for EBM, which is driven by understanding the

ecological interactions and processes necessary to sustain ecosystem structure and function (Trenkel et al., 2011).

Ecosystem Based Fisheries Management (EBFM) focuses on the fisheries sector of marine resources. To advance implementation of EBFM, NOAA Fisheries has developed implementation plans that identify priority actions and milestones for the next five years. The Alaska region EBFM plan is defined as "a systematic approach to fisheries management in a geographically specified area that contributes to the resilience and sustainability of the ecosystem; recognizes the physical, biological, economic, and social interactions among the affected fishery-related components of the ecosystem, including humans; and seeks to optimize benefits among a diverse set of societal goals." The Alaska region EBFM implementation plan focuses on the eastern Bering Sea Large Marine Ecosystem (LME), and robust management practices will be assessed for applicability to surrounding other LME's which include the Gulf of Alaska, Aleutian Islands, and Chukchi and Beaufort Seas of the U.S. Arctic (NOAA Fisheries 2017). The Alaska region depends on collaborative partnerships to develop and implement fishery management decisions and programs. The North Pacific Research Board (NPRB) is considered a key partner and has provided supplemental funding for this project to J.J.Johnson through the Graduate Student Research Award in 2019. The potential to apply acoustical techniques and methods explored in this study, to nearby regions of the eastern Bering Sea, can result in a more comprehensive understanding of Arctic ecosystems and fisheries impacts that contribute to NOAA's EBFM mission.

1.4 Goal and Objectives

The major goal of this project was to gain an understanding of zooplankton dynamics associated with Cold Pool variation (Figure 11). This project contributes knowledge to

understanding the relationship of physical oceanographic changes and the biological variability of zooplankton communities by analyzing differences in the Warm and Cold regimes (Figure 1).

The two main objectives included:

A) Determine the relationship of acoustic backscatter indicative of zooplankton abundance relative to Cold Pool variation. The null hypothesis (H_o) was that Cold Pool presence, bottom temperature, duration at freezing temperatures, and regional and local sea ice area would not affect zooplankton abundance.

B) Develop a predictive model between Cold Pool variation and zooplankton abundance.

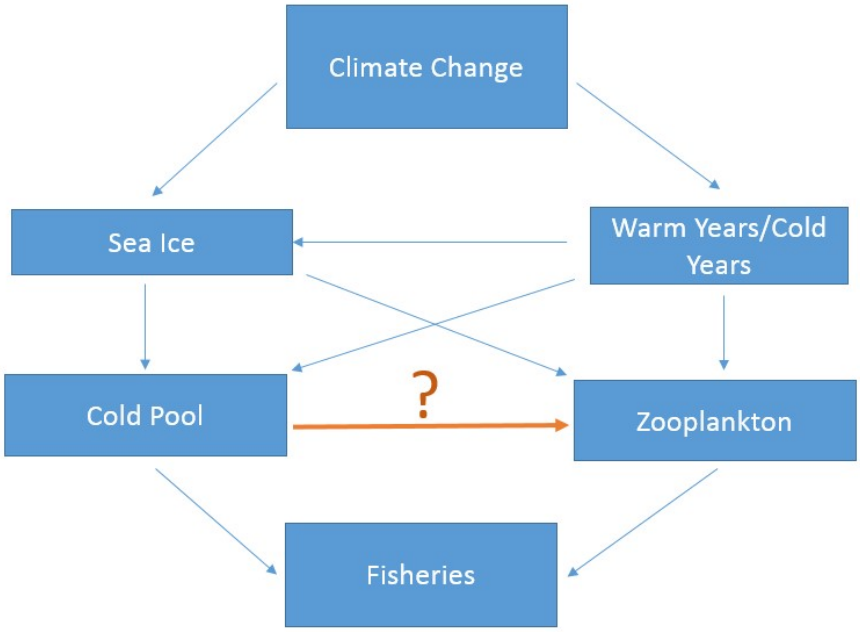

Figure 11. Schematic flow of variables and impacts on the eastern Bering Sea ecosystem, highlighting the need to understand the relationship between year-round zooplankton dynamics and inter-annual Cold Pool variation.

CHAPTER 2: METHODOLOGY

2.1 Study Site

Mooring sites along the EBS shelf, in the Middle domain, have been monitoring the ecosystem via NOAA's North Pacific Climate Regimes and Ecosystem Productivity Program (NPCREP) biophysical observing network since 2005 (Stabeno et al., 2010). The mooring systems are deployed along the 70m isobath on the EBS shelf. Acoustical mooring sites "M5" (59 54.285N, 171 42.285W), "M2" (56 51.989N, 164 3.002), and "M8" (62 11.62N, 174 40.06W) (Figure 12) are changed seasonally or annually by the Ecosystems & Fisheries Oceanography Coordinated Investigations (Eco-FOCI) program (http://ecofoci.noaa.gov). Eco-Foci is a joint research program between the National Marine Fisheries Service (NMFS) AFSC and the Office of Oceanic and Atmospheric Research (OAR) Pacific Marine Laboratory (PMEL). Oceanographic moorings at site M2 have been maintained almost continuously since 1995, while site M5 and site M8 have been maintained since 2005 and 2004, respectively (Stabeno et al., 2012). Since 2008, the oceanographic moorings and additional acoustical moorings were deployed at each site until fall 2019. The hydrographic and acoustical moorings were separated by a kilometer to minimize acoustic noise interference. Each "M" site has similar seasonality, however there are interannual differences in maximum temperature and sea ice formation between sites. For example, the interannual variability in bottom temperature at site M2 is greater than observed at site M8. Vertical stratification between the northern and southern shelves differ as well, with site M2 sharply stratified; site M5 and M8 have weaker thermoclines (Stabeno et al., 2012). Site M5 is centrally located in the Middle domain at the 60˚N transition from North Bering Sea (NBS) and the South Bering Sea (SBS), and site M8 is in the North domain in the NBS. Separated by approximately 300 km (163 nmi), site M8 and M5 were used

in this study and selected due to the relevance of location based on forecasted warming condition differences. With the NBS projected to remain cold and the SBS predicted to be more susceptible warming, site specific ecological processes and Cold Pool variation were likely to occur among the two locations.

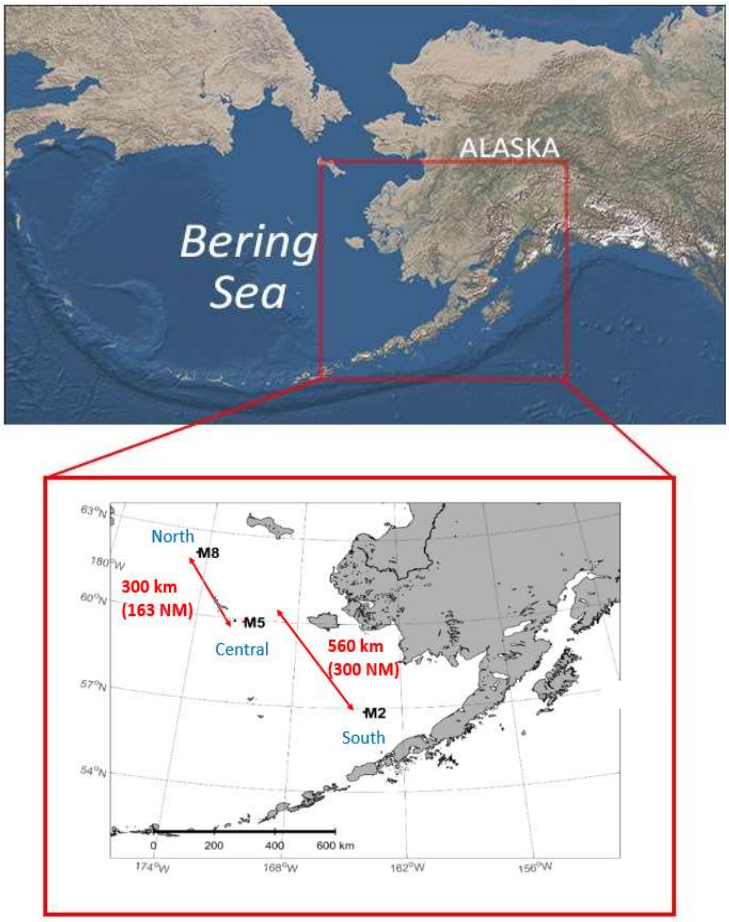

Figure 12. Bering Sea Shelf with labeled mooring locations (Top image: Google Maps).

2.2 Data Collection

The technical approach to achieve the objectives described above utilized multiple time series datasets from 2008-2019 collected from the Bering Sea Middle Domain Shelf at site M5 and M8 (Figure 13). Datasets were divided by Cold and Warm regime time periods, separated on October 1, 2013 (Figure 1).

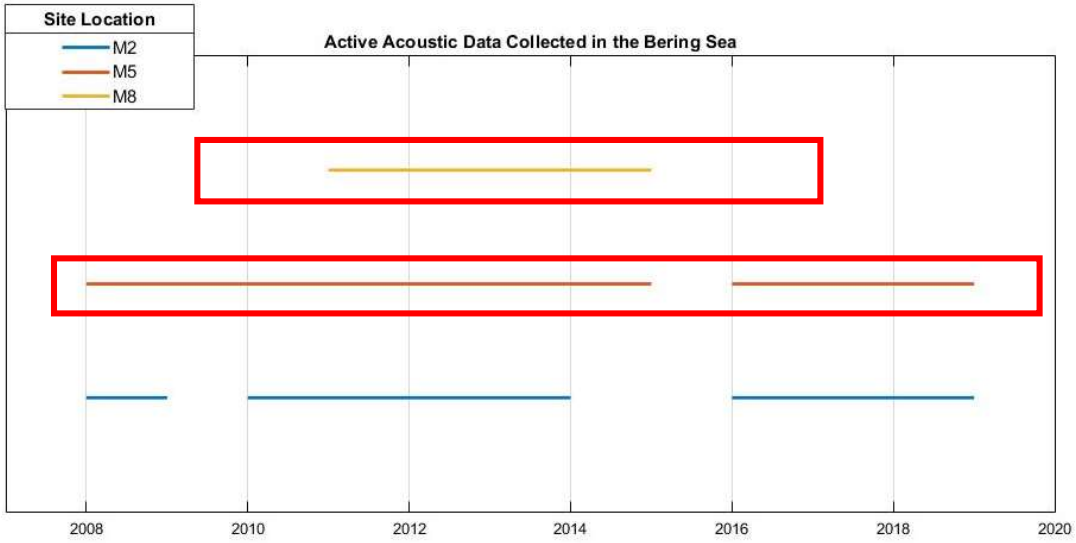

Figure 13. Timeline of acoustic data collected along Bering Sea shelf with study sites M5 and M8 in the red boxes.

2.2.1 Bottom Temperature

Bottom temperature from the Eco-FOCI oceanographic moorings was exported for Cold Pool characterization for 2005-2019. The Eco-FOCI program have utilized the biophysical moorings in the Eco-FOCI network to document full water column temperatures. The oceanographic mooring temperature measurements were recorded using miniature SeaBird temperature recorders SBE-39 sampling every 10 minutes (measurement precision reported to be ±0.0001˚C). The oceanographic mooring measurements agreed with acoustical mooring bottom temperature measurements. Oceanographic measurements were used for analysis due to the longevity of the time series available compared to the acoustical mooring measurements.

2.2.2 Regional Seasonal Sea Ice

Sea ice data were used from the National Snow and Ice Data Center (NSIDC). Regional daily data were used for the Bering Sea with the boundary defined by the Arctic Sea

Ice News and Analysis (ASINA) team using Meier et al. (2007) (Figure 14). Passive microwave satellite derived sampling calculations of 5-day trailing averages for sea ice extent and area have been recorded in square kilometers since 1987. Regional sea ice area "V3 product" (Fetterer et al., 2017) for the Bering Sea region was used for analysis.

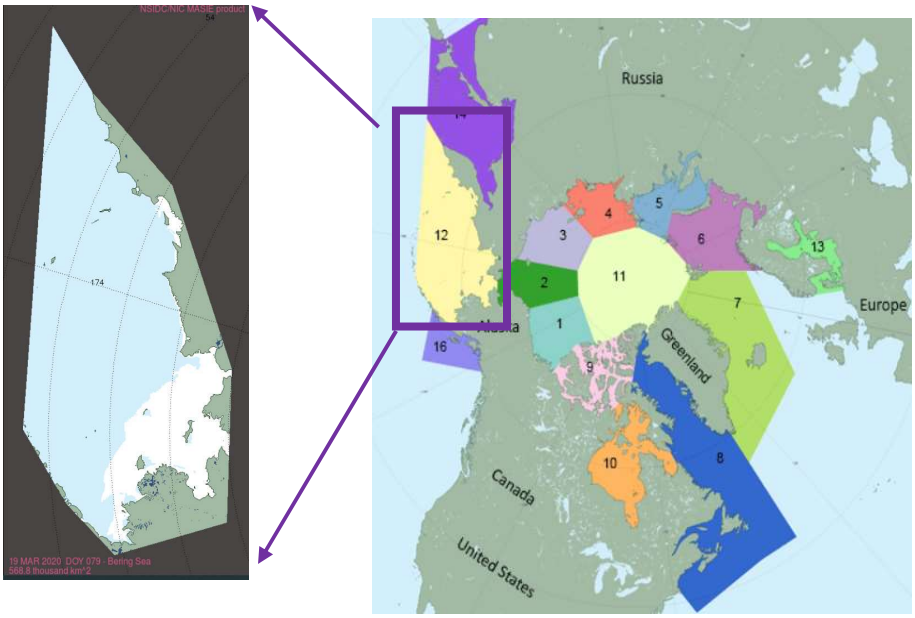

Figure 14. National Snow and Ice Data Center (NSIDC) regions of Arctic (14).

2.2.3 Local Seasonal Sea Ice

Local seasonal sea ice measurements were used from NOAA's National Weather Service (NWS) Alaska Sea Ice Program (ASIP) daily sea ice concentration analysis product (https://portal.aoos.org/old/arctic.php#). Ice measurements were used from the U.S. National Ice Center (NIC) World Meteorological Ice Egg at 4 km^2 resolution. The Ice Egg documents multiple metrics to characterize sea ice by concentration, thickness, and age (Figure 15). The "C_t" section was averaged for daily measurements, interpolating between missing data when ice was present at the site of interest. Local time series were compiled for site M5 and M8.

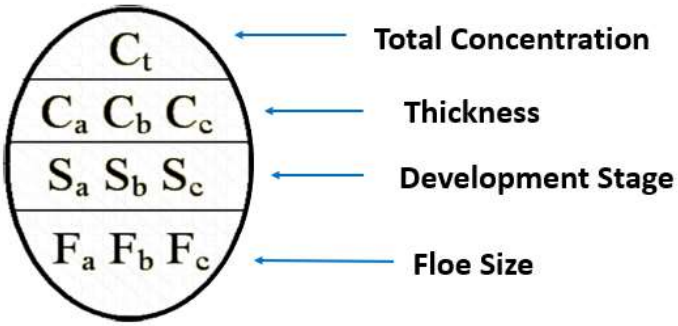

Figure 15. National Ice Center (NIC) World Meteorological Ice Egg

2.2.4 Acoustic Backscatter

Acoustical data were collected with ASL Environmental Sciences Acoustic Water Column Profilers (AWCP) (https://aslenv.com/). AWCPs were attached along bottom-mounted mooring chains and were upward facing (Figure 16). The AWCPs recorded near full water column range of backscatter for 5 minutes every 30 minutes with pulse lengths of 300µs. Site M5 data were collected at acoustic frequencies of 125, 200, and 460 kHz during the time interval 2008-2017 with a year gap in 2015. From 2017-2019, site M5 data were collected at 200, 460, and 775 kHz. Site M8 data were collected at acoustic frequencies of 200, 460, and 775 kHz from 2011-2013, and in 2014-2015 with 125, 200, and 460 kHz.

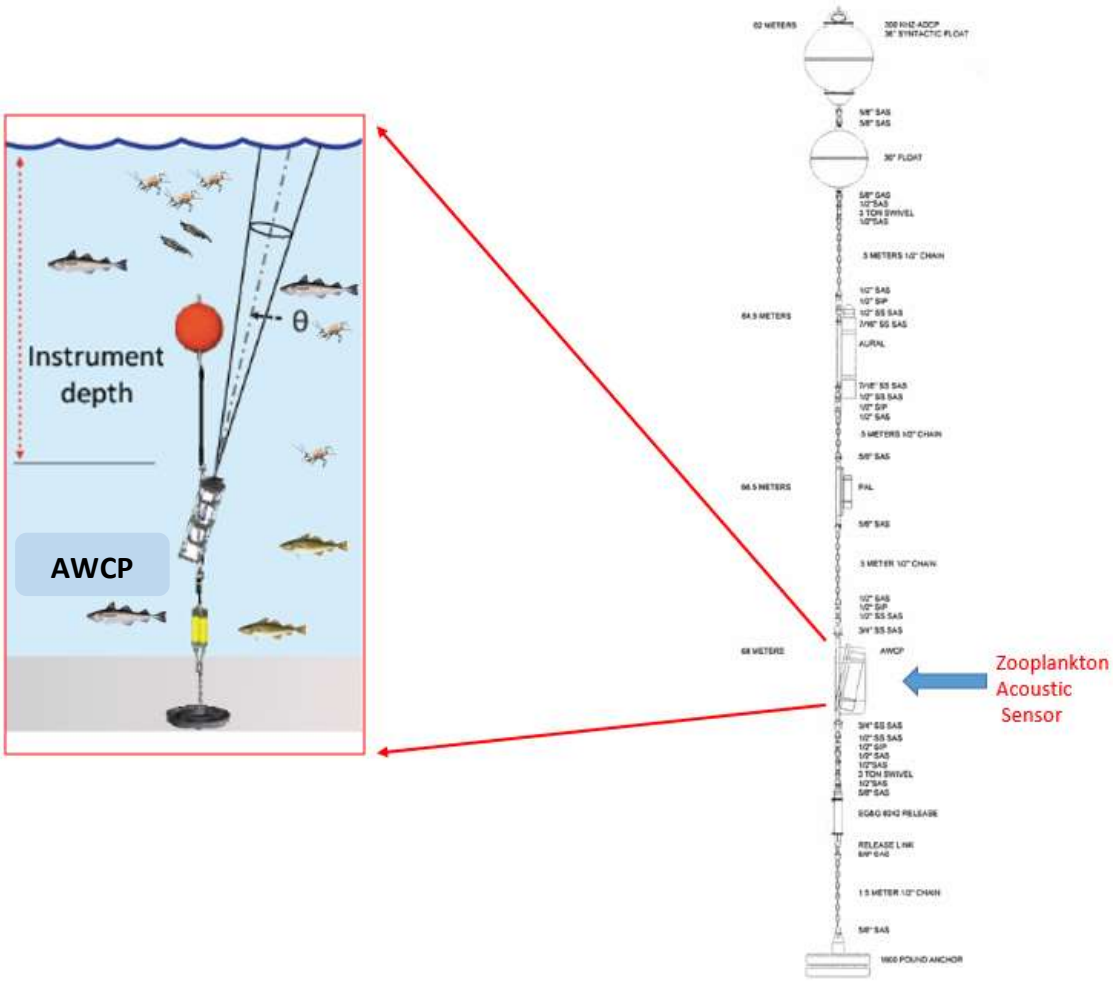

Figure 16. Depiction of acoustical mooring system and sensors attached.

2.3 Data Processing

2.3.1 Cold Pool Presence and Duration

Bottom temperature data sampled at the oceanographic mooring were used to determine Cold Pool presence and duration at each site. Cold Pool metrics were calculated only during the summer season (June-October) based on the seasonal stratified water column structure. To avoid including bottom temperatures with daily values less than 2˚C from water column mixing and winter cooling, solely summer values less than 2˚C were identified and annual Cold Pool presence or absence and duration was determined.

2.3.2 Freezing Bottom Temperature

A freezing temperature was defined when the Bering Sea bottom temperatures reached a minimum of -1.7 ˚C on average. The -1.7 ˚C bottom temperature threshold is indicative of sea ice presence at the surface, as well as the entirety of the water column cooled by winter temperatures. The number of days of bottom temperatures from the oceanographic mooring for each site equal to or less than -1.7 ˚C were identified and summed annually during the spring season (March- April) when historic peak sea ice extent was reached. This was referred to as the duration of *freezing bottom temperature*.

2.3.3 Seasonal Sea Ice

Sea ice covering most of the EBS shelf has been observed with maximum sea ice extent values exceeding 400,000 km^2 by late March. Sea ice presence at the end of the spring season (April-May) is indicative of physical (Cold Pool presence and duration) and biological conditions (recruitment strength) for the shelf during the following summer (Stabeno et al., 2012). NSDIC Bering Sea regional sea ice area values for days that exceeded 400,000 km^2 in May were identified annually.

Local sea ice presence can affect the local biological dynamics of a site. Local sea ice formation and regression time is important for all trophic levels from zooplankton to large marine mammals relying on under ice-algae, spring open water blooms, stability of the water column, and modulation of water temperatures. Timing of the bloom and open water conditions varies depending on the local sea ice concentration, which varies based on ice floe dynamics and wind conditions. NWS local Ice Egg concentration percentage values that exceeded 20% in May were identified, and annual <20% sea ice presence in May were categorized for each site.

2.3.4 Acoustic Data

All AWCP data from 2008-2018 were exported with ASL MFAWCPLink software. Instrument specific deployment settings were applied to all data and documentation of export settings was compiled for all years. The MFAWCPLink software converted linearly detected voltages to S_v (Equation 6). S_v values were processed to remove background, interference, transient, and impulse noise using Myriax Echoview software (https://www.echoview.com/). In addition, data from each instrument (8 total) were corrected for their specific dynamic range or range of values based on frequency and capability of the system (Figure 17). Using the dynamic ranges, data thresholds were applied to mitigate noise.

Data were referenced to zero depth (i.e. the sea surface), so accurate cross-frequency and cross-season comparisons could be made. The variation in the reported bottom depth and sensor placement was consistent within 1-2 meters from season-to-season. Therefore, all data were limited in resolution based on the shallowest sensor deployment. The finest vertical resolution with the dataset was 0.058 meters. Surface lines approximately 1-2 meters below the air-water interface were delineated for data exclusion from unwanted noise from air bubble scattering at the air-water interface.

Acoustic backscatter analysis used the 200 kHz and 460 kHz systems and discarded 125 kHz or 775 kHz data depending on the deployment year. The 200 kHz and 460 kHz were deployed each season across the sampling period for both sites and were used to maintain consistent comparison values across time, while the 125 kHz and 775 kHz were not. Site M5 acoustic backscatter analysis was performed for Fall 2008-Fall 2018 but resulted in data gaps totaling to 11.6% of the averaged daily time series, including Fall 2015-Fall 2016 when instruments were not deployed. Site M8 acoustic backscatter analysis was during the sample

period Fall 2011-Fall 2015 but resulted in data gaps totaling to 13.2% of the averaged daily time series.

$$\boldsymbol{Sv = 20\log_{10} N - G\left(\frac{2R}{c}\right) - OCV - SL + 20\log_{10} R + 2\alpha R - 10\log_{10}\left(\frac{1}{2}c\tau\varphi\right)}$$

Equation 6

Where:

N = The recorded digital value which is linearly related to the output voltage of the detector in the receiver
G=Time varying gain
R = Range (m) for N.
c = Speed of sound (m/s)
OCV= The voltage out of the transducer (dB re 1 volt/micropascal)
SL = source level (dB re 1uPa), which is TVR + $20\log_{10}(V_{TX})$
V_{TX} =The voltage sent to the transducer
α= Absorption coefficient (dB/m)
τ = Transmitted pulse length (s)
Ψ = Two-way beam angle (dB re 1 Sr)

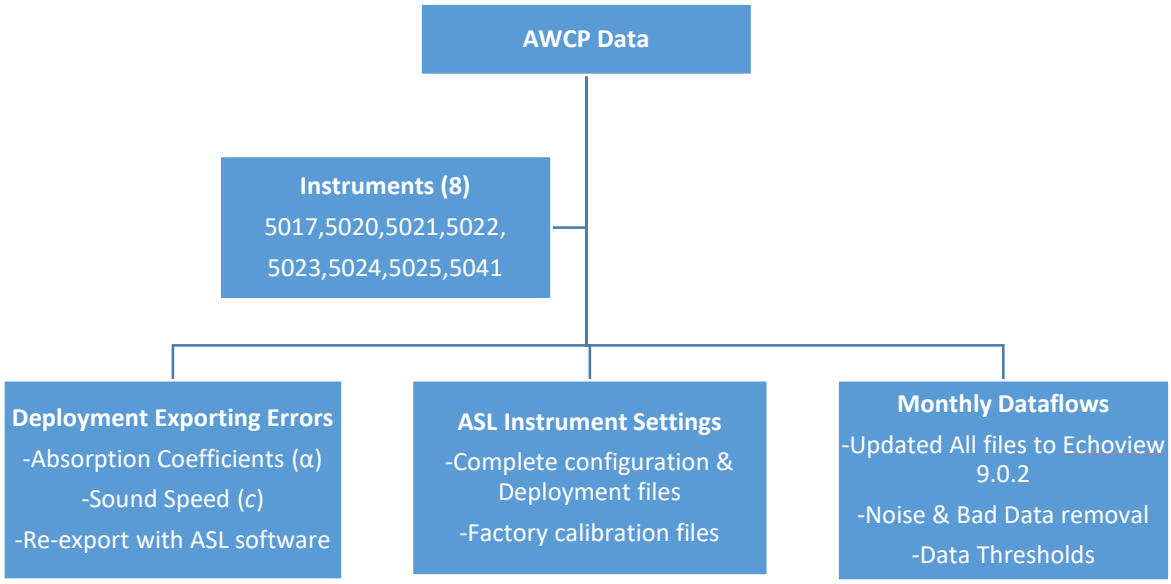

Figure 17. Data flow of Acoustic Water Column Profiler (AWCP) data processing

a. Zooplankton Abundance & Delta-S_v

Acoustical data were exported in daily bins. This resolution captured the entire 5-minute ping cycle for each 30-minute interval in which the instrument sampled per day. These data were averaged over the multiple vertical bins in the water column to generate mean volume backscatter coefficients (S_v units m^2m^{-3}) by integrating data in a 24-hour period for volume backscatter abundance estimation (Figure 18). Area Backscattering Coefficient (m^2 m^{-2}) (ABC) and Mean S_v (m^2m^3) were calculated for daily by 70m bins using the 200 kHz time series for each site. Mean S_v (m^2m^3) values calculated daily by 70m bins for the 200kHz and 460 kHz time series were used with "dB-differencing" or Delta-S_V methodology. Daily Mean 200 kHz S_v values were subtracted from daily Mean 460 kHz S_v values for each site.

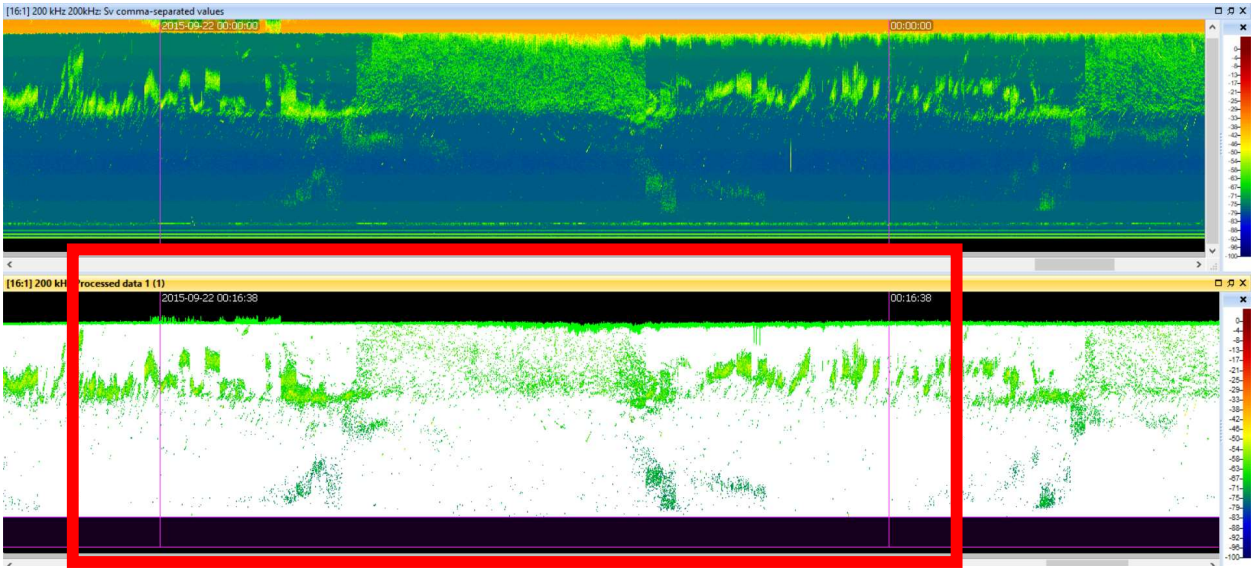

Figure 18. Echogram of upward facing 200 kHz with red box depicting 1 processing bin (24 hours by ~70 m depth)

2.4 Statistical Analysis

2.4.1 Bottom Temperature

Cross-correlations, or cross covariances normalized by the product of the standard deviations of two random variables, were conducted to analyze bottom temperature leads/lags

between the two sites. Monthly bottom temperature averages were computed for each site between the Cold (2006-2013) and Warm (2014-2019) years. 95% confidence intervals (CI) were computed for the data based on the standard error from the t-distribution. Degrees of Freedom (DOF) used to test the t-distribution were calculated based on the independent observations (N*) within each time series.

N* values were calculated using the equation (7):

$$\boldsymbol{N^* = \left(\frac{1-\rho_1}{1+\rho_1}\right) N} \qquad \text{Equation 7}$$

where ρ_1=autocorrelation at time lag (k)=1

Monthly variance for each site for Cold years and Warm years were calculated from σ^2, or the sum of the squared distances of each term in the distribution from the mean. Monthly averages were standardized or rescaled with properties where the mean was equal to 0 and the standard deviation was equal to 1, to analyze seasonal length variation rather magnitude of the signals. Standardized values were calculated using the equation (8):

$$\boldsymbol{Z = \frac{x-\mu}{\sigma}} \qquad \text{Equation 8}$$

Daily anomalies were computed for site M5 bottom temperature based on subtracting the monthly average to find anomalous years (above or below the average) during Cold years and Warm years.

2.4.2 Seasonal Sea Ice

Monthly regional sea ice area averages were computed between the Cold (2006-2013) and Warm (2014-2019) years. Monthly averages were standardized to analyze seasonal length variation rather than magnitude of the signals. Daily anomalies were computed for the regional

sea ice by subtracting the monthly average to find anomalous years during Cold year and Warm year durations.

A cross-correlation between bottom temperature and regional seasonal sea ice for site M5 was conducted between Cold and Warm years to identify leads/lags between the two environmental variables and to analyze the correlation during Cold vs. Warm years. Seasonal lags between the bottom temperature and SSI were estimated from cross-spectra analysis. A cross-correlation between daily anomalies of M5 bottom temperature and regional sea ice was conducted to identify covariance between anomalies. Confidence intervals (CI) for both correlations were calculated based the Percentile bootstrapping method (Efron and Tibshirani, 1986), relying on random sampling with replacement, with 10,000 iterations to determine whether correlations were statistically significant. A cross-correlation between local sea ice for site M5 and regional sea ice was conducted to identify covariance and to identify leads/lags between the two environmental variables.

2.4.3 Acoustic Backscatter

Monthly ABC average were computed between the Cold (2008-2013) and Warm (2014-2018) years for each site. Monthly averages were standardized to analyze seasonal length variation rather than magnitude of the signals. Monthly Delta-S_v averages were computed for site M5 between the Cold (2008-2013) and Warm (2014-2018) years, and between Cold (2011-2013) and Warm (2014-2015) years for site M8. Monthly variance for Delta-S_v was calculated between Warm and Cold years for each site.

2.4.4 Predictive Modelling

Generalized Additive Models (GAMs) allow for combinations of linear and non-linear relationships between the response variable and individual explanatory variables. In terms of this

project, that means the zooplankton ABC response variable can have various relationships with multiple Cold Pool environmental predictive variables while all others are held steady (Table 1). Two GAMs - a Cold regime model and a Warm regime model - using the 'mgcv' package in R (version 1.8-31; R Development Core Team 2012) were fit assuming the effects of the Cold Pool variable predictors were additive. Smoothing splines and tensor product interaction functions (penalized regression splines; Wood & Augustin 2002 and Wood et al., 2006, respectively) were used to model the effect of each term, in their respective units, on the acoustic abundance response variable. Backward variable selection was performed by fitting the full model, then dropping terms with p-values >0.05 one a time.

All predictive models described above were quantified with an Akaike's Information Criteria (AIC) and Deviance Explained (R^2) value. AIC, which measure the goodness of fit and model complexity, were used to indicate the relative quality of the models for model selection. Model performance was evaluated by examining model residual plots and partial residuals of covariates to determine whether model assumptions had been met.

Variable **Description (units)**	**Type**	**Temporal Resolution**	**Vertical Spatial Resolution**	**Data Type**
ABC Area Backscattering Coefficient (m^2 m^{-2})	Response	Daily	Water Column Averaged	Continuous
Bottom_Temp Bottom temperature (°C)	Predictor	Daily	~65 meters	Continuous
Freezing_Temp Bottom temperature (< -1.7°C) in Spring (YES/NO)	Predictor	Daily	~65 meters	Binary
Pres_Cold_Pool Cold Pool presence (YES/NO)	Predictor	Daily	~65 meters	Binary
Regional_SSI Regional sea ice area (km^2)	Predictor	Daily	Surface	Continuous
Local_SSI Local sea Ice coverage (%)	Predictor	Daily	Surface	Continuous
Year, Month, Day Year, Month, Day	Predictor	Daily	NA	Categorical
fracyear Fraction of year (years)	Predictor	Daily	NA	Continuous

Table 1. GAM predictor and response variables

CHAPTER 3: RESULTS

This chapter presents results from the analysis of the environmental and acoustical time series. It begins with bottom temperature analysis that includes data from the beginning of the Cold regime in 2006 and relays information about the Cold Pool dynamics. SSI data is then presented with regional SSI encompassing the Cold regime (2006-2013) and Warm regime (2014-2019) time period, and the local SSI time series matching each respective site's acoustical sampling time period. The SSI analysis demonstrates regional and local commonalities, differences, and how respective equilibriums changed after the regime shift. This is followed by the relationship of bottom temperature and SSI between the regimes. Acoustic backscatter results are then presented for site M5 for 2008- 2018 and site M8 for 2011- 2015 and linked with environmental results. Lastly, the predictive modelling results are presented for site M5, as it is the longer time series of the two sites analyzed.

3.1 Bottom Temperature

The bottom temperature seasonal cycle differed between the NBS (site M8) and CBS (site M5) sites. Historically, site M8 has been observed to reach a minimum in late December or January with the arrival of sea ice and remained < 1˚C until the beginning of fall, while the warmest M8 temperatures occurred during the fall from wind driven water column mixing. Site M5 bottom temperatures historically have been observed to reach a minimum later in February or March with warmest temperatures occurring in the fall (Stabeno et al., 2012). Monthly averages with recent increased Warm year bottom temperatures have resulted in a delayed minimum, with site M8 reaching its bottom temperature minimum during February, and site M5 reaching its minimum bottom temperature during March or April (Figure 19).

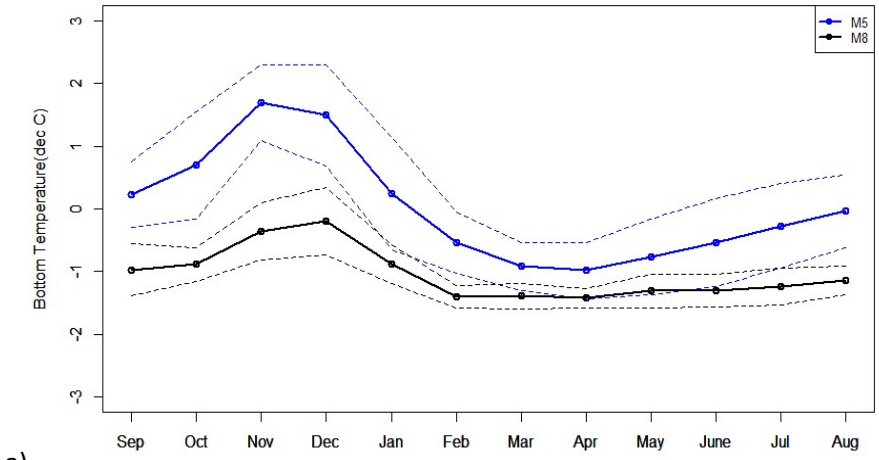

a)

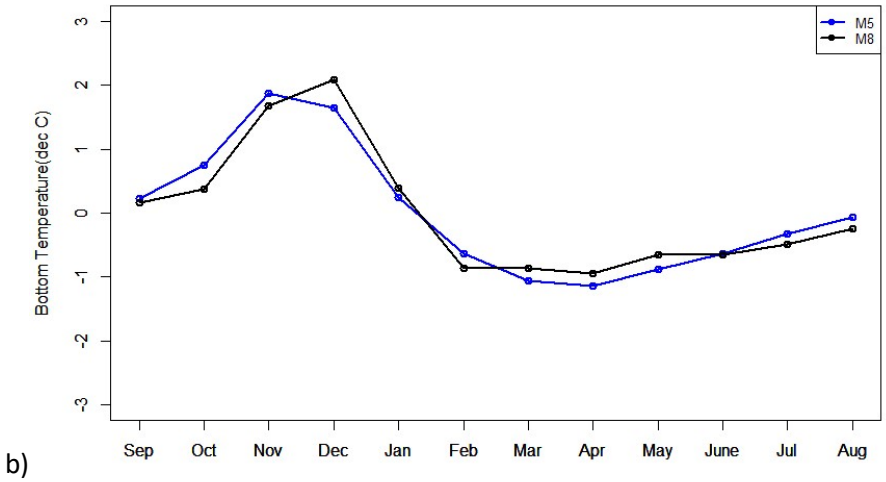

b)

Figure 19. Site M5 and M8 2005-2019 bottom temperature a) monthly averages and b) standardized monthly averages

Site M5 bottom temperatures were generally warmer than site M8, with M5 leading or warming faster and cooling later (Figure 20), which was expected as site M5 is farther south. Site M5 and M8 bottom temperature cross-correlation had a ϱ ~0.6 value but with high correlation due to the seasonal cycle. Cross-correlation results demonstrated lags between the two sites' peaks in both the Cold and Warm years (Figure 21).

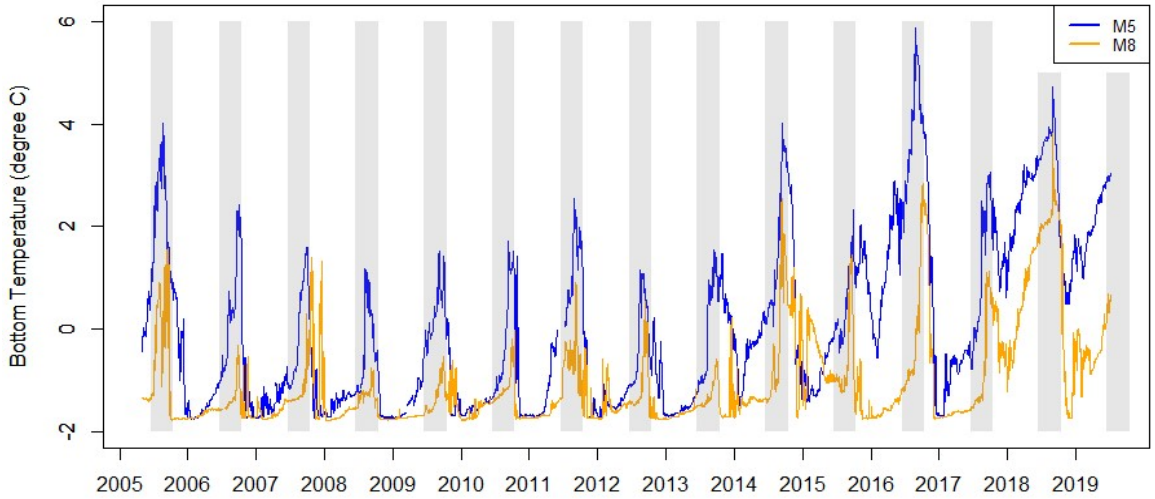

Figure 20. Site M5 and M8 bottom temperature with shaded regions September 1-December 31 annually.

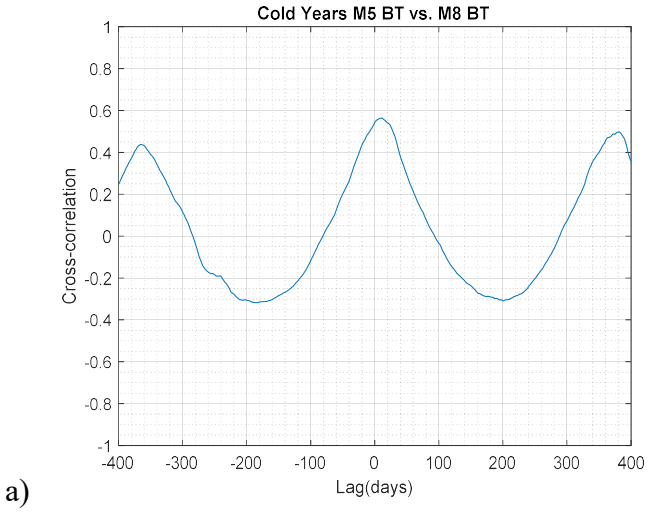

a)

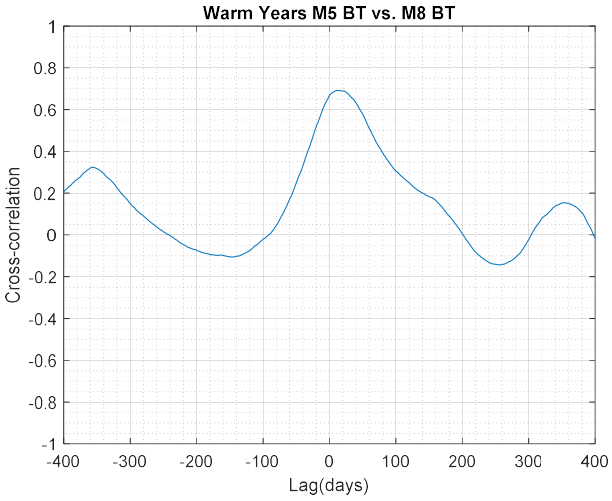

b)

Figure 21. Site M5 and M8 bottom temperature cross-correlation during a) Cold years (2006-2013) and b) Warm years (2014-2019).

Monthly averages of both sites varied between Cold and Warm years as well as between sites (Figure 22). The 95% CIs range and variance increased in Warm years for both sites (Figure 23). Magnitude of the site M8 Warm year fall-winter average trend was similar to the site M5 fall-winter Cold year average, with a large degree of overlap between site M8 Warm year and site M5 Cold year standardized variance values. The site M8 Warm year average trend suggests the NBS is starting to experience dynamics of the CBS during Cold years.

Site M5 monthly average anomalies were calculated in the Cold regime and in the Warm regime separately (Figure 24). The Cold year anomaly patterns were seasonally related and followed by a below average Warm regime year in 2014. The subsequent Warm years were observed to have high amplitude and more erratic seasonal patterns. Increasing bottom temperature variance with time has resulted in a greater range of monthly bottom temperature values and therefore less ability to confidently forecast bottom temperatures for both sites, but especially at site M5 (Figure 24).

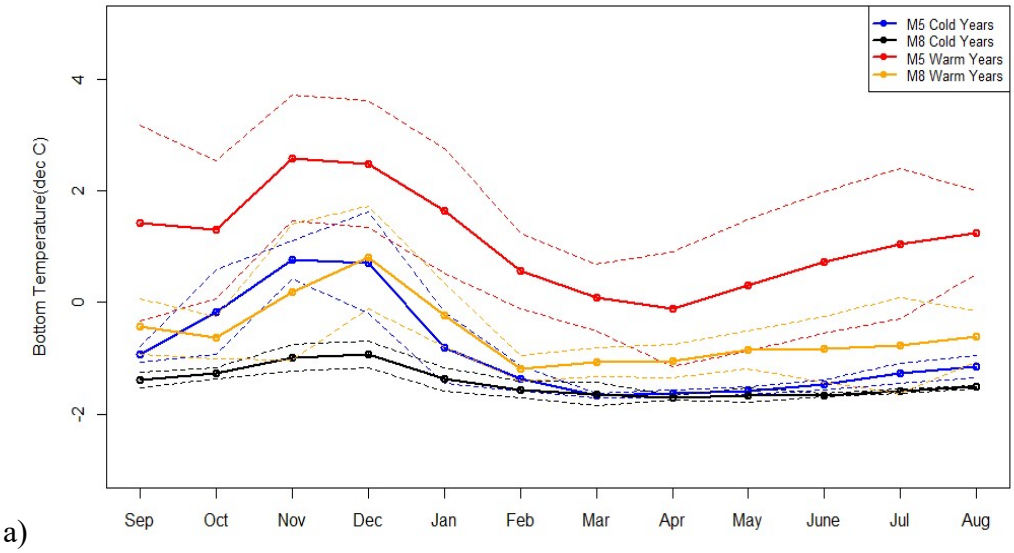

a)

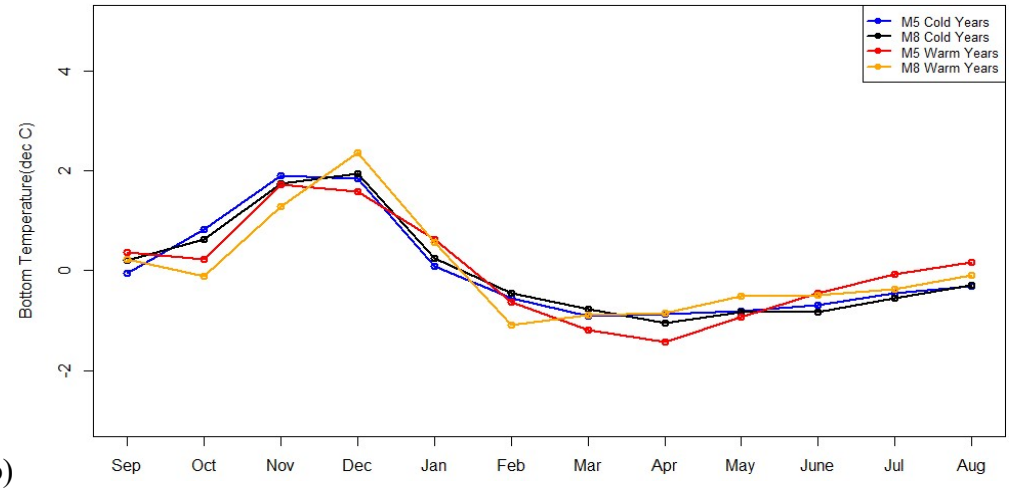

b)

Figure 22. Site M5 and M8 2005-2019 bottom temperature Cold and Warm year a) monthly averages with 95% CI, and b) standardized monthly averages

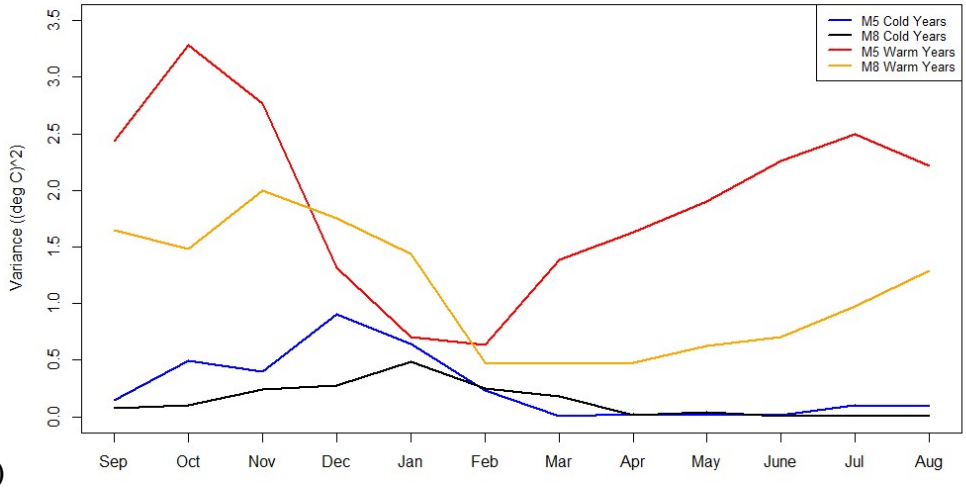

a)

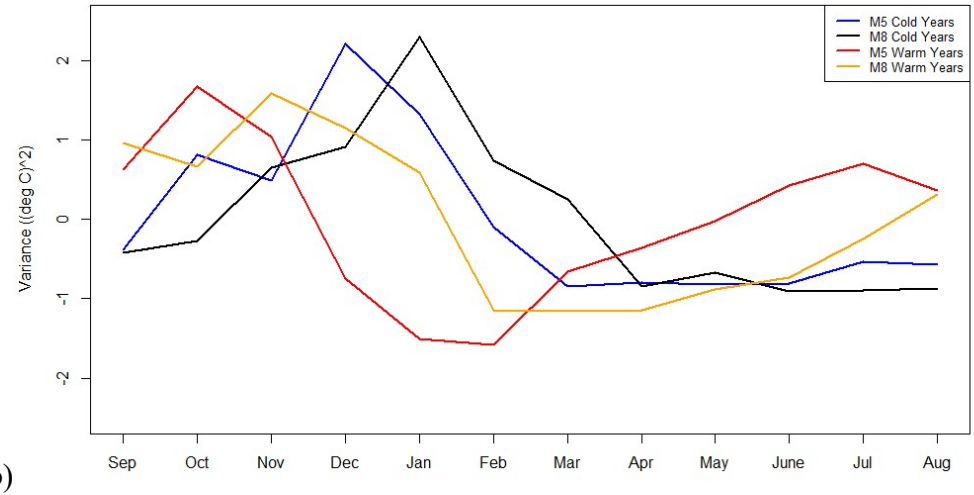

b)

Figure 23. Site M5 and M8 2005-2019 Cold and Warm year a) monthly variance and b) standardized monthly variance

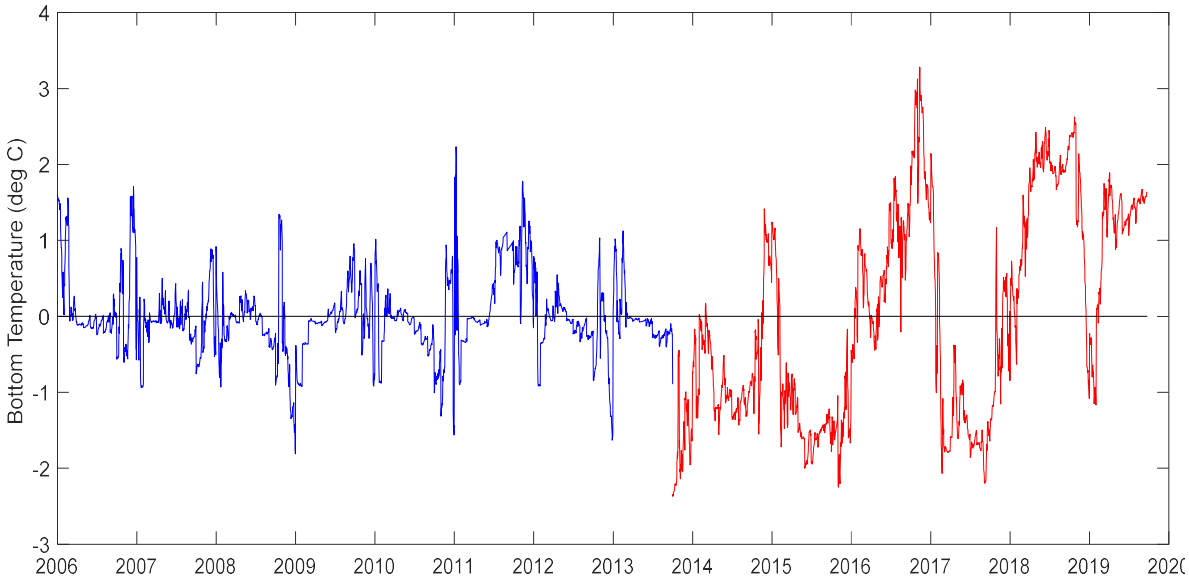

Figure 24. Site M5 bottom temperature monthly average anomalies during Cold years (2006-2013) and Warm years (2014-2020)

3.1.1 Cold Pool Variables

Summer bottom temperatures varied from -1.7 ˚C to 4˚C at site M5 and -1.7 ˚C to 2 ˚C at site M8 from 2006-2019 (Figure 25a and b, respectively). The Cold Pool was absent during 2018 at site M5 and present at site M8, but quickly dissipated at the end of the summer season (Figure 26). Cold Pool duration was consistent for all years during the summer season, or 91 days for the analysis period June 1- August 31 annually at site M8. Site M5 Cold Pool annual 91-day duration was consistent during Cold years for the summer season, except during 2011 with a decrease of ~16 days. Cold Pool duration at site M5 during Warm years was more variable with ~34 days and ~24 days in 2016 and 2019 respectively (Figure 27). As Warm year bottom temperature increased, so did Cold Pool duration variance at Site M5. Site M8 duration was not indicative of change in Warm years, but Cold Pool dissipation in the fall immediately after the summer season foreshadows changes in NBS Cold Pool dynamics within the current Warm regime.

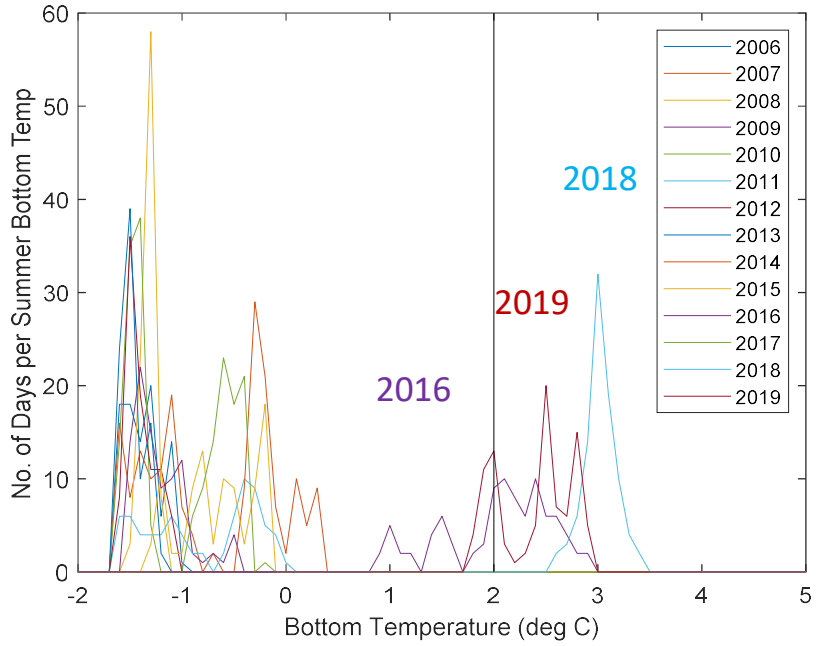

a)

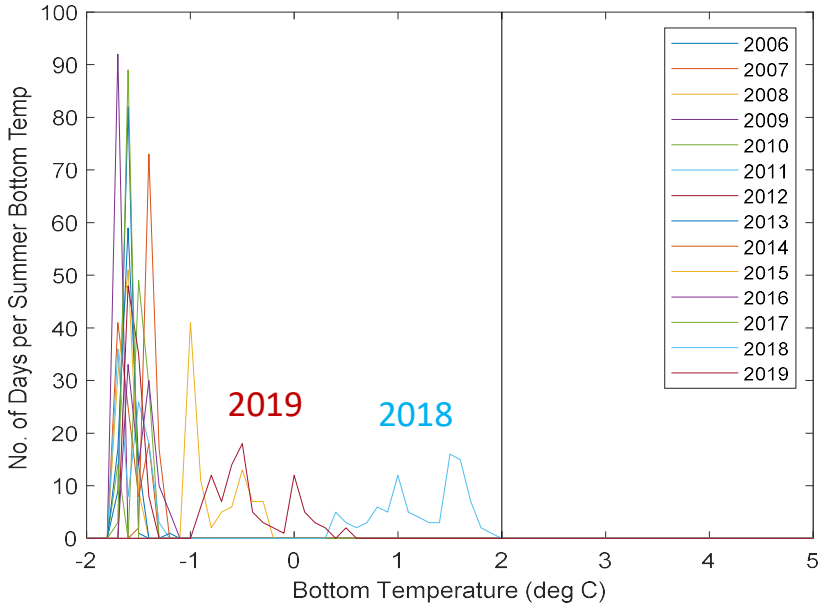

b)

Figure 25. Histogram of daily summer bottom temperatures (June 1-August 31) for a) site M5, and b) site M8

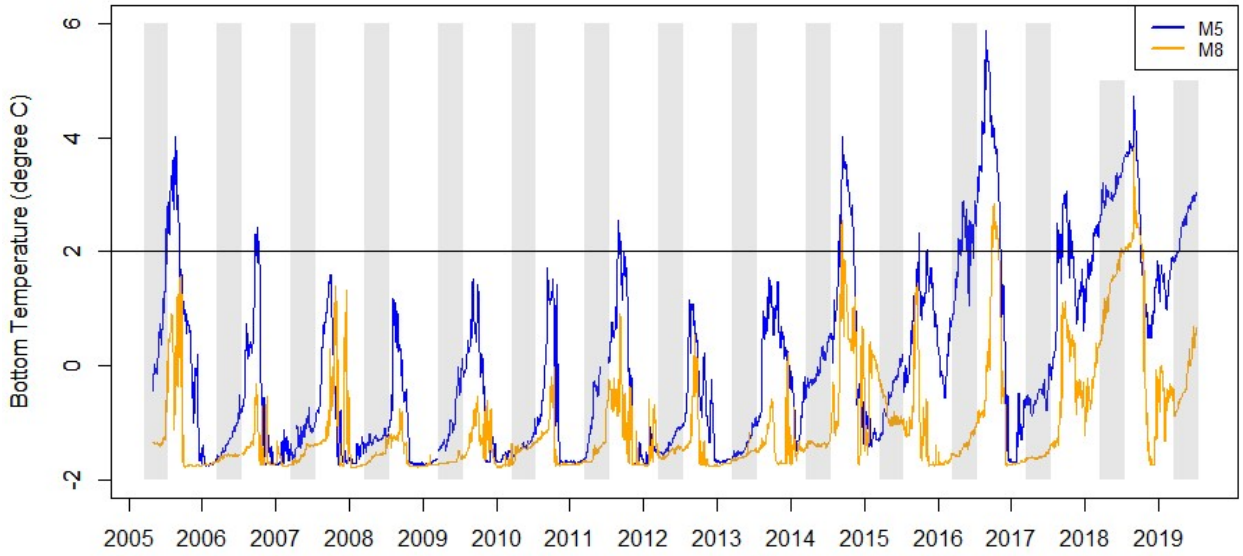

Figure 26. Bottom temperatures for site M5 and M8 with shaded regions during annual summer months with 2˚C Cold Pool threshold

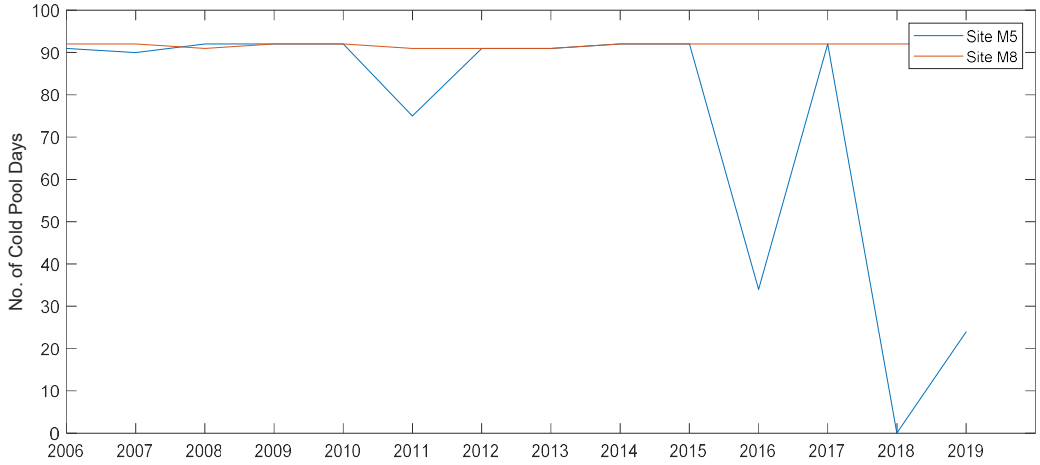

Figure 27. Site M5 and M8 annual duration of Cold Pool presence (< 2 ˚C bottom temperature)

Spring bottom temperatures ranged from -1.7 ˚C to 2.3 ˚C at site M5 and -1.7 ˚C to 1.3 ˚C at site M8 (Figure 28a & Figure 28b, respectively). Bottom temperatures reached their average minimum (-1.7 ˚C) when the water column was fully cooled by winter sea ice from March to the end of April. The number of days when the -1.7 ˚C threshold was met was variable at site M5 with an overall decreasing trend between Cold and Warm years (Figure 29), while the number of

days where the threshold was met was on average ~50 days at site M8, and matched annual decreasing trends with site M5, with a (<10) day duration in 2014, 2015, and 2019 (Figure 30). A decrease in the spring freezing temperature duration when the water column was fully cooled, was based on reduced ice extent leading to reduced available ice melt. Weak vertical stratification allows surface heating to penetrate near bottom depths during the summer which impacts Cold Pool presence and duration (Stabeno and Bell, 2018). Forecasted reduced sea ice and warmer bottom temperatures affect the integrity of Cold Pool bottom temperatures to sustain for the entirety of future summer seasons.

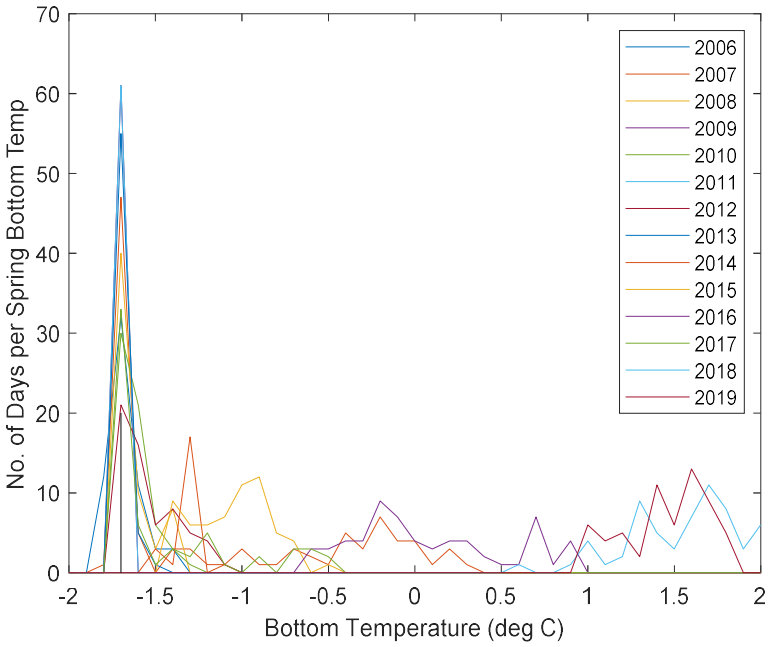

a)

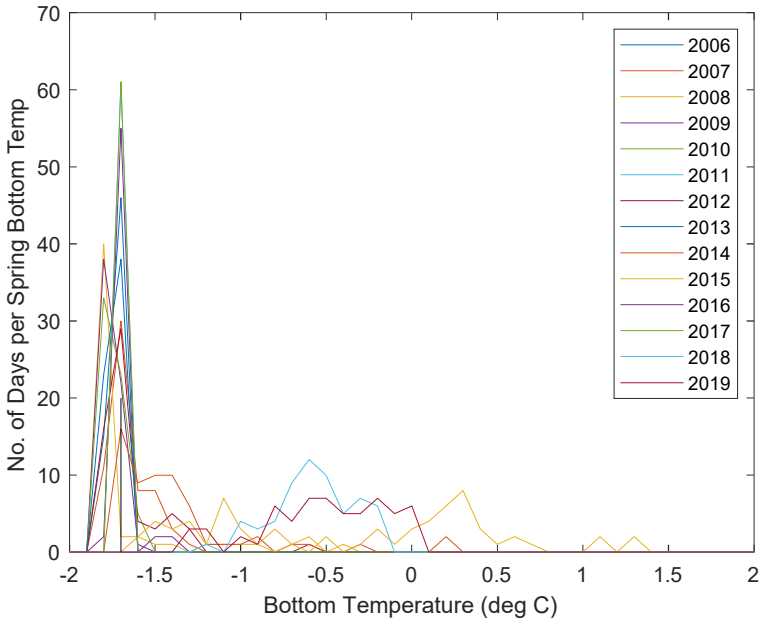

b)

Figure 28. Histogram of daily spring bottom temperatures (March-April 31) for a) site M5, and b) site M8

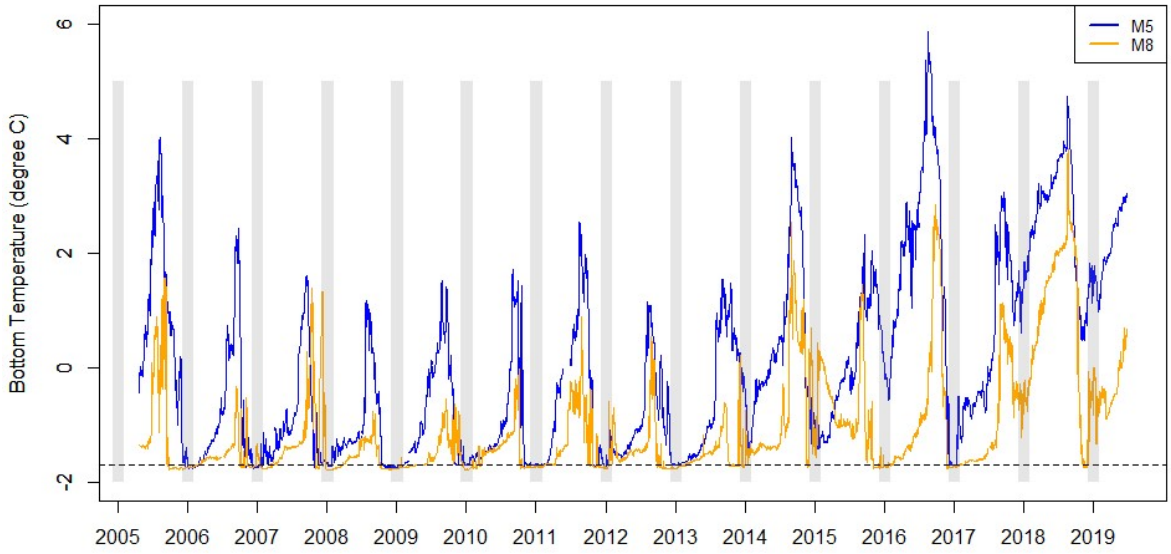

Figure 29. Bottom temperatures for site M5 and M8 with shaded regions during annual spring months with -1.7˚C freezing temperature threshold (dashed line)

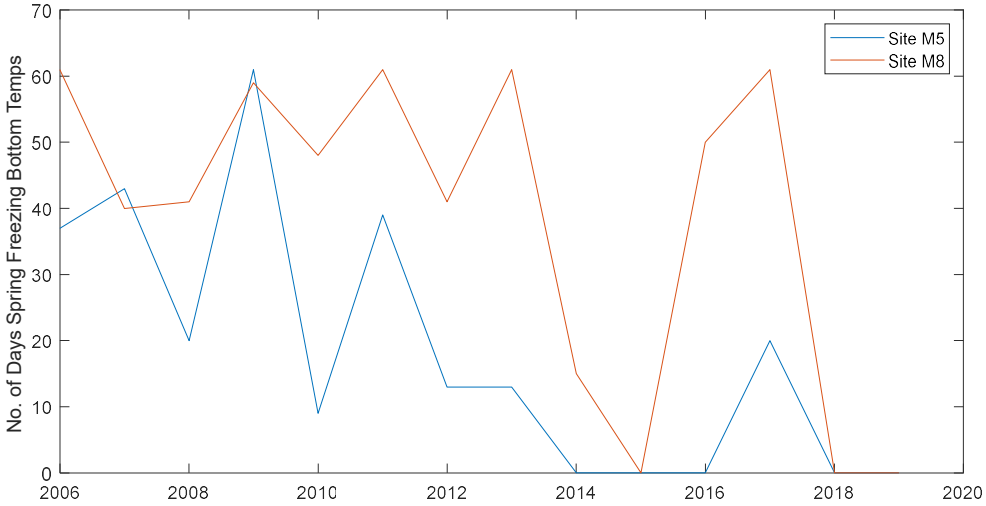

Figure 30. Site M5 and M8 annual duration of freezing bottom temperatures (≤ -1.7 ˚C)

3.2 Seasonal Sea Ice

There was interannual variability of sea ice within regimes (Figure 31), but there was a distinct difference in the average maximum area of sea ice coverage between Cold and Warm regimes (Figure 32a). The monthly regional SSI area average between Cold and Warm years

were non-overlapping except for late summer-fall when sea ice was absent. Bering Sea regional sea ice monthly anomalies were above the average during the last two years of the Cold regime and first three years during the Warm regime (Figure 33). Historically, varying interannual sea ice area maximums within a regime has shown no trend (Stabeno et al., 2019). Recent Warm year sea ice area maximums are representative of annual atmospheric forcing such as wind direction and ocean temperatures (Stabeno and Bell, 2018). Conditions that are conducive to lower ice concentrations caused by southerly winds appear more often during the Warm regime.

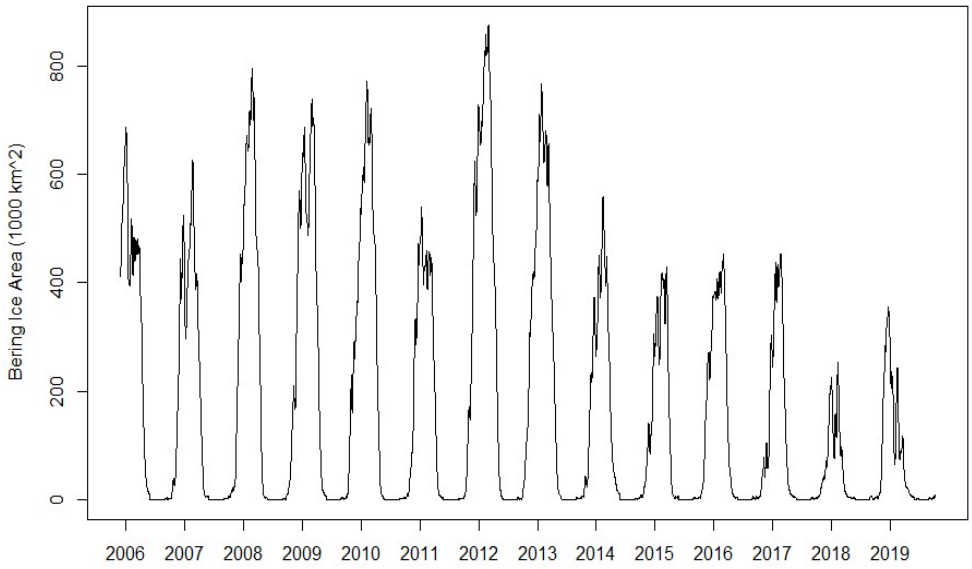

Figure 31. National Sea Ice Data Center (NSIDC) Bering Sea regional sea ice area

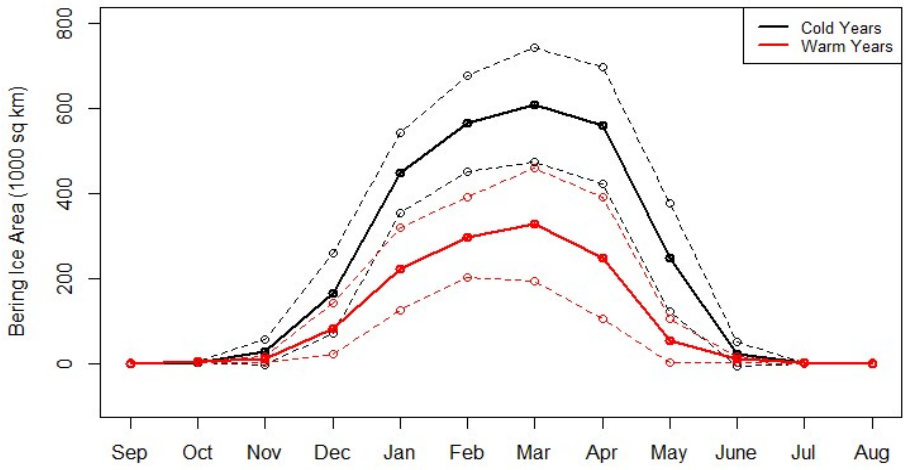

a)

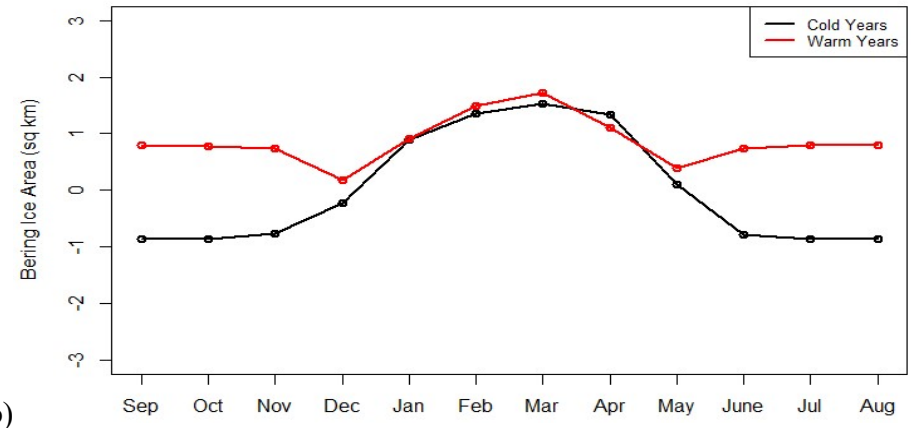

b)

Figure 32. 2006-2019 Bering Sea regional sea ice a) monthly averages, and b) standardized monthly averages

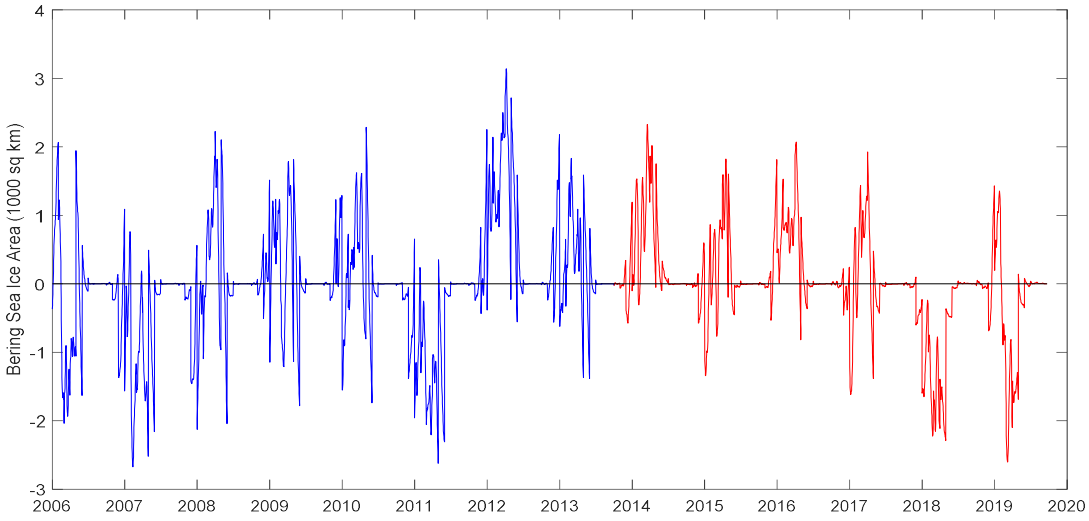

Figure 33. Bering Sea regional sea ice anomalies during Cold years (2006-2013) and Warm years (2014-2020)

Regional SSI area maximum varied annually, while local sea ice time series at each site varied annually in maximum percent cover and duration of coverage (Figure 34). Regional SSI led local sea ice in both Cold and Warm years by ~20 days (Figure 35). During the regime shift (Fall 2013-Spring 2014) regional and local sea ice dynamics changed at both sites. There was an increased rate of regional SSI regression, or a steeper decline of average values March - May from Cold years to Warm years (Figure 36), resulting in a decrease in maximum sea ice area in May between regimes, affecting the timing of the spring bloom. Regional SSI area >400,000 km^2 during May was indicative of above average ice area anomalies during Cold years (Figure 33). Bering Sea regional SSI area >400000 km^2 during May occurred in Cold years 2008- 2010 and 2012-2013, and no Warm years. Historically, spring local sea ice cover prior to full retreat was <20% as early as the end of April to as late as the beginning June at site M8, and at site M5 occurring as early as the end of March to as late as mid-May (Stabeno et al., 2019 and Stabeno et al., 2012, respectively). After fall 2013, both sites had local sea ice regress and coverage fell below 20% during May 2014 and 2015 with site M8 leading site M5 (Figure 34). The regime shift from Cold to Warm resulted in the reduction of regional sea ice maximum and local ice maximum percent cover duration in May. Timing of sea ice arrival and retreat directly impacts the ecosystem shelf-wide and locally as it is the basis for the environmental conditions for months to follow, especially in May which impacts the timing of the spring bloom.

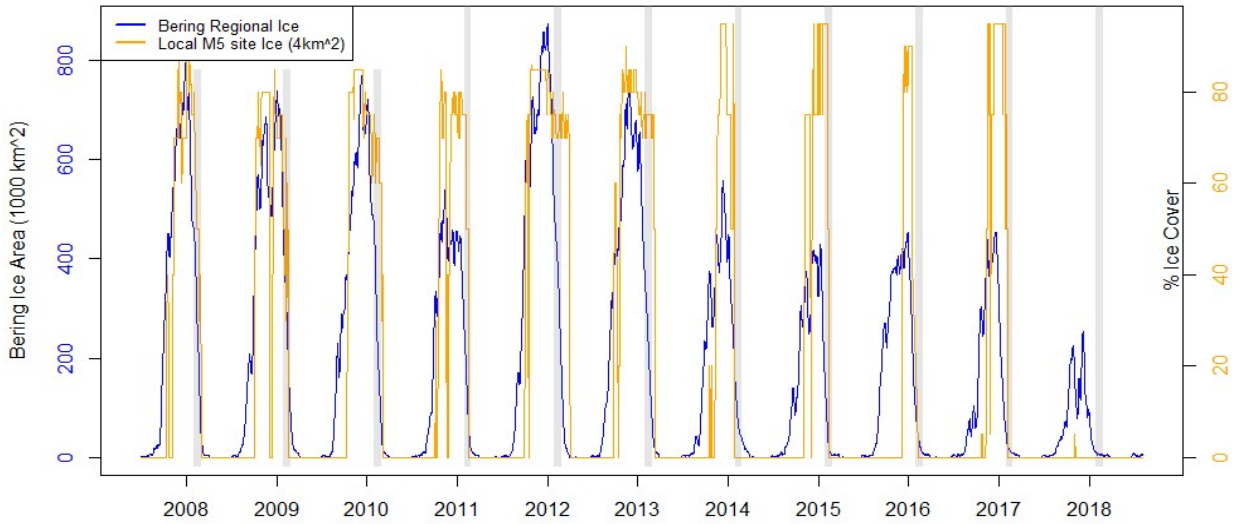

Figure 34. Regional seasonal sea ice area and local seasonal sea ice cover for site M5 with shaded regions annually during May

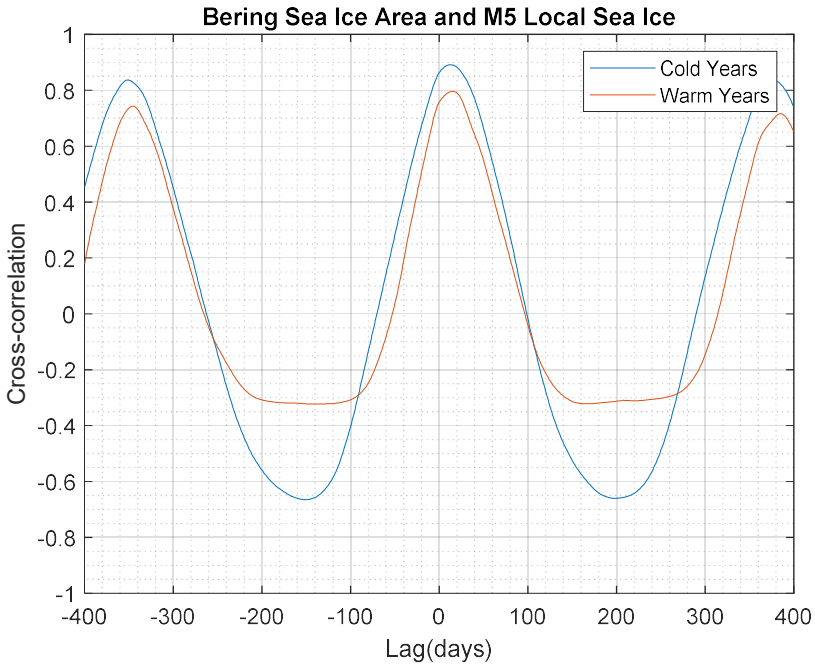

Figure 35. Bering Sea regional sea ice area and local M5 sea ice cover cross-correlation during Cold years (2007-2013) and Warm years (2014-2018)

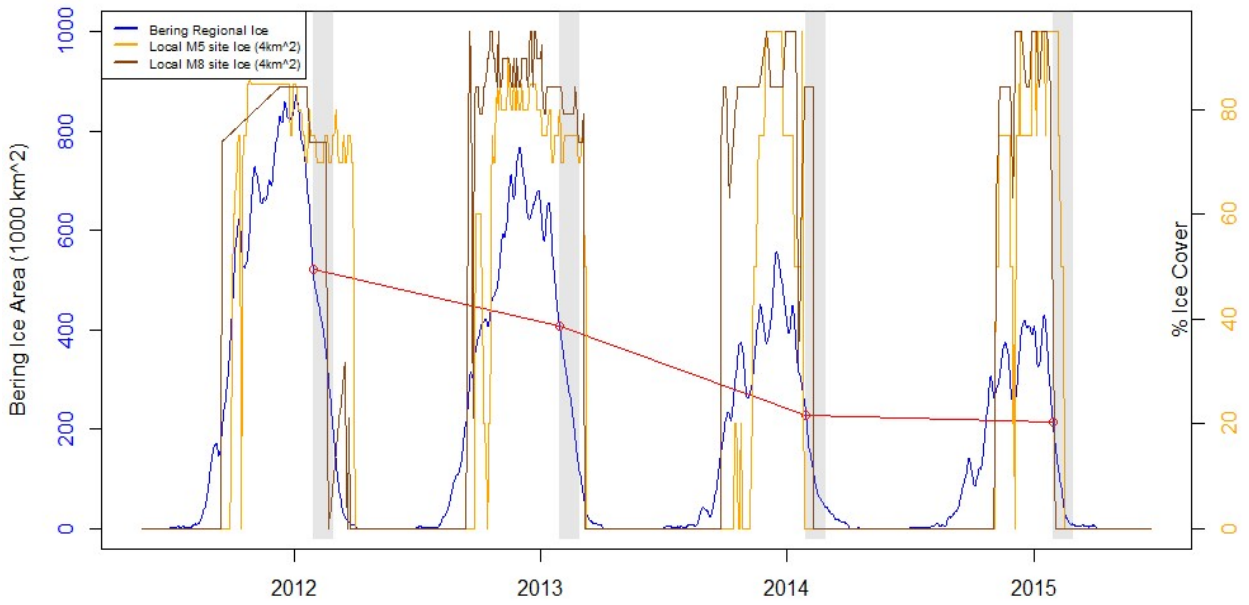

Figure 36. Bering Sea regional sea ice and site M5 and M8 local sea ice during regime shift (2013) with red line depicting the regional sea ice value on May 1 and shaded areas representing all of May

3.3 Bottom Temperature and Seasonal Sea Ice

Site M5 bottom temperature and regional sea ice cross-correlation exceeded the 95% CI during Cold years with a lag ~110 days, while Warm year cross-correlation did not exceed the 95% CI and decreased in lag to ~90 days, i.e. Cold year cross-correlations were significant while Warm years were not. Phase between bottom temperature and SSI at the annual frequency was strongly coupled with high squared coherence (0.96 for Cold years, 0.91 for Warm years) and used to calculate the seasonal lags. (Figure 37). The ~20 day lag decrease in Warm years was attributed to early sea ice retreat and increased bottom temperatures. Cross-correlations of site M5 bottom temperature and Bering Sea regional sea ice with seasonality removed (i.e. anomalies) were not significant in Warm or Cold years (Figure 38). Due to the cyclical nature of the data and interannual variation in leads/lags, phasing differences in bottom temperature and

sea ice time series occur. Thus, removing the seasonality was not useful in determining significant relationships.

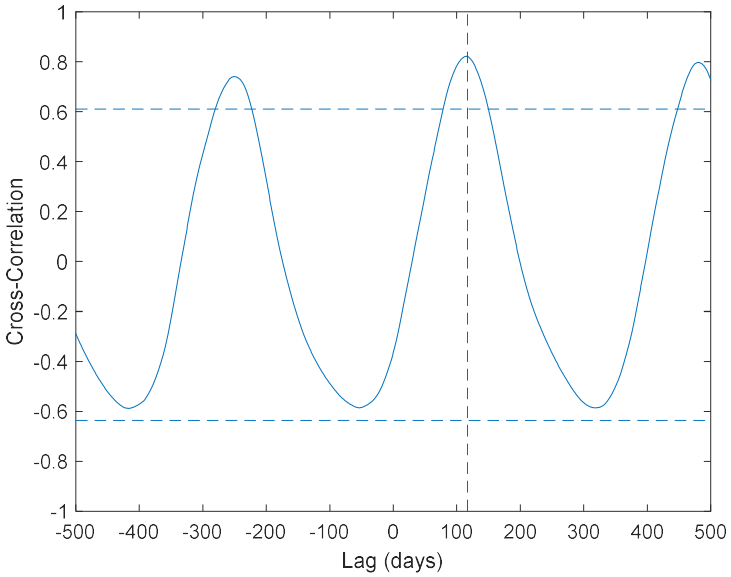

a)

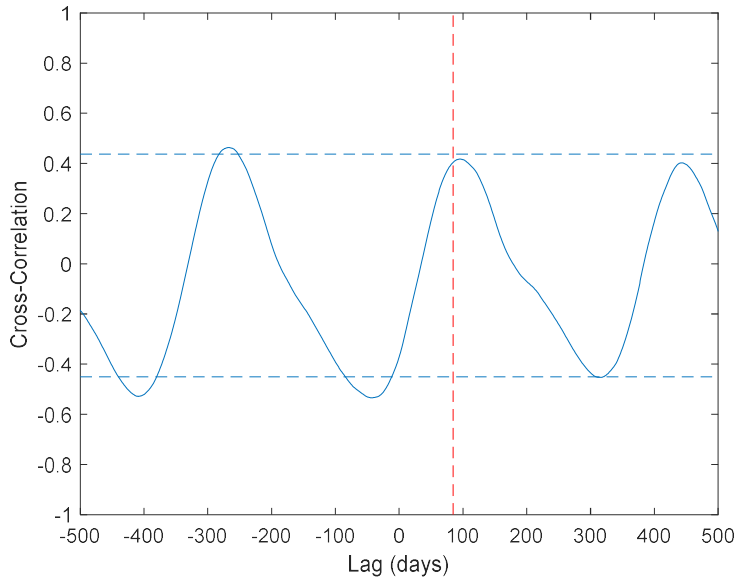

b)

Figure 37. Site M5 bottom temperature and Bering Sea regional sea ice area cross-correlation with dashed red line depicting lag and blue dashed lines depicting 95% CI during a) Cold years (2006-2013), and b) Warm years (2014-2019)

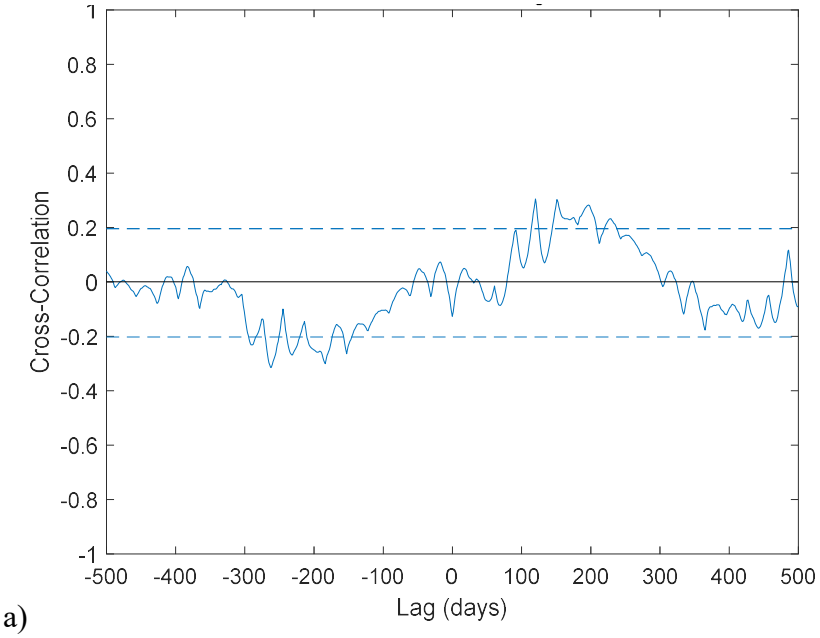

a)

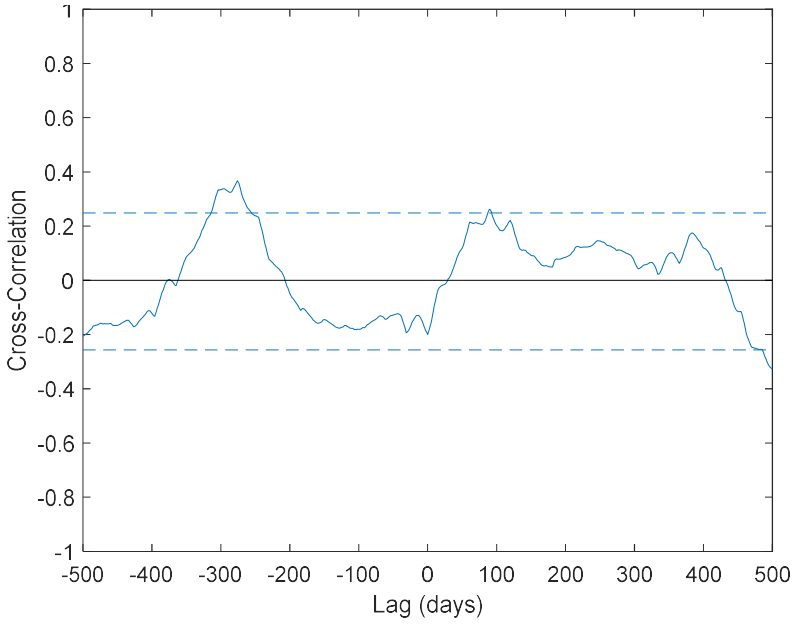

b)

Figure 38. Site M5 bottom temperature anomaly and Bering Sea regional sea ice area anomaly cross-correlation with blue dashed lines depicting 95% CI during a) Cold years (2006-2013), and b) Warm years (2014-2019)

3.4 Acoustic Backscatter

Site M5 and M8 acoustical metrics, daily 200 kHz ABC, 200 kHz Mean S_v, and 460-200 kHz Delta-S_v, varied seasonally, interannually, and between Cold and Warm years

(Figure 39). Both sites' Cold year Delta-S_v monthly averages exhibited similar patterns, while Warm year monthly average patterns were different between sites (Figure 40a). The monthly variance increased for both sites in Warm years with the highest variance during March at site M8 and April at site M5, and the lowest Warm year variance in April at site M8 and September at site M5 (Figure 40b).

ABC and Mean S_v values were ~ 2 orders of magnitude greater during Cold years when compared to Warm years, with the highest variability between the two during August and lowest variability during February (Figure 41). ABC values can be used to calculate the abundance of mono-scattering zooplankton groups, such as small scatterers-copepods and large scatterers-euphausiids, based on literature S_v values (Equation 4). Relative to one another, smaller or more negative dB values are associated with copepod S_v, while larger, more positive dB values are associated with euphausiid S_v (Figure 8). Using theoretical S_v scattering curves, results suggest smaller bodied crustacean zooplankton such as copepods dominate volume scattering in Warm years, resulting in decreased ABC values while larger bodied crustacean species such as euphausiids dominate volume scattering in Cold years, resulting in increased ABC values

Site M5 Mean S_v (Figure 39b) was 180˚ out of phase or exhibited a negative relationship with Delta-S_v (Figure 39c). Mean S_v value decreases indicated increases in small zooplankton species and occurred when positive Delta-S_v values increased and vice-versa. This study's results aligned with Stauffer et al.'s (2015) EBS 2009-2012 observations. For example, Figure 39b shows 2009 Mean S_v values ½ negative and ½ positive throughout the year where small zooplankton scatterers comprised ≥50% of the community. A small portion of negative Mean S_v values was observed in 2012 followed by the majority of the year consisting of positive values where <10% of small scatterers comprised the community.

The regime shift and seasonality are qualitatively depicted in the Mean S_v and Delta-S_v values. During the first cycle post-regime shift 2015, Delta-S_v values were positive throughout the year until late fall, whereas site M8 Delta-S_v values were observed at a higher amplitude than site M5. While this further supports the shift to increased abundance of smaller copepod species *Pseduocalanus spp* coupled with the environmental shift, it also suggests the average volume scattering strength varies regionally between sites for the same groups of scatterers (i.e. copepods). Thus, post-regime shift acoustical data indicates a decrease in overall abundance of animals per volume in the water column coupled with the shift from euphausiid dominant to copepod dominant communities.

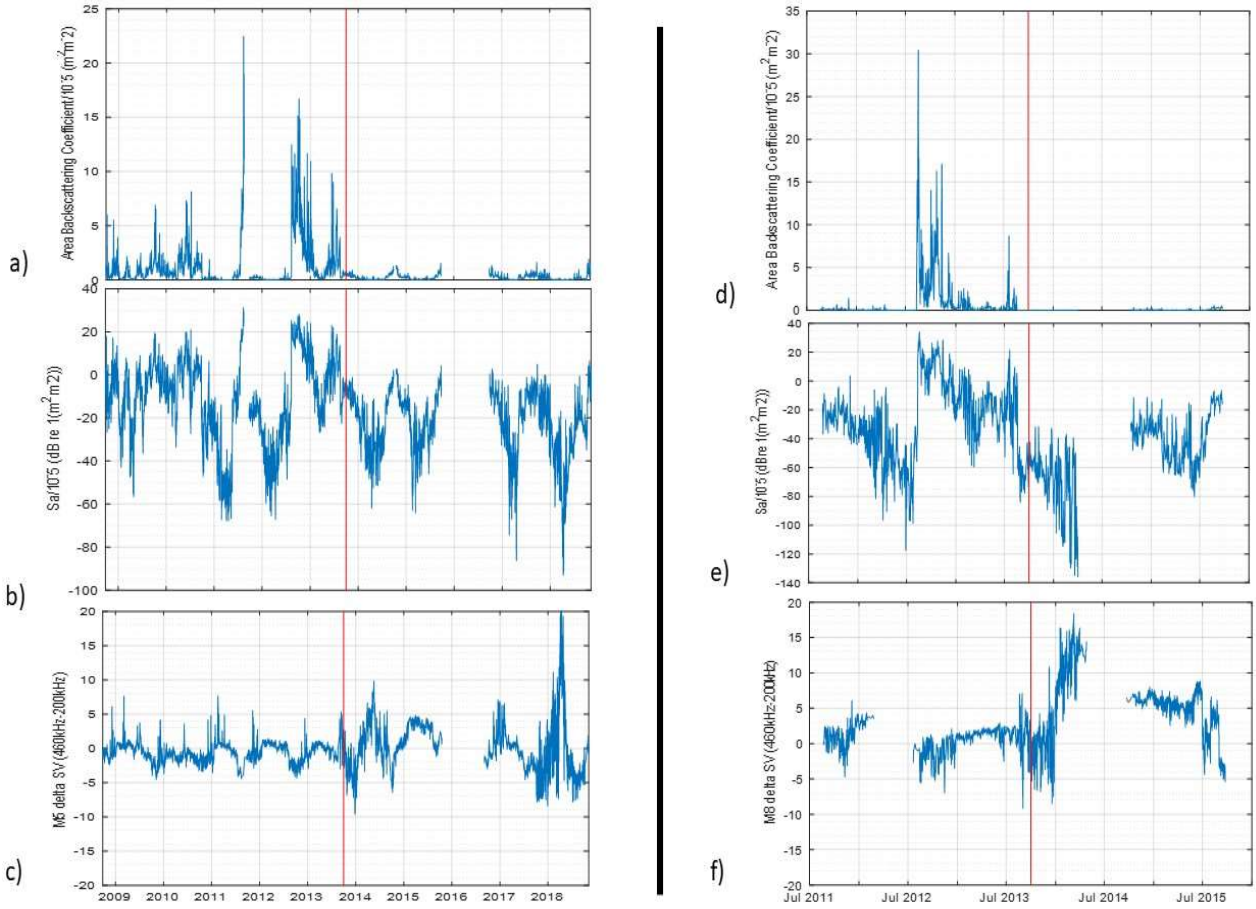

Figure 39. Site M5 daily time series 2008-Fall 2018 for a) 200 kHz ABC, b) 200 kHz Mean S_v, and c) Delta-S_v (460 kHz-200 kHz). Site M8 daily time series 2011-Fall 2015 for d) 200 kHz ABC, e) Mean S_v, and f) Delta-S_v (460 kHz-200 kHz). The red line depicts the Cold to Warm regime demarcation.

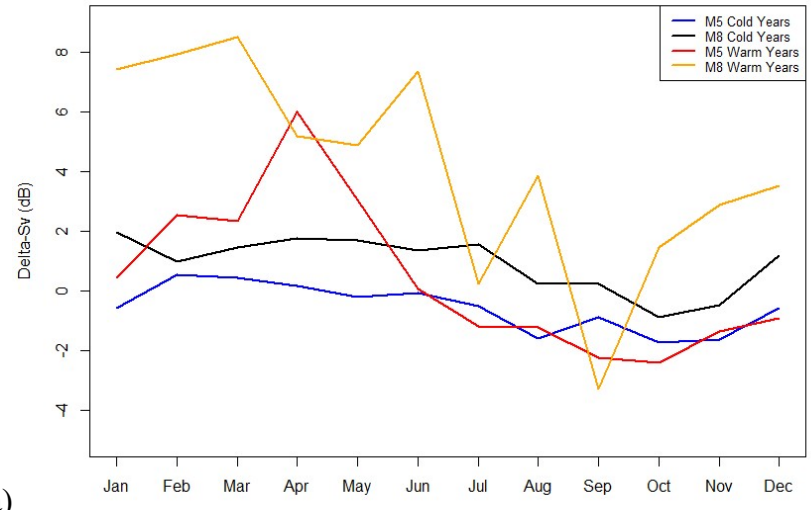

a)

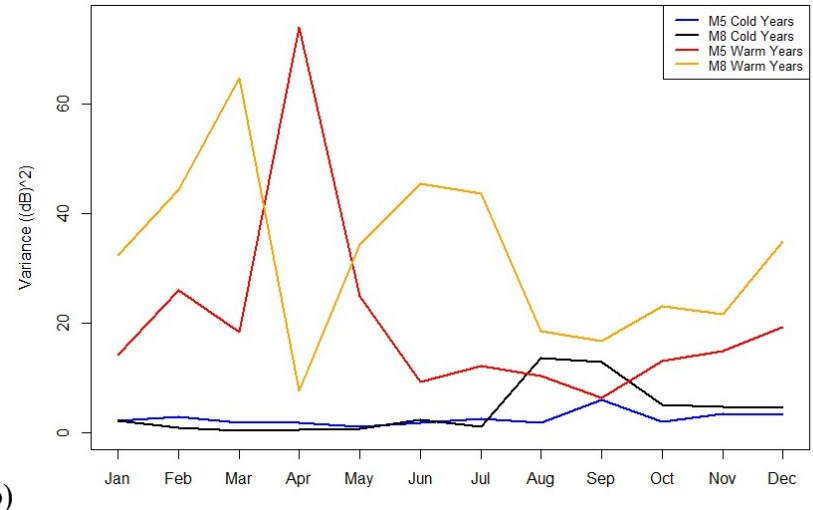

b)

Figure 40. Site M5 and M8 Cold Years (2008-2013 and 2011-2013, respectively) and site M5 and M8 Warm Years (2014-2018 and 2014-2015, respectively) Delta-S_v a) monthly averages, and b) monthly variances (σ^2)

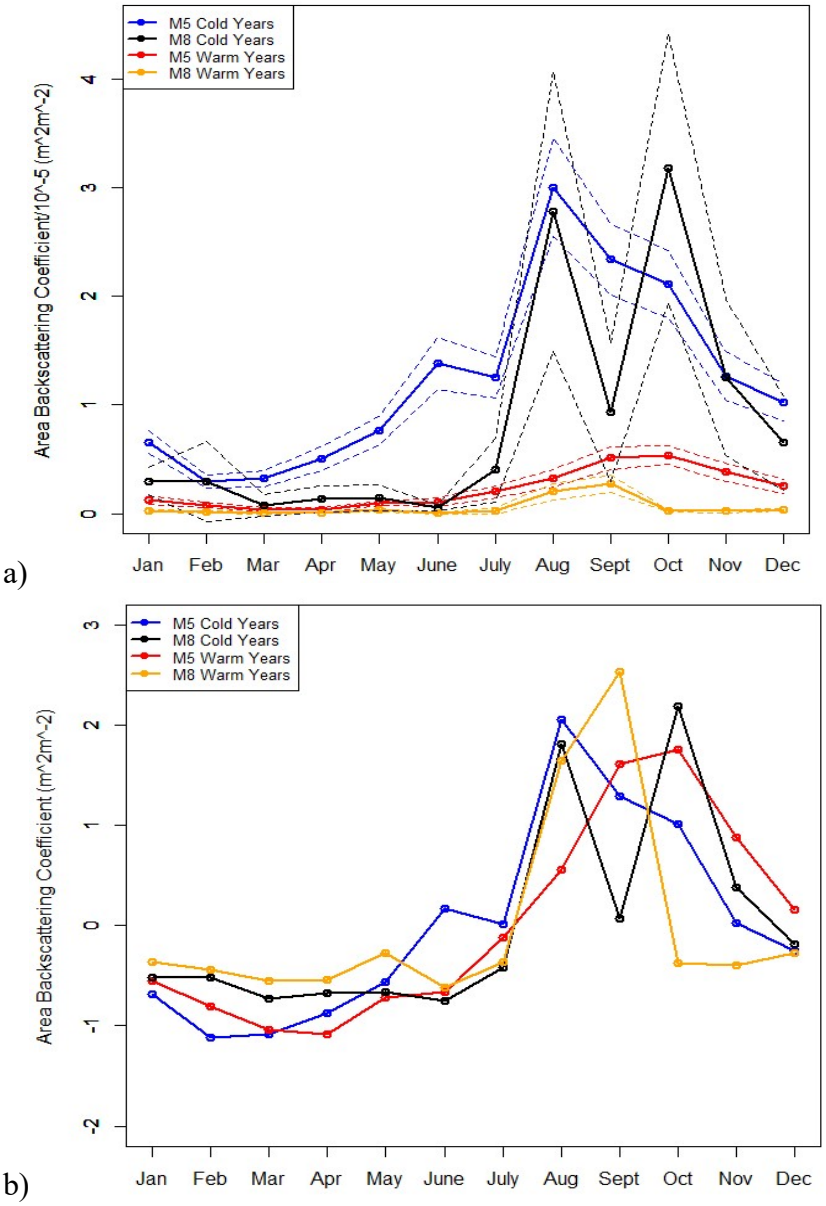

Figure 41. Site M5 (2008-2018) and M8 (2011-2015) Cold and Warm Year ABC a) monthly averages, and b) standardized monthly averages

Bottom temperature led acoustic backscatter annually or started increasing earlier, but acoustic backscatter reached annual maximum peaks faster, during Cold and Warm years. Increased temperature variability during Warm years was coupled with decreased backscatter abundance values for both sites (Figure 42). Detrended monthly Delta-S_v variance increased when bottom temperature detrended monthly variance decreased in Warm years, while Cold year

Delta-S_v and bottom temperature corresponded with little variance, suggesting Warm year average scattering strengths were not solely temperature related (Figure 43). Low frequency seasonal patterns were observed during Cold years with long cycles repeating annually each spring and fall in the Delta-S_v time series (Figure 39c). Backscatter seasonality is based on the range of conditions from the seasonal cycle from surface sea ice covering bottom temperatures reaching near freezing -1.7˚C to 4˚C in the spring. Seasonal acoustic variation is attributed to water properties (i.e. water temperature, salinity, acidity) and result in variation of absorption of sound in seawater as part of the transmission loss of sound from a source to a receiver (biological scatterer to echosounder). Warm year backscatter increased variance patterns suggest community wide changes occurred between Cold and Warm years that are not solely based on water property variance, but rather variation that is attributed to g and h physiological changes in the organisms themselves (i.e. lipid content), physical (i.e. size, length), or groups of community structure shifts (i.e. water column dominated by smaller bodied copepods vs. large copepods and euphausiids). Warm year acoustic backscatter amplitude increased in Warm years where the greatest amplitude spike occurred in 2018. The 2018 peak suggests a community change that was affected by the lack of the Cold Pool that acts functionally as a refuge from warmer higher trophic level predators, such as pollock, which may have increased predation rates. Site M5 200 kHz ABC was not qualitatively different in Warm years when the Cold Pool was present or absent, but Mean S_v and Delta-S_v were qualitatively different in Warm years when the duration of the Cold Pool presence was reduced or absent. Though Cold Pool variation has increased in the current Warm regime, the acoustic backscatter time record is too short to identify trends that may be lagged or delayed to more recent Warm years based on changing Cold Pool conditions.

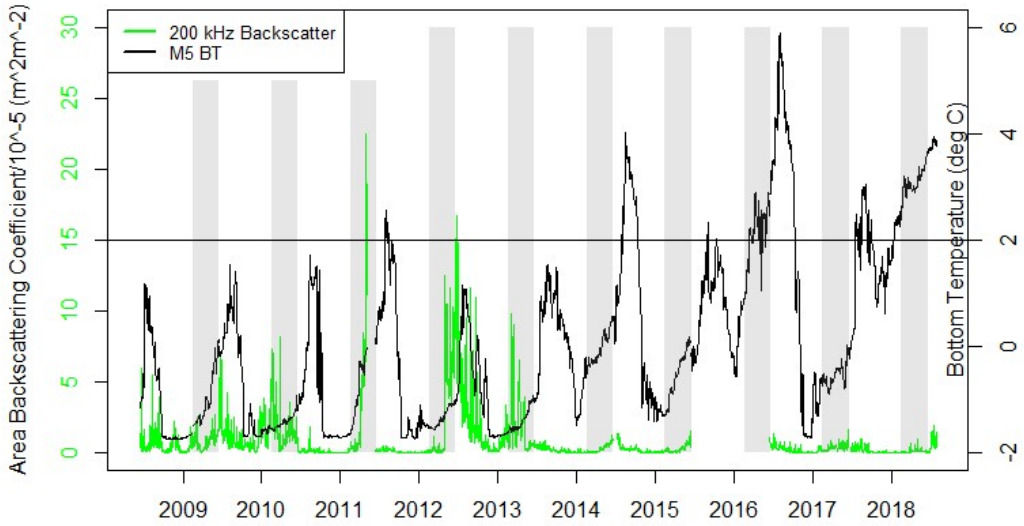

a)

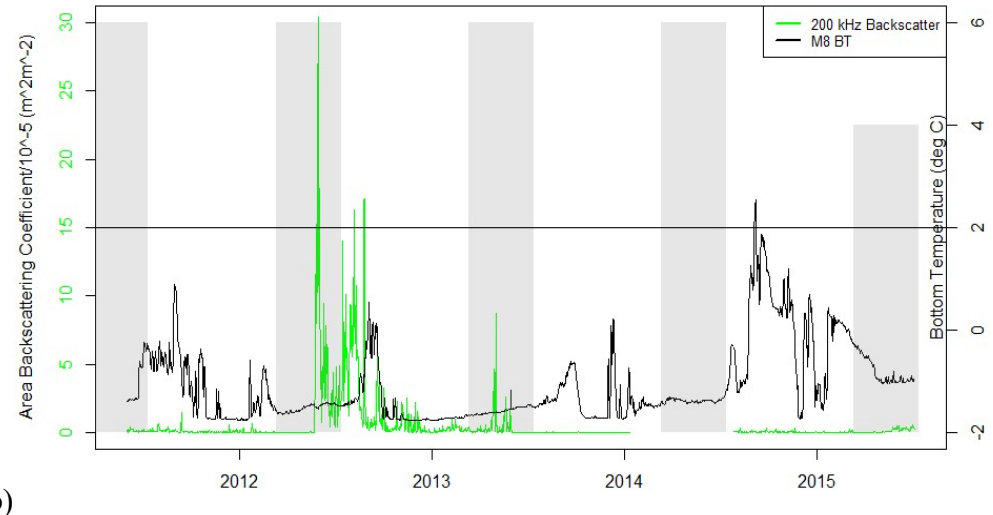

b)

Figure 42. 200 kHz ABC (green) and bottom temperature (black) with horizontal line depicting Cold Pool threshold (<2˚C) with annual shaded areas during summer months (June-October) at a) site M5 during 2008-2018 and b) site M8 during 2011-2015

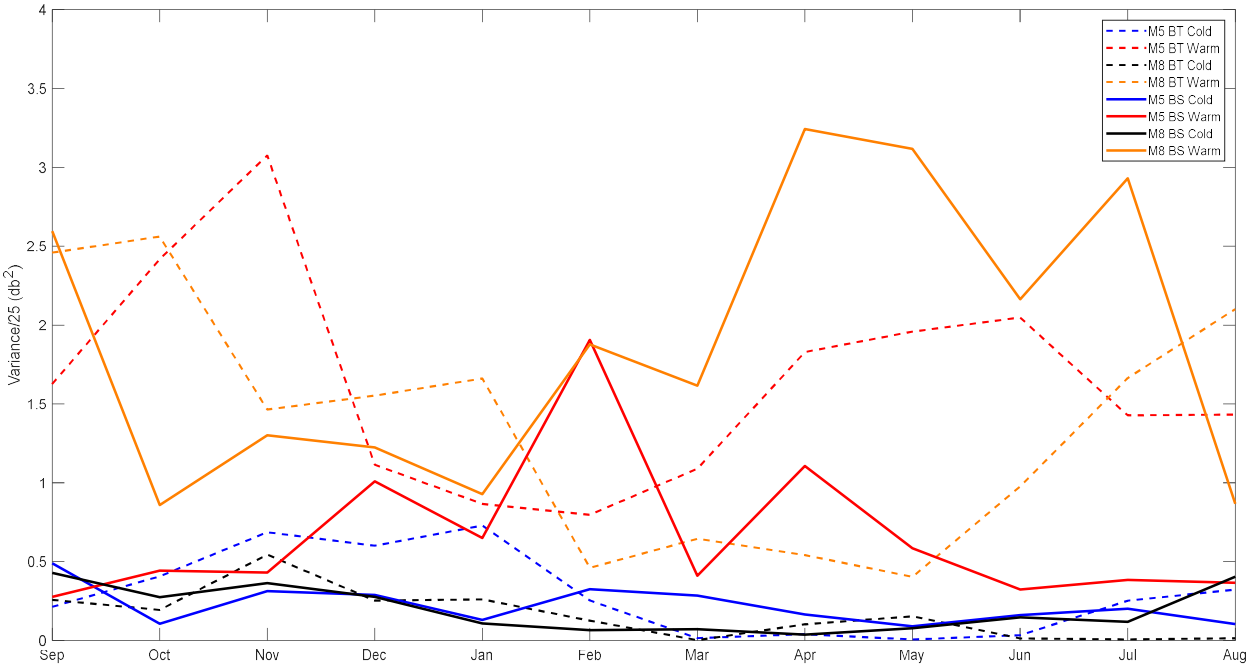

Figure 43. Site M5 (2008-2018) and M8 Delta-S_v (2011-2015) monthly variance (solid lines) and bottom temperature monthly variance (dashed lines)

Generally, CBS site M5 acoustic backscatter maximum peaks led bottom temperature maximum's followed by regional SSI then local SSI for Cold and Warm years (Figure 44). The NBS site M8, followed similar temporal patterns; however, there was less lag between regional and local SSI reaching peaks at M8 (Figure 45). Acoustic backscatter increased earlier and reached annual maximum peaks before regional SSI area during Cold and Warm years, with a decrease in average maximum sea ice area during Warm years coupled with relatively small backscatter values indicative of a decrease in abundance for both sites (Figure 46). Monthly averages decreased in 200 kHz ABC, increased in bottom temperature, and decreased in regional SSI during all months (Figure 47), and the annual seasonal peak was delayed, in Cold years when compared to Warm years. In general, fall bloom abundances were greater than spring blooms abundances, with a slower rate of increased backscatter observed during Warm year summer months for both sites. Site M5's largest bloom occurred in 2011 (2008-2018) while site

M8's largest occurred in 2012 (2011-2015). Site M8 daily 200 kHz ABC overall was less variable than at site M5, with minimal to no ABC for the duration (2011-2015) except during the 2012 fall bloom and 2013 spring bloom (Figure 39d). Site M5 and M8 maximum 200 kHz blooms aligned when sampling time overlapped (fall 2011- fall 2015), with the greatest peak in the fall 2012 followed by the second largest for spring 2013 (Figure 48). The sites therefore are observed to be linked with the documented increased nutrient and phytoplankton biomass that occurred in the summer 2012 following the coldest year with the most extensive SSI within the Cold regime (Stauffer et al., 2015, Danielson et al., 2017) (Figure 49). SSI maximum area are indicative of annual shelf conditions for primary producer blooms and higher predatory zooplankton group dynamics (Stabeno et al., 2019). Average maximum SSI extent during Warm years were coupled with reduced zooplankton blooms observed in the acoustic backscatter that are indicative of phenology challenges during the regime. Temporally, the regional SSI retreat increased quickly during April and May, while backscatter abundance quickly decreased during the late summer months July and August (Figure 50). The lag between the bottom temperature and regional sea ice reaching their maximum peak decreased, and was more synchronous, from Cold to Warm years for both sites during 2014 (Figure 51). Bottom temperature bimodal peaks were observed for site M5 (2016-2018) and site M8 (2015), while regional SSI area maximum variability increased during sea ice "peak time." Thus, backscatter abundance is being affected in the spring based on phytoplankton ice edge and the summer open water bloom timing after SSI retreat. Increased frequency of bimodal maximum peaks and instability of bottom temperature and SSI during Warm years are indicative of match-mismatched temporal cues throughout the food web that are essential for survival, maturation, diapause, and reproduction success.

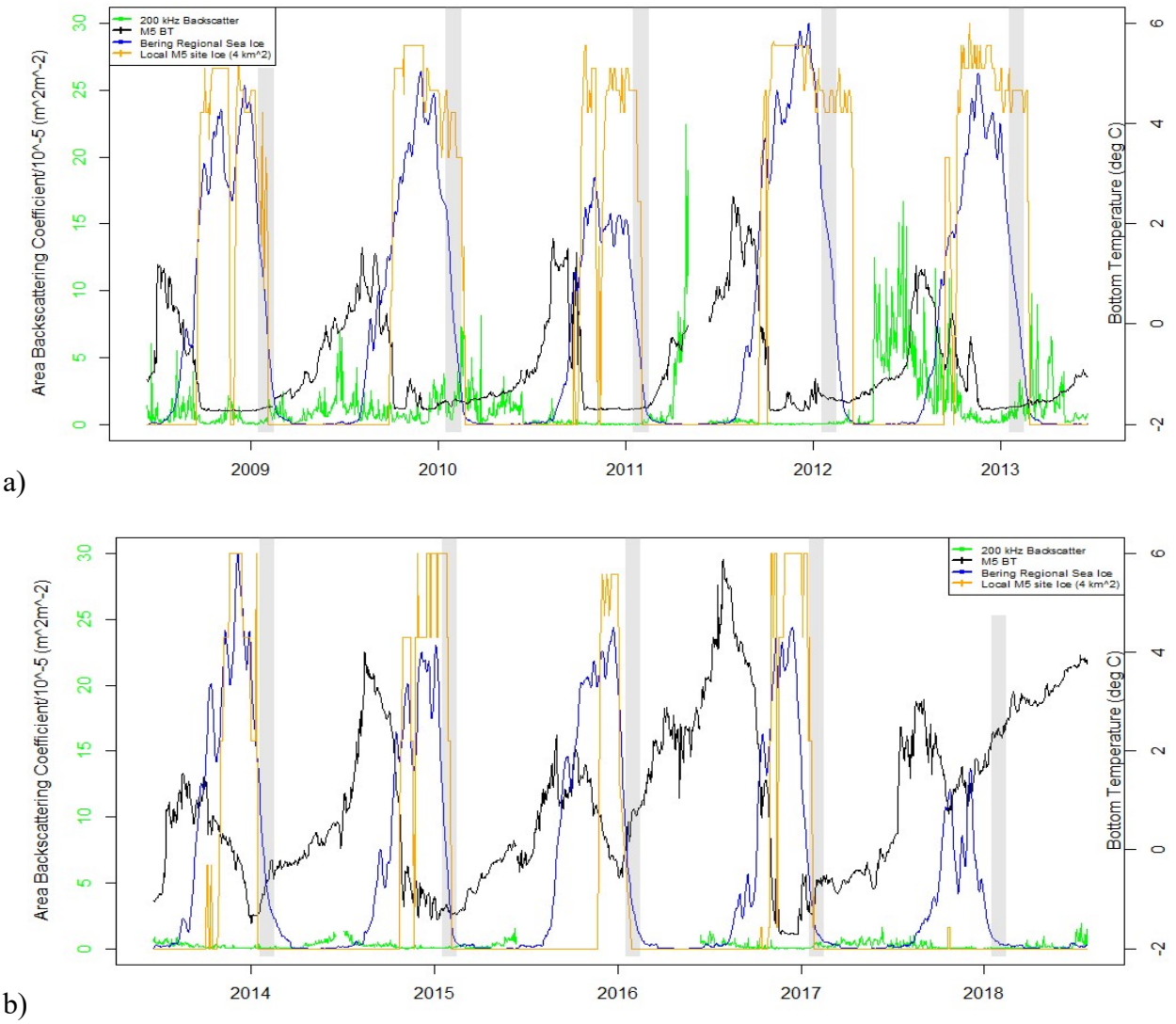

Figure 44. Site M5 200 kHz ABC (green), bottom temperature (black), Bering Sea regional sea ice (blue), and local sea ice (orange) with shaded areas during May, during a) Cold years (2008-2013) and b) Warm years (2014-2018)

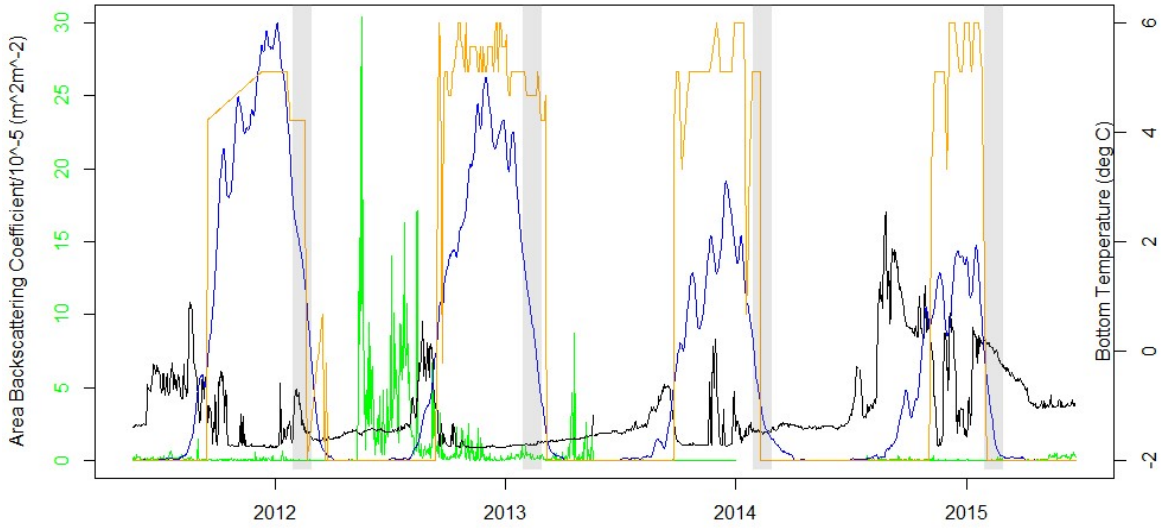

Figure 45. Site M8 200 kHz ABC (green), bottom temperature (black), Bering Sea regional sea ice (blue), and local sea ice (orange) during Cold years (2011-2013) and Warm years (2014-2015) with shaded areas during May

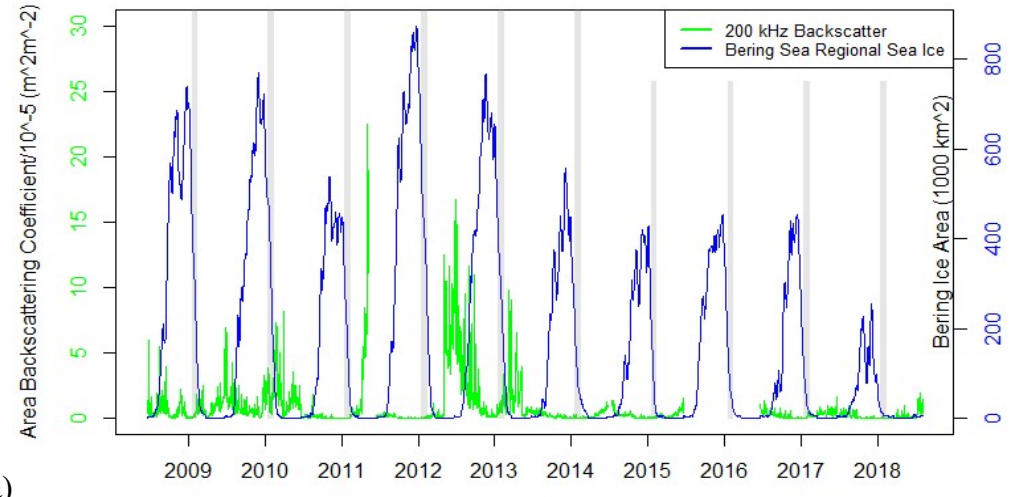

a)

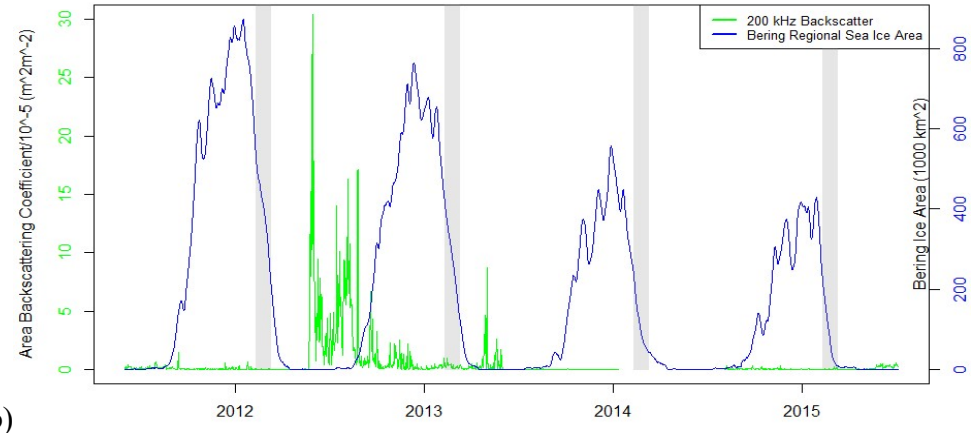

b)

Figure 46. 200 kHz ABC (green) and regional SSI area (blue) with annual shaded areas during May for a) site M5 during 2008-2018, and b) site M8 during 2011-2015

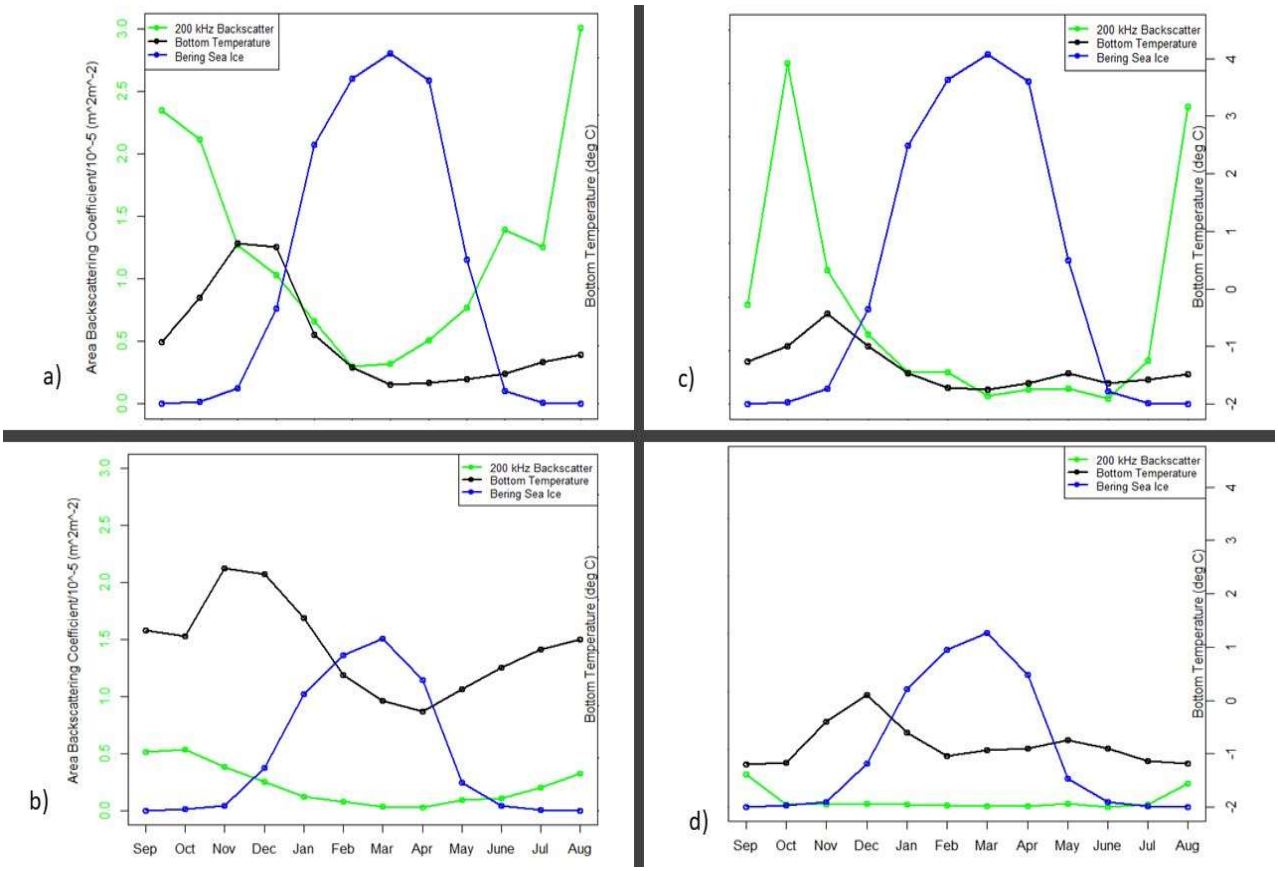

Figure 47. Monthly average plots for 200 kHz ABC (green), bottom temperature (black), and Bering Sea regional sea ice (blue) for a) site M5 during Cold years (2008-2013), b) site M5 during Warm years (2014-2018), c) site M8 during Cold years (2011-2013), and d) site M8 during Warm years (2014-2015)

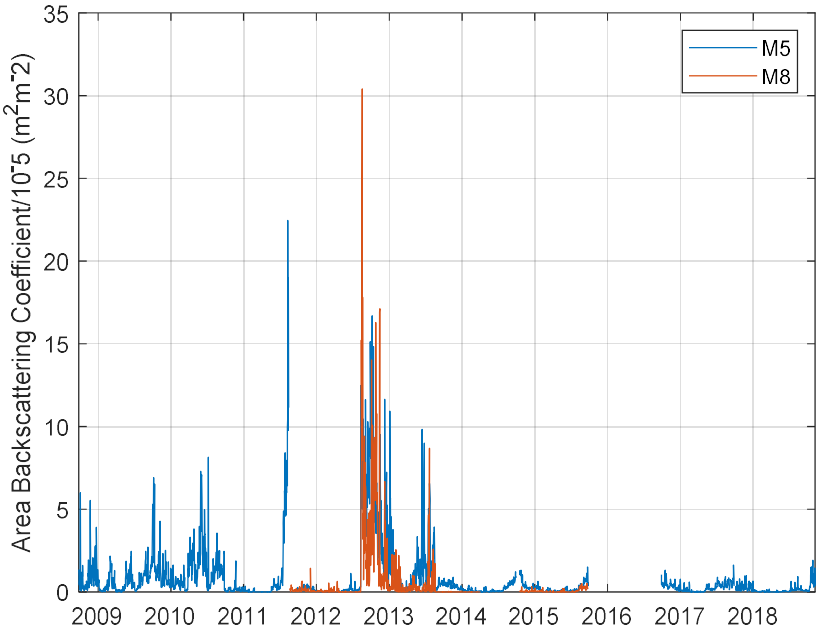

Figure 48. Site M5 (Fall 2008- Fall 2018) and M8 (Fall 2011- Fall 2015) 200 kHz ABC time series

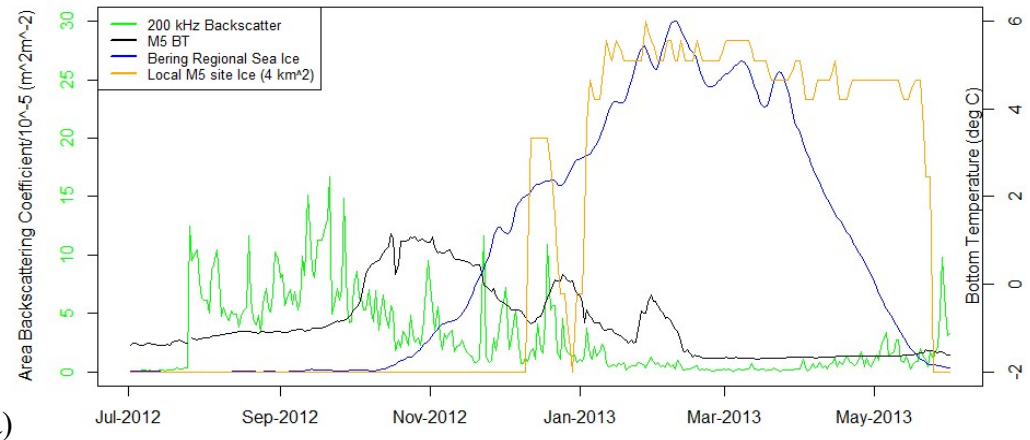

a)

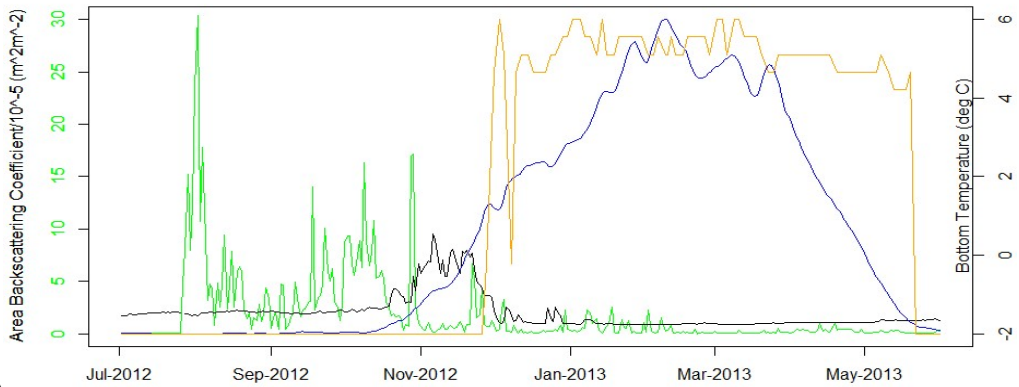

b)

Figure 49. 200 kHz ABC (green), bottom temperature (black), Bering regional sea ice (blue), and local sea ice (orange) prior to the fall 2013 regime shift for a) site M5, and b) site M8

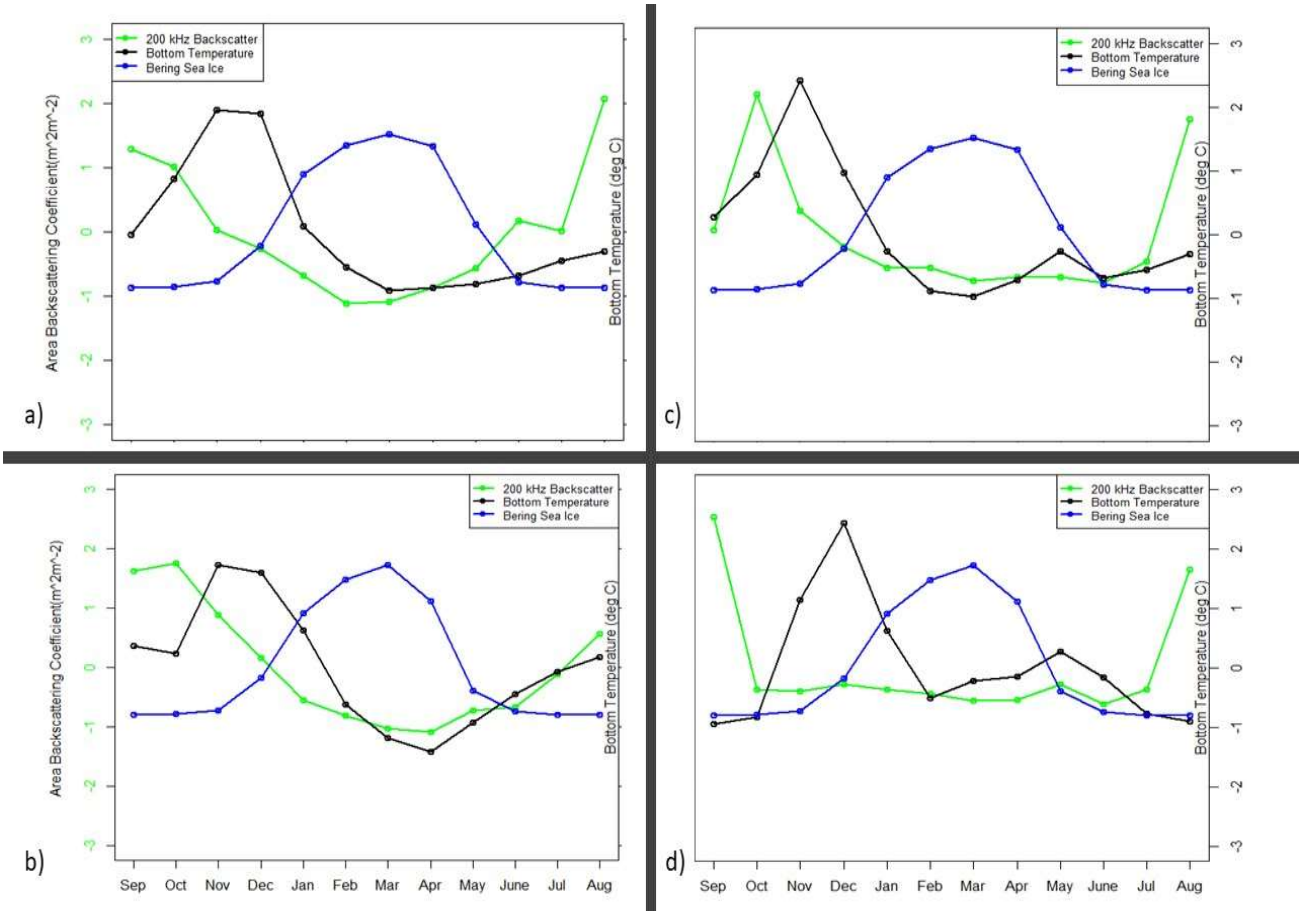

Figure 50. Standardized monthly average plots for 200 kHz ABC (green), bottom temperature (black), and Bering Sea regional sea ice (blue) for a) site M5 during Cold years (2008-2013), b) site M5 during Warm years (2014-2018), c) site M8 during Cold years (2011-2013), and d) site M8 during Warm years (2014-2015)

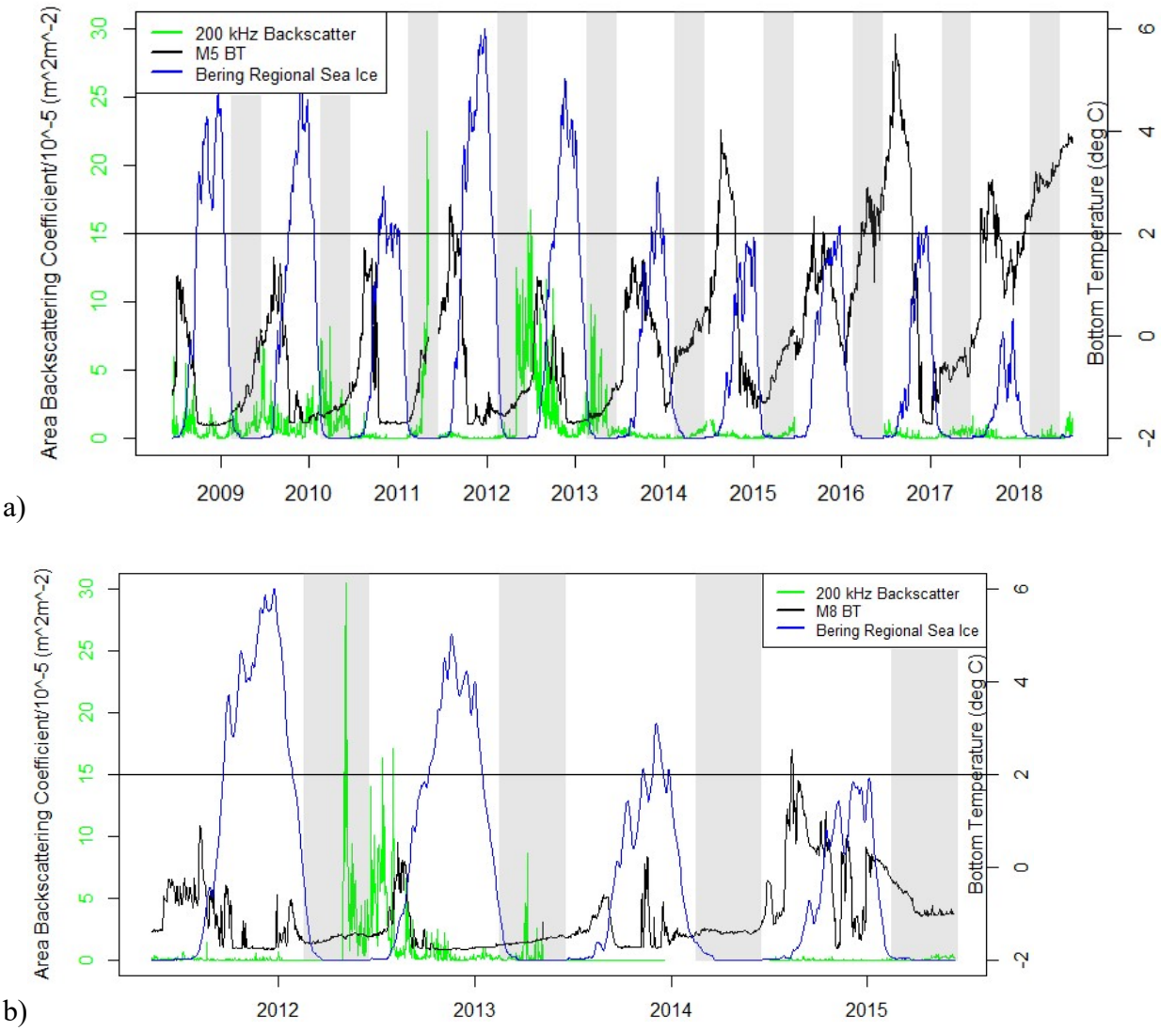

Figure 51. 200 kHz ABC (green), bottom temperature (black), Bering Sea regional sea ice (blue) with horizontal black line depicting Cold Pool threshold (<2˚C) and shaded areas during summer months for a) site M5 (2008-2018), and for b) site M8 (2011-2015)

3.5 Predictive Models

Multiple GAMs were used to evaluate the importance of Cold Pool variables in predicting acoustic backscatter as a proxy for zooplankton abundance. The predictive models were divided by Cold and Warm regimes for site M5. Due to the nature of the 2013 bloom the GAMs were not capable of predicting the 2013 anomalous regime shift year, and therefore not used in the Cold regime or Warm regime models. Acoustic ABC values were logarithmically

transformed and multiplied by a constant to approximate normally distributed model residuals. Regional SSI values were orders of magnitude larger than the other variables, and therefore logarithmic transformed to allow for better Cold regime model convergence. Transformed ABC values varied inversely with bottom temperature (negative relationship) and directly with regional seasonal sea ice (positive relationship). Local seasonal sea ice was collinear with the fraction of a year (*fracyear*) variable and therefore not used in the models. A cyclical cubic regression spline was needed to account for the zooplankton abundance seasonal nonlinearity. Interactions between 1) bottom temperature and Cold Pool presence, 2) spring freezing temperature presence and regional SSI, and 3) bottom temperature and regional SSI was expected. Examinations of these interactions were used with bivariate smooths and tensor products in the full models. The full (best) model equations for the Cold (Equation 9) and Warm (Equation 10) years were:

a) $$\log_{10}(10^6 ABC) \sim s(fracyear, bs = \text{c}) + s(Bottom\ Temp) + s(Regional\ SSI) + s(Bottom\ Temp, by = Pres\ Cold\ Pool) + s(Regional\ SSI, by = Freezing\ Temp) + ti(fracyear, Bottom\ Temp) + ti(fracyear, \log_{10} Regional\ SSI) + ti(Bottom\ Temp, Regional\ SSI)$$ Equation 9

b) $$\log_{10}(10^6 ABC) \sim s(fracyear, bs = \text{c}) + s(Bottom\ Temp) + s(Regional\ \ SSI) + s(Bottom\ Temp, by = Pres\ Cold\ Pool) + ti(fracyear,\ \ Bottom\ Temp) + ti(fracyear, Regional\ SSI) + ti(Bottom\ Temp, Regional\ SSI)$$ Equation 10

where: s(x) indicates a smooth of the effect of each covariate, s(x, by=y) indicates smooth interaction, s(x, bs= 'cc') indicates a cyclic cubic regression spline smooth, and ti(x, x) indicates a tensor product interaction of smooth covariates in their scales.

The effect of regional SSI on ABC values was strong in the Cold regime final model, and ~2x the effect as bottom temperature. Comparatively, bottom temperature and regional SSI had an almost equal effect in the Warm regime final model. Bottom temperature explained ~9% of the deviance, or goodness-of-fit (R^2) for the Cold regime model, and regional SSI explained

~22% (Table 2). Bottom temperature increased to ~12% and regional sea ice decreased to ~10% deviance explained in the Warm regime model (Table 3). Bottom temperature alone did not provide as much predictive power compared to when being used with interactions for both regime models. The greatest decrease in prediction error (AIC) and increase in deviance explained in both regime models was attributed to the bottom temperature interaction terms in the full models (10.7% Cold regime and 6% Warm regime). Bottom temperature linkage with regional SSI and zooplankton abundance seasonality is an integral part of the EBS ecosystem and had two distinct equilibriums between regimes.

The summer Cold Pool presence binary covariate explained ~3% of the deviance for the Cold regime model and only ~1% of the Warm regime model. Both Cold Pool specific binary variables (presence and spring freezing bottom temperatures days) decreased in predictive power in the Warm years, but environmental variables that characterize the Cold Pool (bottom temperature and SSI) increased in predictive power. This suggests Cold Pool presence and previous winter water column cooling exclusively may not be significant variables of zooplankton abundance in the Warm regime. Thus, the predictive models suggest Cold regime Cold Pool relationships are more stable and known, whereas Warm regime Cold pool dynamics warrant more investigation.

ABC confidence Intervals (CI) increased from the Cold regime compared to the Warm regime when regressed against *fracyear* showing annual variability between the two regimes. Coefficient variance increased and were coupled with greater CI, for bottom temperatures greater than 1˚C and 3˚C, for the Cold and Warm regime, respectively. Regional SSI coefficient variance and CI increased greater than 5×10^5 km^2 in the Cold regime and 3.25×10^5 km^2 in the Warm regime (Figure 52).

Description	**Formulation**	**Deviance Explained**	**AIC**
No *Bottom_Temp or Regional_SSI*	log10(ABC*10^06) ~ s(fracyear,bs="cc")	32.3%	5897.9
No Bottom_Temp	log10(ABC*10^06) ~ s(fracyear,bs="cc")+ s(Regional_SSI))	36.2%	5823.8
No *Regional_SSI*	log10(ABC*10^06) ~ s(fracyear,bs="cc")+ s(Bottom_Temp))	35.2%	5805.1
No tensor product or Cold Pool interactions	log10(ABC*10^06) ~ s(fracyear,bs="cc") + s(Bottom_Temp) + s(Regional_SSI))	39.1%	5728.2
No *Regional_SSI* or interactions	log10(ABC*10^06) ~ s(fracyear,bs="cc") + s(Bottom_Temp) + s(Bottom_Temp,by = Pres_Cold_Pool)+ ti(fracyear,Bottom_Temp)	40.9%	5711.2
No tensor product	log10(ABC*10^06) ~ s(fracyear,bs="cc") + s(Bottom_Temp) + s(Regional_SSI) + s(Bottom_Temp,by = Pres_Cold_Pool) + s(Regional_SSI, by = Freezing_Temp)	43.2%	5655.6
No *Bottom_Temp* or interactions	log10(ABC*10^06) ~ s(fracyear,bs="cc") + s(Regional_SSI) + s(Regional_SSI, by = Freezing_Temp)+ ti(fracyear,log10(Reg_SSI))	53.9%	5379.8
No *Freezing_Temp* or *Pres_Cold_Pool*	log10(ABC*10^06) ~ s(fracyear,bs="cc") + s(Bottom_Temp) + s(Regional_SSI) + ti(fracyear,Bottom_Temp) + ti(fracyear,log10(Reg_SSI)) + ti(Bottom_Temp, Regional_SSI)	64.6%	4998.8
No *Freezing_Temp*	log10(ABC*10^06) ~ s(fracyear,bs="cc") + s(Bottom_Temp) + s(Regional_SSI) + s(Bottom_Temp,by = Pres_Cold_Pool) + ti(fracyear,Bottom_Temp) + ti(fracyear,log10(Reg_SSI)) + ti(Bottom_Temp, Regional_SSI))	65.8%	4966.4
No *Pres_Cold_Pool*	log10(ABC*10^06) ~ s(fracyear,bs="cc") + s(Bottom_Temp) + s(Regional_SSI)+ s(Regional_SSI, by = Freezing_Temp) + ti(fracyear,Bottom_Temp) + ti(fracyear,log10(Reg_SSI)) + ti(Bottom_Temp, Regional_SSI))	67.4%	4889.8
Full Model	log10(ABC*10^06) ~ s(fracyear,bs="cc") + s(Bottom_Temp) + s(Regional_SSI) + s(Bottom_Temp,by = Pres_Cold_Pool) + s(Regional_SSI, by = Freezing_Temp)+ ti(fracyear,Bottom_Temp) + ti(fracyear,log10(Reg_SSI)) + ti(Bottom_Temp, Regional_SSI)	68.6%	4855.4

Table 2. EBS zooplankton abundance Cold regime GAMs

Description	**Formulation**	**Deviance Explained**	**AIC**
No *Bottom_Temp* or *Regional_SSI*	log10(ABC*10^06) ~ s(fracyear,bs="cc"))	55.2%	4261.3
No *Bottom_Temp*	log10(ABC*10^06) ~ s(fracyear,bs="cc")+s(Regional_SSI))	59%	4147.8
No *Regional_SSI*	log10(ABC*10^06) ~ s(fracyear,bs="cc")+s(Bottom_Temp))	61.8%	4035.6
No tensor product or Cold Pool interactions	log10(ABC*10^06) ~ s(fracyear,bs="cc") + s(Bottom_Temp) + s(Regional_SSI))	63.6%	3981.9
No tensor product	log10(ABC*10^06) ~ s(fracyear,bs="cc") + s(Bottom_Temp) + s(Regional_SSI) + s(Bottom_Temp,by = Pres_Cold_Pool) + s(Regional_SSI, by = Freezing_Temp))	64.1%	3970.3
No *Bottom_Temp* or interactions	log10(ABC*10^06) ~ s(fracyear,bs="cc") + s(Regional_SSI) + ti(fracyear,Regional_SSI))	64.7%	3960.9
No *Regional_SSI* or interactions	log10(ABC*10^06) ~ s(fracyear,bs="cc") + s(Bottom_Temp)+ s(Bottom_Temp,by = Pres_Cold_Pool) + ti(fracyear,Bottom_Temp))	67.4%	3835.9
No *Pres_Cold_Pool*	log10(ABC*10^06) ~ s(fracyear,bs="cc") + s(Bottom_Temp) + s(Regional_SSI)+ ti(fracyear,Bottom_Temp) + ti(fracyear,Regional_SSI) + ti(Bottom_Temp, Regional_SSI))	73.4%	3596.5
Full Model	log10(ABC*10^06) ~ s(fracyear,bs="cc") + s(Bottom_Temp) + s(Regional_SSI) + s(Bottom_Temp,by = Pres_Cold_Pool) + ti(fracyear,Bottom_Temp) + ti(fracyear,Regional_SSI) + ti(Bottom_Temp, Regional_SSI))	74.5%	3559.7

Table 3. EBS zooplankton abundance Warm regime GAMs

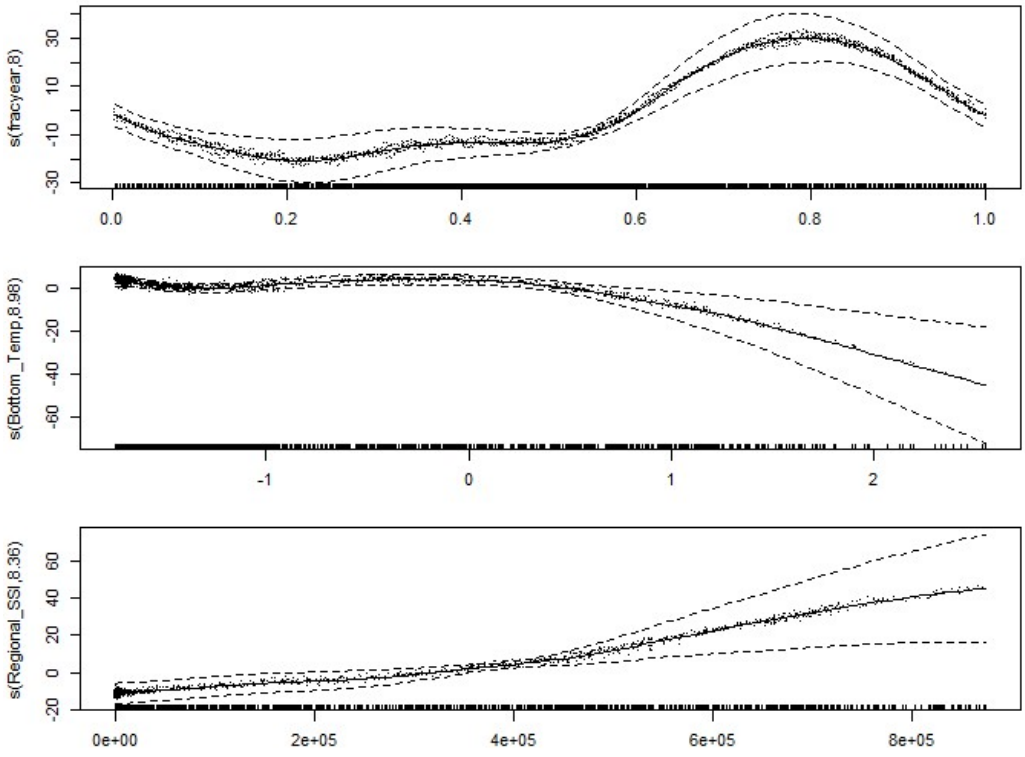

a)

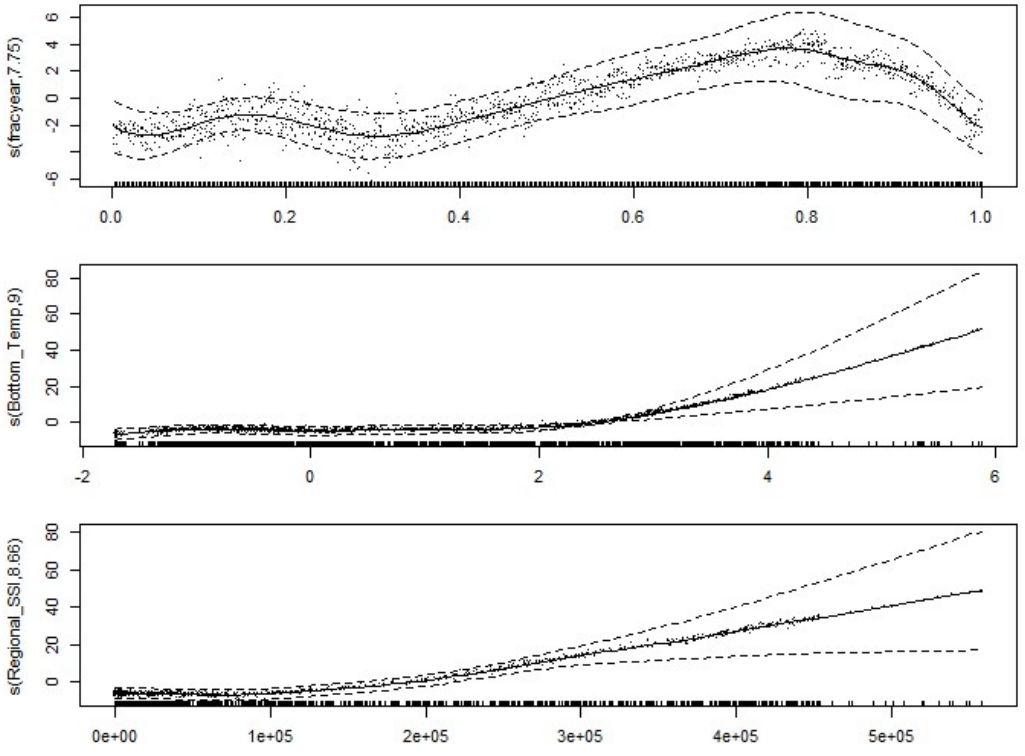

b)

Figure 52. Linear coefficients for predictive model explantory variables with 95% CI for final a) Cold regime and b) Warm regime

CHAPTER 4. DISCUSSION

Though the Cold Pool and zooplankton populations have been studied along the EBS shelf, year-round full water column representation of the communities have yet to be observed while undergoing a regime shift. This is the first study to link the EBS Cold Pool with shelf zooplankton dynamics across two regimes by utilizing a long-term acoustical monitoring dataset. From assessing the differences between the two regimes and two regions, it was determined that the Warm regime Cold Pool truncated duration or absence alone did not have as much of an affect as anticipated on the zooplankton communities or was not observed to have an immediate impact within the scope of this study. However, variables that characterize Cold Pool extent and duration, i.e. bottom temperature and regional SSI, had more of an impact on Warm regime zooplankton dynamics than in the Cold regime. Environmental and ecological insights concluded from this analysis contributes to the comprehensive understanding of the EBS regional warming and current observations of lower trophic level climate-mediated changes occurring at different time scales.

Indications of the NBS following similar environmental trends as the SEBS has been in question (Stabeno and Bell, 2019). While the SEBS and the CBS have been dominated by multiyear Cold and Warm regimes, the NBS was predicted to remain cold with continued extensive SSI during winter and early spring (Stabeno et al., 2012, Wang and Overland 2009). However, from recent observations, Stabeno and Bell (2019) hypothesized the NBS may be experiencing the same variability as the SEBS. Site M5 Cold regime and site M8 Warm regime monthly bottom temperature averages were observed to have similar magnitude and temporal scales in this study. In recent Warm years increased variability of bottom temperature, regional

SSI extent, and the decreasing number of days of full water column cooling, suggest site M8, or the NBS, is experiencing site M5 or CBS Cold year conditions. These observations support Stabeno and Bell (2019) recent hypotheses of NBS variability, however with an implied delay between the sites with active warming.

EBS warming bottom temperature and SSI between the Cold and Warm regime affected the Cold Pool. The 2018 absence of the Cold Pool at site M5 was due to above average winter temperature anomalies in 2017 that resulted from the lack of SSI and persistence of southerly winds coupled with southern advection of warm water. Isolated from advective warming due to weak northward flow, site M8 experienced the presence of the Cold Pool in 2018, but it quickly diminished from weakened salinity vertical stratification. As a result of the cascading events in 2017, winter bottom tempeatures were the warmest on record at site M5 and M8 in 2018 (Stabeno and Bell, 2019). Forecasted temperature increases suggest Cold Pool absence at site M5 will be more regular, and site M8 Cold Pool decreases in duration will be likely. Furthermore, observed northern Cold Pool component (58˚N and northward) and a SE Cold Pool component (centered at 57˚N) (Stabeno et al,. 2012) documented farther south may have similar properties to the differences now being seen in the NBS and CBS Cold Pool. Though ABC values were not qualitatively different in Warm years when the Cold Pool was present or absent, Mean S_v and Delta-S_v metrics were qualitatively different when Cold Pool was absent or duration was variable. Perhaps an increased response in zooplankton communities will occur from the 2018 absence and current Cold Pool dynamics in the coming years.

CBS site M5 and NBS site M8 reflected the same magnitude of backscattered zooplankton abundances during overlapped sample periods that included immediate pre and post regime shift. The similarity in abundances at each site foreshadows further change in the NBS

ecosystem, if the NBS is only currently experiencing CBS Cold regime environmental conditions. Increased rates of change have been observed with higher mean annually integrated gross primary production (GPP) values in the northern domains during Warm years and in the SEBS domains during Cold years (Liu et al., 2016). Warm regime predctive models had higher R^2 values than Cold regime models when modelling the CBS backscatter abundances. The Cold regime response variables included large spring and fall bloom backscattered values, while the Warm regime did not. Warm regime environmental variables were more variable than Cold regime explanatory variables, but Warm regime backscatter abundance was consistently low and exhibited annual seasonlity resulting in greater predictability. The Cold regime full predictive model supports Eisner et al.,'s (2014) hypothesis of larger zooplankton species having a direct relationship with SSI as a strong predtictor variable, and a negative relationship with bottom temperature with ½ of the predictive power as SSI. The Warm regime full predictive model further supports Eisner et al., (2014) hypothesis where small zooplankton taxa have a direct relationship to surface and bottom temperature, with regional SSI decreasing in predicting power and equalling bottom temperature affects. Surface temperature should be explored in current Warm regime predictive models with Cold Pool variables for further examination and improved model performance. Cold Pool proxy relationships within the Cold regime are stable and more understood, whereas Warm regime relationships, that are linked with higher trophic level predation, warrant more inquiry due to increased predictive power coupled with increased Cold Pool variable variation. Further investigation of predictive regime models can utilize leads/lag information paired with explanatory variables for more parsimonious models, and should be considered when analyzing alternate regions along the EBS such as the NBS site M8. In current forecasts of sustained warming of the EBS, the range in magnitude of GPP is expected to expand

in the NBS, however with warming temperatures detrimentally impacting ecosystem stability and zooplankton community composition, hindrance of enhanced GPP flow to higher trophic levels may occur.

Though limited by a lack of biological samples to pair with the acoustical time series analyzed, Delta-S_v methods provided insight to the shift in zooplankton community structure and year-round dynamics from Cold to Warm years that support traditional net survey observations (Stabeno et al., 2019, Eisner e al., 2014, Sigler et al., 2014, Miksis-Olds et al., 2013, Coyle et al., 2008). Figure 43 highlighted Delta-S_v monthly variance lagged negative relationship with bottom temperature monthly variance during Warm years, and variances approximately collinear during Cold Years. These observations suggest that during Cold years when bottom temperature variance increases during the fall and winter, zooplankton community changes are occurring due to the temperature changes in the water i.e. phenology along the EBS shelf. During Warm years, Delta-S_v and bottom temperature variance is greatly increased at different times of year. The lack of Delta-S_v variance during peak bottom temperature variance would suggest the Warm year backscatter variance is not based solely on temperature- but rather a shift in organism physiology, physical characteristics, and/or community structure. In the EBS all changes have possibly occurred, where shifts to *Psuedocalanus spp* as the dominant species from lipid rich *Calanus spp* and euphausiids has been documented, as well as physiological and size shifts in the *Pseudocalanus* themselves are possible.

Cold Pool presence alone offers refuge to larval fish from warmer bodied predators and therefore AWCP backscatter from the 200 kHz can be dominated by larval fish acoustic signals, which make it difficult to distinguish zooplankton signals such as krill, pteropods, and amphipods. Sampling spatial or temporal overlap can lead to underestimates of euphausiid

densities. To address over or under abundance estimates of backscatter dominated by euphausiids, copepods, or fish, biomass can be computed using the range of S_v values for each type of scatterer (i.e. small scatterers such as copepods, medium scatterers such as juvenile krill, large scatterers such as adult euphuasiids, and resonant scatterers such as swim bladdered fish), and application of *a priori* knowledge of temporal patterns and behaviors of higher trophic levels are needed to tease out acoustic overlap. Acoustic zooplankton backscatter from this study corroborates current studies (NOAA NMFSC RACE, Ressler et al., De Robertis et al., Kimmel et al.,) that have documented water column dominant species to shift from large bodied copepod *C. Marshallae* and euphausiid *T. raschii* to smaller bodied *Psedocalanus spp* from Cold to Warm years during summer surveys. However, with the observed community shift both biologically with nets and acoustically, further physiological (density and sound speed) and/or physical (size, length) changes may be occurring in the smaller bodied zooplankton species based on Warm year increased variable conditions and increased amplitude of acoustical metrics. Increased sampling and TS studies are needed within the Warm regime for comprehensive individual and community wide changes within the system.

4.1 EBS and Ecosystem Resiliency

Increased rates of environmental change and loss of biodiversity and biomass continue to affect ecosystem functions and services globally. Maintenance of these functions and services, or 'resilience' is crucial under substantial predicted environmental change. The stability and speed of which an ecosystem can return to an equilibrium state following a disturbance is known as resilience. An extension of resiliency is the Ecological Resiliency Theory (Oliver et al., 2015) and is the ability of a system to resist regime shifts to maintain ecosystem function by which systems can be susceptible to stochasticity close to critical tipping points that result in a new

equilibrium. The 2012 and 2013 seasons leading up to the fall 2013 regime shift in the EBS were more variable and stochastic with above average bottom temperatures. The regional SSI 2011 maximum peak was lower than average then followed by the highest maximum peak within the Cold regime in 2012. The acoustic backscatter was also observed to have more variability and larger peaks in 2011- spring 2013, coupling with the extensive sea ice in May (Figure 48). During the 2013 transition year, the system experienced a change that resulted in a new equilibrium for average annual bottom temperature, backscatter abundance, and sea ice extent.

Increased stochasticity near the 2013 climatic regime shift is not the only example of EBS resiliency. Oliver et al. (2015) identified a range of mechanisms that create foundations of resilient ecosystems across three ecological scales: species, communities, and landscapes. Ecosystem states maintain their stability through internal feedback mechanisms, such as the EBS Cold year lipid rich zooplankton communities that enhance stock recruitment (Coyle et al., 2011), which confer resistance in ecosystem functions. *Response traits* of species under environmental perturbations and turnover in species communities have been thought to facilitate resilient functions. Intraspecific *response traits,* or changes in biophysical (g, h, and length) properties among individuals, are linked with sensitivity to environmental change which result *in effect traits.* Effect traits are seen as maintenance of ecosystem functions, such as zooplankton physical characteristics that vary seasonally and geographically (Smith et al., 2010, McQuinn et al., 2013). Interspecific community wide shifts such as EBS *Pseduocalanus spp* dominant species during Warm years that are better fitted for warmer conditions (Hunt et al., 2011, Kimmel et al., 2018), are suggestive of important trophic links for resiliency on the shelf. Increases in diversity result in community wide resilience and has been observed in the Bering

Sea in the demersal community from warming conditions (Mueter and Litzow 2008, Stabeno et al., 2012).

Observed increases in diversity may also attribute to hysteresis in an ecosystem. Hysteresis, where increases or decreases of forcing environmental variables result in response biological variables following a different equilibrium trajectory, may be characteristic of a diversifying community response to changing temperature driven by differences in Cold and Warm EBS community states. A comprehensive understanding of the underlying mechanisms of EBS zooplankton community regime specific equilibriums are required for hysteresis categorization of the system. Further exploration is needed if the EBS undergoes subsequent shifts in which the EBS experiences Cold year conditions, but biological zooplankton communities fail to reorganize to their Cold regime community structure previous states.

4.2 Detecting Future Regime Shifts

Coupling between variability of ocean conditions and the response of marine populations is observed when high-frequency weather patterns are attenuated by the heat capacity of the ocean which results in low-frequency, low trophic level production variation that propagates up the food chain (Cushing 1990, Steele 1985, and Aebisher et al., 1990). Biological regime shifts are characterized by low-frequency, high-amplitude changes in oceanic conditions that may be pronounced in biological variables and can propagate through several trophic levels (Collie et al., 2004), such as the EBS regime shift in trawl community composition during the mid-1980's (Connors and Brown 2002, Litzow and Hunsicker, 2016). Biological regime shifts can be classified as smooth, abrupt, or discontinuous based on the relationship between biotic ecosystem response variables and some external forcing or condition. Smooth shifts are linear or semi-linear transitions, while abrupt shifts have non-linear relationships between forcing environmental

variables and biological response variables. Alternative stable states are associated with discontinuous shifts or tipping points in ecosystems where environmental perturbations can increase the likelihood of a regime shift leading to a fundamental change in the assemblages in species. Hysteresis is associated with discontinuous regime shifts. The EBS exhibited characteristics of a discontinuous regime shift with coupled zooplankton community and acoustic backscatter equilibria shift and diversifying traits of a hysteresis system.

Regime shifts often result in conflicting Ecosystem Based management (EBM) perspectives. New ecological states are often just as resilient as previous states, and thus creates challenges for managers interested in reversing an ecosystem state or situation. However, early detection of tipping points prior to a regime shift for critical transitions is possible with Early Warning Signals (EWS) (Wouters et al., 2014). EWS are statistical indicators that measure the phenomenon 'critical slowing down' (CSD) or the decreased recovery rate of an ecosystem with low resilience (Sheffer, 2010). EWS in unstable ecosystems and increased loss of resiliency approaching a transition are identified with increases in variation and spatial/temporal autocorrelation of variables leading up to a tipping point. EWS have been used successfully in mostly non-linear systems, and have been demonstrated to occur in paleoclimate, lake eutrophication, trophic cascades, experimental zooplankton extinctions, and collapse of photo-inhabited green algae (Dakos et al., 2008, Wang et al., 2012, Carpenter et al., 2012, Drake and Griffen , 2010, and Veraart etl., 2012, respectively). Building on the results of this study, the EBS can be further assessed using acoustical time series for EWS. Robust detection of EWS depends on the length of the time series, with shorter time series limiting long signal discernment, therefore further continuous acoustical monitoring is needed in the EBS as shifts may occur more often under forecasted climatic conditions. Filtered high frequency or low

frequency trends can be further analyzed for hidden signals that are present within acoustical and environmental data sets (Bendat and Piersol, 1986) (Figure 53). Further analysis is needed for autocorrelation rates pre and post the 2013 regime shift for identifying hindcasted EWS within the current Warm regime.

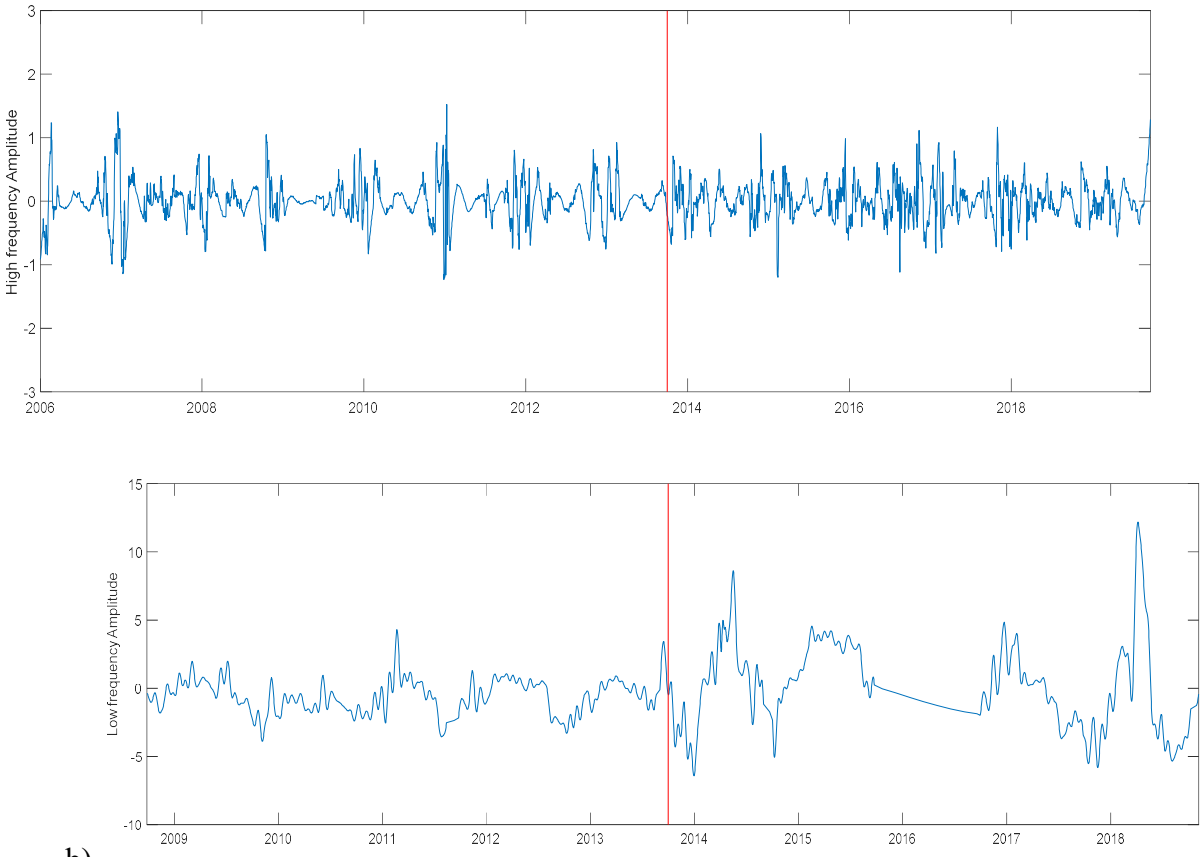

Figure 53. Filtered time series data with red line depicting fall 2013 regime shift demarcation for a) 2006-2018 high band pass bottom temperature amplitude, and b) 2008-2018 low band pass Delta-S_v amplitude

EWS are important in EBM and integration of regime shift information into Integrated Ecosystem Assessment (IEA) is needed for tactical implementation in management (Levin and Mollman 2015). Predicting future tipping points or regime shifts will be needed for predicted climatic conditions. Identifying non-linearity within EBS zooplankton communities with coupling environmental variables to help predict future shifts is vital for fishery ecosystem

needs, as critical tipping points may be reached more frequently with increases in environmental variation in Warm years. While IEAs are evolving as an EBM approach, more analytical and statistical modelling is needed to incorporate tactical management in marine ecosystems that undergo discontinuous regime shifts for sustainable ecosystem stewardship. Tactical management objectives include defining ecosystem specific reference points, which require documentation of the range of variability to distinguish normal variability from changes signaling a major shift (Cormier et al., 2017). While examples of operational, cross-sectoral EBM in marine and coastal ecosystems with current policies are lacking, one adaptive management technique using primary indicators is highlighted with Alaska LME with Ecosystem Approach Fisheries Management (EAFM) report cards (Zador et al., 2017). EAFM report cards have been used with the North Pacific Fishery Management Council, one of eight regional councils established by the Magnuson-Stevens Fishery Conservation and Management Act in 1976, to manage fisheries in the 200-mile Exclusive Economic Zone (NOAA, 2015). Alaska LME EAFM report cards are abbreviated in the information conveyed and use for tactical quota decisions has not yet been established. The use of EWS to identify regime shifts may facilitate more informative report cards, where certain primary indicators are highlighted depending on the regime state for splitting fishery quota by Alaskan LME. This study's results increased the comprehensive understanding of Cold and Warm year zooplankton communities in the NBS and CBS. Neighboring LME can be further monitored for acoustical equilibria shifts as an innovative practice in NOAA's EBFM mission.

V. CONCLUSION

Long-term acoustical monitoring platforms are useful tools for monitoring spatial and temporal ecosystem change. In the fall of 2013, the EBS encountered a regime shift that was characterized by less SSI, early receding SSI, increased bottom temperatures, and a zooplankton community structure shift. Due to the changes in environmental conditions, an alternative equilibrium was established in the current Warm regime that was coupled with noteworthy differences in water column acoustic backscatter averages. Decreased abundances of lipid rich species on the EBS shelf in the Warm regime have been observed in zooplankton biological net surveys (Stabeno et al., 2019, Kimmel et al., 2018, Eisner et al., 2014), and this study captured those community changes acoustically across two climactic regimes. With future predictions of warming temperatures and little to no SSI, the NBS may be starting to be experience parameters similarly to the SEBS Cold regime conditions. Delayed warming impacts forecast a higher rate of ecosystem change than previously anticipated, leaving investigation for further acoustic variation in Warm regime zooplankton size, physiology, and community structure. The most recent Warm regime years have resulted in little to no Cold Pool formation along the EBS shelf, and while changes have occurred in zooplankton communities between regimes, Warm regime specific Cold Pool dynamics are yet to be fully understood and perhaps their impact on secondary producer communities are delayed. Region specific changes calls for management to make informed decisions based on ecosystem regime state and utilization of acoustical EWS are possible for predicting future shifts. EWS detection in acoustical metrics highlighted in this study emphasizes the importance of continued acoustical monitoring on the EBS shelf where ecosystem changes are occurring with rapid environmental warming.

LIST OF REFERENCES

Aebischer, N. J., J. C. Coulson, and J. M. Colebrookl. "Parallel long-term trends across four marine trophic levels and weather." *Nature* 347.6295 (1990): 753-755.

Baker, Matthew R., and Anne B. Hollowed. "Delineating ecological regions in marine systems: Integrating physical structure and community composition to inform spatial management in the eastern Bering Sea." *Deep Sea Research Part II: Topical Studies in Oceanography* 109 (2014): 215-240.

Bendat, Julius S., and Allan G. Piersol. "Decomposition of wave forces into linear and non-linear components." *Journal of Sound and Vibration* 106.3 (1986): 391-408.

Benoit-Bird, Kelly J., and Gareth L. Lawson. "Ecological insights from pelagic habitats acquired using active acoustic techniques." *Annual Review of Marine Science* 8 (2016): 463-490.

Benoit-Bird, Kelly J., Neal E. McIntosh, and Scott A. Heppell. "Nested scales of spatial heterogeneity in juvenile walleye pollock Theragra chalcogramma in the southeastern Bering Sea." *Marine Ecology Progress Series* 484 (2013): 219-238.

Brodeur, Richard D., Matthew T. Wilson, and Lorenzo Ciannelli. "Spatial and temporal variability in feeding and condition of age-0 walleye pollock (Theragra chalcogramma) in frontal regions of the Bering Sea." *ICES Journal of Marine Science* 57.2 (2000): 256-264.

Brown, Zachary W., and Kevin R. Arrigo. "Contrasting trends in sea ice and primary production in the Bering Sea and Arctic Ocean." *ICES Journal of Marine Science* 69.7 (2012): 1180-1193.

Carpenter, S. R., Arrow, K. J., Barrett, S., Biggs, R., Brock, W. A., Crépin, A. S., ... & Li, C. Z. “General resilience to cope with extreme events.” *Sustainability 4*(2012), 3248-3259.

Chen, Zhuomin. *Dynamics and spatio-temporal variability of the Mid-Atlantic Bight Cold Pool*. Diss. Rutgers University-School of Graduate Studies, 2018.

Chu, Dezhang, Kenneth G. Foote, and Timothy K. Stanton. "Further analysis of target strength measurements of Antarctic krill at 38 and 120 kHz: Comparison with deformed cylinder model and inference of orientation distribution." *The Journal of the Acoustical Society of America* 93.5 (1993): 2985-2988.

Collie, Jeremy S., Katherine Richardson, and John H. Steele. "Regime shifts: can ecological theory illuminate the mechanisms?" *Progress in Oceanography* 60.2-4 (2004): 281-302.

Conners, M. E., A. B. Hollowed, and E. Brown. "Retrospective analysis of Bering Sea bottom trawl surveys: regime shift and ecosystem reorganization." *Progress in Oceanography* 55.1-2 (2002): 209-222.

Conti, Stéphane G., and David A. Demer. "Improved parameterization of the SDWBA for estimating krill target strength." *ICES Journal of Marine Science* 63.5 (2006): 928-935.

Cormier, Roland, et al. "Moving from ecosystem-based policy objectives to operational implementation of ecosystem-based management measures." *ICES Journal of Marine Science* 74.1 (2017): 406-413.

Coyle, Kenneth O. "Acoustic estimates of zooplankton biomass and distribution: application of canonical correlation to scaling of multifrequency acoustic data." *Canadian Journal of Fisheries and Aquatic Sciences* 57.11 (2000): 2306-2318.

Coyle, K. O., et al. "Climate change in the southeastern Bering Sea: impacts on Pollock stocks and implications for the oscillating control hypothesis." *Fisheries Oceanography* 20.2 (2011): 139-156.

Cornwall, Warren. "Vanishing Bering Sea ice poses climate puzzle." *Science* (2019): 616-617.

Cushing, D. H. "Plankton production and year-class strength in fish populations: an update of the match/mismatch hypothesis." *Advances in Marine Biology* 26 (1990): 249-293.

Dakos, Vasilis, et al. "Slowing down in spatially patterned ecosystems at the brink of collapse." *The American Naturalist* 177.6 (2011): E153-E166.

Danielson, Seth L., et al. "A comparison between late summer 2012 and 2013 water masses, macronutrients, and phytoplankton standing crops in the northern Bering and Chukchi Seas." *Deep Sea Research Part II: Topical Studies in Oceanography* 135 (2017): 7-26.

Danielson, Seth, et al. "On ocean and sea ice modes of variability in the Bering Sea." *Journal of Geophysical Research: Oceans* 116.C12 (2011).

Dell'Apa, Andrea, et al. "The status of marine and coastal ecosystem-based management among the network of US federal programs." *Marine Policy* 60 (2015): 249-258.

Demer, David A., and Stéphane G. Conti. "Validation of the stochastic distorted-wave born approximation model with broad bandwidth total target strength measurements of Antarctic krill." *ICES Journal of Marine Science* 60.3 (2003): 625-635.

De Robertis, Alex, Denise R. McKelvey, and Patrick H. Ressler. "Development and application of an empirical multifrequency method for backscatter classification." *Canadian Journal of Fisheries and Aquatic Sciences* 67.9 (2010): 1459-1474.

De Robertis, Alex, and Edward D. Cokelet. "Distribution of fish and macrozooplankton in ice-covered and open-water areas of the eastern Bering Sea." *Deep Sea Research Part II: Topical Studies in Oceanography* 65 (2012): 217-229.

Drake, J. M., and Griffen, B. D. "Early warning signals of extinction in deteriorating environments." *Nature* 467 (2010): 456-459.

Efron, Bradley, and Robert Tibshirani. "Bootstrap methods for standard errors, confidence intervals, and other measures of statistical accuracy." *Statistical science* (1986): 54-75.

Eisner, Lisa. "The Bering Sea: Current status and recent trends." *PICES Press* 26.1 (2018): 29-36.

Eisner, Lisa B., et al. "Climate-mediated changes in zooplankton community structure for the eastern Bering Sea." *Deep Sea Research Part II: Topical Studies in Oceanography* 109 (2014): 157-171.

Gallager, Scott M., Hidekatsu Yamazaki, and Cabell S. Davis. "Contribution of fine-scale vertical structure and swimming behavior to formation of plankton layers on Georges Bank." *Marine Ecology Progress Series* 267 (2004): 27-43.

George, John C., et al. "Observations on shorefast ice dynamics in arctic Alaska and the responses of the Inupiat hunting community." *Arctic* 57.4 (2004).

Guy, Lisa Sheffield, et al. "Understanding climate control of fisheries recruitment in the eastern Bering Sea: long-term measurements and process studies." *Oceanography* 27.4 (2014): 90-103.

Haynie, Alan, and Henry Huntington. "Strong connections, loose coupling: the influence of the Bering Sea ecosystem on commercial fisheries and subsistence harvests in Alaska." *Ecology and Society* 21.4 (2016).

Horsburgh, K. J., et al. "Seasonal evolution of the cold pool gyre in the western Irish Sea." *Progress in Oceanography* 46.1 (2000): 1-58.

Howe, Bruce M., et al. "Observing the oceans acoustically." *Frontiers in Marine Science* 6.426 (2019).

Hunt Jr, George L., et al. "Climate change and control of the southeastern Bering Sea pelagic ecosystem." *Deep Sea Research Part II: Topical Studies in Oceanography* 49.26 (2002): 5821-5853.

Ianelli, James N., et al. "Assessment of the walleye Pollock stock in the Eastern Bering Sea." *NOAA Library Repository* (2016).

Jech, J. Michael, et al. "Comparisons among ten models of acoustic backscattering used in aquatic ecosystem research." *The Journal of the Acoustical Society of America* 138.6 (2015): 3742-3764.

Kang, Myounghee, Masahiko Furusawa, and Kazushi Miyashita. "Effective and accurate use of difference in mean volume backscattering strength to identify fish and plankton." *ICES Journal of Marine Science* 59.4 (2002): 794-804.

Levin, Phillip S., and Christian Möllmann. "Marine ecosystem regime shifts: challenges and opportunities for ecosystem-based management." *Philosophical Transactions of the Royal Society B: Biological Sciences* 370.1659 (2015): 20130275.

Litzow, Michael A., and Mary E. Hunsicker. "Early warning signals, nonlinearity, and signs of hysteresis in real ecosystems." *Ecosphere* 7.12 (2016): e01614.

Liu, C. L., Zhai, L., Zeeman, S. I., Eisner, L. B., Gann, J. C., Mordy, C. W., and Lomas, M. W. "Seasonal and geographic variations in modeled primary production and phytoplankton losses from the mixed layer between warm and cold years on the eastern Bering Sea shelf." *Deep Sea Research Part II: Topical Studies in Oceanography 134* (2016): 141-156.

Maeda, T. "Relationship between annual fluctuation of oceanographic conditions and abundance of year classes of the yellow-fin sole in the eastern Bering Sea." *Special Bulletin of Research Institute of North Pacific Fisheries Hokkaido University* (1977).

McQuinn, Ian H., Maxime Dion, and Jean-François St. Pierre. "The acoustic multifrequency classification of two sympatric euphausiid species (Meganyctiphanes norvegica and Thysanoessa raschii), with empirical and SDWBA model validation." *ICES Journal of Marine Science* 70.3 (2013): 636-649.

Meier, Walter N., Julienne Stroeve, and Florence Fetterer. "Whither Arctic sea ice? A clear signal of decline regionally, seasonally and extending beyond the satellite record." *Annals of Glaciology* 46 (2007): 428-434.

Miksis-Olds, Jennifer L., et al. "Ecosystem response to a temporary sea ice retreat in the Bering Sea: Winter 2009." *Progress in Oceanography* 111 (2013): 38-51.

Mueter, Franz J., and Michael A. Litzow. "Sea ice retreat alters the biogeography of the Bering Sea continental shelf." *Ecological Applications* 18.2 (2008): 309-320.

Niebauer, H. J. "Effects of El Nino-Southern Oscillation and North Pacific weather patterns on interannual variability in the subarctic Bering Sea." *Journal of Geophysical Research: Oceans* 93.C5 (1988): 5051-5068.

Okkonen, Stephen R., et al. "Satellite and hydrographic observations of the Bering Sea 'Green Belt'." *Deep Sea Research Part II: Topical Studies in Oceanography* 51.10-11 (2004): 1033-1051.

Oliver, Tom H., et al. "Biodiversity and resilience of ecosystem functions." *Trends in Ecology and Evolution* 30.11 (2015): 673-684.

Ressler, Patrick H., Alex De Robertis, and Stan Kotwicki. "The spatial distribution of euphausiids and walleye pollock in the eastern Bering Sea does not imply top-down control by predation." *Marine Ecology Progress Series* 503 (2014): 111-122.

Ressler, Patrick H., et al. "Developing an acoustic survey of euphausiids to understand trophic interactions in the Bering Sea ecosystem." *Deep Sea Research Part II: Topical Studies in Oceanography* 65 (2012): 184-195.

Ressler, Patrick H., Alex De Robertis, and Stan Kotwicki. "The spatial distribution of euphausiids and walleye pollock in the eastern Bering Sea does not imply top-down control by predation." *Marine Ecology Progress Series* 503 (2014): 111-122.

Scheffer, Marten. "Foreseeing tipping points." *Nature* 467.7314 (2010): 411-412.

Secor, David H., et al. "Ocean destratification and fish evacuation caused by a Mid-Atlantic tropical storm." *ICES Journal of Marine Science* 76.2 (2019): 573-584.

Simmonds, John, and David N. MacLennan. "Fisheries acoustics: theory and practice." *John Wiley & Sons* (2008).

Smith, Joy N., Patrick H. Ressler, and Joseph D. Warren. "A distorted wave Born approximation target strength model for Bering Sea euphausiids." *ICES Journal of Marine Science* 70.1 (2012): 204-214.

Smith, Joy N., Patrick H. Ressler, and Joseph D. Warren. "Material properties of euphausiids and other zooplankton from the Bering Sea." *The Journal of the Acoustical Society of America* 128.5 (2010): 2664-2680.

Smith, Sharon L. "Growth, development and distribution of the euphausiids Thysanoessa raschi (M. Sars) and Thysanoessa inermis (Krøyer) in the southeastern Bering Sea." *Polar Research* 10.2 (1991): 461-478.

Springer, A. M., and Roseneau, D. G. "Copepod-based food webs: Auklets and oceanography in the Bering Sea," *Marine Ecology Progress Series* 21 (1985): 229–237.

Stabeno, Phyllis J., et al. "A comparison of the physics of the northern and southern shelves of the eastern Bering Sea and some implications for the ecosystem." *Deep Sea Research Part II: Topical Studies in Oceanography* 65 (2012): 14-30.

Stabeno, P. J., et al. "Variability of physical and chemical characteristics along the 70-m isobath of the southeastern Bering Sea." *Deep Sea Research Part II: Topical Studies in Oceanography* 49.26 (2002): 5931-5943.

Stabeno, Phyllis, et al. "Factors influencing physical structure and lower trophic levels of the eastern Bering Sea shelf in 2005: Sea ice, tides and winds." *Progress in Oceanography* 85.3-4 (2010): 180-196.

Stabeno, P. J., et al. "Variability of physical and chemical characteristics along the 70-m isobath of the southeastern Bering Sea." *Deep Sea Research Part II: Topical Studies in Oceanography* 49.26 (2002): 5931-5943.

Stabeno, Phyllis J., and Shaun W. Bell. "Extreme Conditions in the Bering Sea (2017–2018): Record-Breaking Low Sea-Ice Extent." *Geophysical Research Letters* 46.15 (2019): 8952-8959.

Stauffer, Beth A., Jennifer Miksis-Olds, and Joaquim I. Goes. "Cold regime interannual variability of primary and secondary producer community composition in the Southeastern Bering Sea." *PloS One* 10.6 (2015): e0131246.

Steele, John H. "A comparison of terrestrial and marine ecological systems." *Nature* 313.6001 (1985): 355-358.

Stroeve, Julienne C., et al. "Trends in Arctic sea ice extent from CMIP5, CMIP3 and observations." *Geophysical Research Letters* 39.16 (2012).

Thoman, Rick, and John E. Walsh. *Alaska's Changing Environment: Documenting Alaska's Physical and Biological Changes Through Observations*. International Arctic Research Center, University of Alaska Fairbanks, 2019.

Trenkel, Verena M., et al. "Underwater acoustics for ecosystem-based management: state of the science and proposals for ecosystem indicators." *Marine Ecology Progress Series* 442 (2011): 285-301.

Trenkel, Verena M., and Laurent Berger. "A fisheries acoustic multi-frequency indicator to inform on large scale spatial patterns of aquatic pelagic ecosystems." *Ecological indicators* 30 (2013): 72-79.

Urmy, Samuel S., John K. Horne, and David H. Barbee. "Measuring the vertical distributional variability of pelagic fauna in Monterey Bay." *ICES Journal of Marine Science* 69.2 (2012): 184-196.

Veraart, A. J., Faassen, E. J., Dakos, V., van Nes, E. H., Lürling, M., & Scheffer, M. "Recovery rates reflect distance to a tipping point in a living system." *Nature* 481 (2012): 357-359.

Vidal, Julio, and Sharon L. Smith. "Biomass, growth, and development of populations of herbivorous zooplankton in the southeastern Bering Sea during spring." *Deep Sea Research Part A. Oceanographic Research Papers* 33.4 (1986): 523-556.

Wang, Rong, et al. "Flickering gives early warning signals of a critical transition to a eutrophic lake state." *Nature* 492.7429 (2012): 419-422.

Wood, N. "S. Generalized Additive Models: An Introduction With R. Vol. 66." (2006).

Wood, Simon N., and Nicole H. Augustin. "GAMs with integrated model selection using penalized regression splines and applications to environmental modelling." *Ecological Modelling* 157.2-3 (2002): 157-177.

Wouters, N., et al. "Evidencing a regime shift in the North Sea using early-warning signals as indicators of critical transitions." *Estuarine, Coastal and Shelf Science* 152 (2015): 65-72.

Wyllie-Echeverria, T. I. N. A., and Warren S. Wooster. "Year-to-year variations in Bering Sea ice cover and some consequences for fish distributions." *Fisheries Oceanography* 7.2 (1998): 159-170.

Zador, S. G., Holsman, K. K., Aydin, K. Y., & Gaichas, S. K. “Ecosystem considerations in Alaska: the value of qualitative assessments.” *ICES Journal of Marine Science* 74 (2017): 421-430.

APPENDIX A: Matlab and R Codes

The following Matlab and R codes were used to calculate figures and statistics for this study.

Bottom Temperature (R)

```
# Load Packages
library(lubridate)
library(xts)
library(dplyr)

# Load Files
#Bottom Temps
#.csv files contain daily bottom temperature values in one column and the
date in another
BT=read.csv(file=paste(datapath,"M5_2005-2019_NaNs.csv", sep="/"),
header=TRUE, sep=",") #M5
BT1=read.csv(file=paste(datapath,"M8_2005-2019_NaNs.csv", sep="/"),
header=TRUE, sep=",") #M8

Temp=BT$Temperature
Temp2=BT1$Temperature

# Format Time
#Tempstab=BTstab$temp
date=BT$Date
date<-as.Date(date,format="%m/%d/%Y")

date1=BT1$Date
date1=as.Date(date1,format="%m/%d/%Y")

#Plotting for 2008-2019 Site M5
plot(date,Temp,type='l',xaxt='n',ylab='Bottom Temperature (degree
C)',xlab='')

#axes options for different subsets of data
datelabels=seq(as.Date("2005-01-01", format="20%y"), tail(date,1), by="1
year")
axis.Date(side=1, date, at=datelabels, format="20%y")

#M8 BT plot
plot(date1,Temp2,type='l',xaxt='n',ylab='Bottom Temperature (degree
C)',xlab='')
#axes options for differents subsets of data
datelabels=seq(as.Date("2005-01-01", format="20%y"), tail(date,1), by="1
year")
axis.Date(side=1, date, at=datelabels, format="20%y")

#Plot M5 and M8 overlaid on another to visualize lead and lags between sites
plot(date[74:5255],Temp[74:5255],type='l',xaxt='n',ylab='Bottom Temperature
(degree C)',xlab='',col='blue',ylim=c(-2,6))
par(new=TRUE)
plot(date1,Temp2,type='l',xaxt='n',ylab='Bottom Temperature (degree
C)',xlab='',ylim=c(-2,6),col='orange')
datelabels=seq(as.Date("2005-01-01", format="20%y"), tail(date,1), by="1
year")
```

```
axis.Date(side=1, datelabels[1:15], at=datelabels[1:15], format="20%y")
legend("topright", legend=c("M5", "M8 "),col=c("blue", 'orange'),
cex=0.8,lwd=2)

#Freezing bottom temperature plot
plot(date[74:5255],Temp[74:5255],type='l',xaxt='n',ylab='Bottom Temperature
(degree C)',xlab='',col='blue',ylim=c(-2,6))
par(new=TRUE)
plot(date1,Temp2,type='l',xaxt='n',ylab='Bottom Temperature (degree
C)',xlab='',ylim=c(-2,6),col='orange')
datelabels=seq(as.Date("2005-01-01", format="20%y"), tail(date,1), by="1
year")
axis.Date(side=1, datelabels[1:15], at=datelabels[1:15], format="20%y")
legend("topright", legend=c("M5", "M8 "),col=c("blue", 'orange'),
cex=0.8,lwd=2)
abline(h=-1.7, col="black",lty=(2))

#Bottom Temperature Statistics
# Continuous Average (monthly)
M5_monthlyavg=tapply(BT$Temperature, format(date, '%m-%Y'), mean, na.rm=TRUE)
M8_monthlyavg=tapply(BT1$Temperature, format(date1, '%m-%Y'),
mean,na.rm=TRUE)
M5_monthlysd=tapply(BT$Temperature, format(date, '%m-%Y'), sd, na.rm=TRUE)

#BT 2008-2019 Climatology
#Monthly average across all years (climatology)
M5=tapply(BT$Temperature, month(date), mean,na.rm=TRUE) #Average (mu)
M5sd=tapply(BT$Temperature, month(date), sd,na.rm=TRUE) #Standard Deviation
(sigma)
M5=c(M5[9:12], M5[1:8]) #rearrange months to be Sept-Aug instead of Jan-Dec
M5dates=format(seq(as.Date("2005-09-01"), by="month", length.out=12),'%m')
M5sd=c(M5sd[9:12], M5sd[1:8])

M8=tapply(BT1$Temperature, month(date1), mean,na.rm=TRUE)
M8sd=tapply(BT1$Temperature, month(date1), sd,na.rm=TRUE)
M8=c(M8[9:12], M8[1:8])
M8sd=c(M8sd[9:12], M8sd[1:8])

# BT Climatology Cold Years
#monthly average across cold years Jan 1,2006-Oct 1, 2013
Datesc=BT[243:3437,] #M5
Datesc8=BT1[170:3364,] #M8

M5c=tapply(BT$Temperature[243:3073], month(date[243:3073]), mean,na.rm=TRUE)
M5sdc=tapply(BT$Temperature[243:3073], month(date[243:3073]), sd,na.rm=TRUE)
M5c=c(M5c[9:12],M5c[1:8])
M5sdc=c(M5sdc[9:12],M5sdc[1:8])

M8c=tapply(BT1$Temperature[170:3000], month(date1[170:3000]),
mean,na.rm=TRUE)
M8sdc=tapply(BT1$Temperature[170:3000], month(date1[170:3000]),
sd,na.rm=TRUE)
M8c=c(M8c[9:12],M8c[1:8])
M8sdc=c(M8sdc[9:12],M8sdc[1:8])

#BT Climatology Warm Years
#monthly average across warm years Oct 2, 2013-Aug 31, 2019
```

```
Datesw=BT[3438:5233,] #M5
Datesw8=BT1[3365:5160,] #M8 Oct 2,2013-Sept 31, 2019

M5w=tapply(BT$Temperature[3074:5254], month(date[3074:5254]),
mean,na.rm=TRUE)
M5sdw=tapply(BT$Temperature[3074:5254], month(date[3074:5254]),
sd,na.rm=TRUE)
M5w=c(M5w[9:12],M5w[1:8])
M5sdw=c(M5sdw[9:12],M5sdw[1:8])

M8w=tapply(BT1$Temperature[3001:5181], month(date1[3001:5181]),
mean,na.rm=TRUE)
M8sdw=tapply(BT1$Temperature[3001:5181], month(date1[3001:5181]),
sd,na.rm=TRUE)
M8w=c(M8w[9:12],M8w[1:8])
M8sdw=c(M8sdw[9:12],M8sdw[1:8])
```

% BT separated by Cold Year/Warm Year Statistics (Matlab)

```
%Calculate Number of Observations and N*
% Observations time series ex. (01/01/2006-10/1/2013) by month (since 2006)
N=RegionalIceArea(1:3195,:); %Cold years
N=RegionalIceArea(3196:5021,:); %Warm years (10/2/2013-09/30/2019)

%Take care of leap years (Feb 29 days)
%M5 and Regional SSI Cold Years (01/01/2006-9/30/2014)
N(2251,:)=[];
N(790,:)=[];

%Site M5 &M8 and Regional SSI Warm years
N(517,:)=[];

%M8 Cold Years (01/01/2006-9/30/2014)
N(790,:)=[];
N(2250,:)=[];

%loop for each month for total observations by each month
for i=1:12
O=find(month(N.Date)==i);
Nobs(i)=length(O);
end

%Check to make sure number of observations matches the total number in the
%time series (matches length of "N")
sum(Nobs)

%write values (change order based on what first month is used for analysis-
%default is Jan-Dec)
csvwrite('Nobvw8Final.txt',[Nobs(8:12) Nobs(1:7)]); %write text files to be
used in R stats (Total observations)

%Divide the same months (all Januarys) into individual time series
%ex. 9 time series of daily values for each Jan (01/01/2006-9/30/2014)

%change number by month Jan=1 Dec=12 For each month compute a "monthvals" &
%run autocorrelation to sum N* values.

%Bottom Temperature
```

```
x1=08;
Month=find(month(N.Date)==x1);

a=table2array(N(Month,3));
a=str2double(a);

%Regional Sea Ice
% x1=12;
% Month=find(month(N.date)==x1);
%
% a=table2array(N(Month,2));

%Reshape [row column] row=number of days in each month column=how many of
%the same month in time period

x=31; %how many days in a month
y=5; %how many of the same month in the time period

%check to see if the number of days matches how many months are in the time
%period (does this match the number of values in "a"?
check=x*y

Monthvals=reshape(a,[x,y]);
csvwrite('M8_Augustw.txt',Monthvals) %exports to be used in R statistics and
Cold Pool variables

%Run cross-correlations of every month in every year to find N*
for i=1:y %change value for how many columns are in monthvals
ts1=Monthvals(:,i);
ts2=ts1;
[lags,corr]=crcov1(ts1,ts2,nlags,deltat);

%compute N* (calculation of independent observations) with autocorrelation of
first lag
%(1-corr(lag=1)/1+corr(lag=1))*Nobs for ts
Nstar(i,:)=((1-(corr(end)))/(1+(corr(end))))*length(ts1);
end
csvwrite('DecwarmyearM8N.txt',Nstar) %Write exports for N* to use in R

#R Statistics (Use Number of observations and N* value exports for the t-stat
CI calculations)
Month=rbind('Sep','Oct','Nov','Dec','Jan','Feb','Mar','Apr',"May",'June','Jul
','Aug')

#Total Observations
Nobsc=read.table('NobvcFinal.txt', header = FALSE, sep = ",", dec = ".")
#calculated in Matlab

#Independent Observations (N*)
Nstarc=read.table('Nstarvaluesc_Final.txt', header = FALSE, sep = ",", dec =
".") #calculated in Matlab

#Site M5 Stats
NobsM5=(Nobsc+Nobsw)
NstarM5=(Nstarc+Nstarw)
tstatvals95=c(1.95996,2.11991,2.05553,2.17881,2.17881,2.06866,1.95996,2.05183
,2.09302,2.10092,2.07961,2.04841)
```

```
stderror<-0
for(i in 1:12){stderror[i]<-
  ((tstatvals95[i]*M5sd[i])/sqrt(NstarM5[i]))}
stderror<-unlist(stderror,use.names=FALSE)
M5stats=cbind(Month, M5,M5sd,t(NobsM5),t(NstarM5),stderror)

#M8 Stats
NobsM8=(Nobsc8+Nobsw8)
NstarM8=(Nstarc8+Nstarw)
tstatvals95=c(2.07387,1.95996,2.04841,2.05954,1.95996,1.95996,1.95996,1.95996
,2.05553,2.04523,2.05183,1.95996)

stderror8<-0
for(i in 1:12){stderror8[i]<-
  ((tstatvals95[i]*M8sd[i])/sqrt(NstarM8[i]))}
stderror8<-unlist(stderror8,use.names=FALSE)
M8stats=cbind(Month, M8,M8sd,t(NobsM8),t(NstarM8),stderror8)

# M5 Cold Year Stats
#Standard error calculations based on tstat values in table for 95% CI and
N*(independent #observations
tstatvals95=c(2.04227, 2.57058, 2.13145, 2.44691, 2.26216, 2.08596, 2.10092,
2.09302, 2.17881, 2.16037, 2.13145, 2.17881)

stderror<-0
for(i in 1:12){stderror[i]<-
((tstatvals95[i]*M5sdc[i])/sqrt(Nstarc[i]))}
stderrorc<-unlist(stderror,use.names=FALSE)

#Compile all stats for M5 Cold years into a table
M5statsc=cbind(Month,M5c,M5sdc,t(Nobsc),t(Nstarc), stderrorc)

# M5 Warm Year Stats
tstatvals95=c(2.77645, 2.22814, 2.2284, 2.44691, 4.30265, 3.18245, 2.11991,
2.36462, 2.36462, 2.77645, 2.44691, 2.11991)

stderror<-0
for(i in 1:12){stderror[i]<-
  ((tstatvals95[i]*M5sdw[i])/sqrt(Nstarw[i]))}
stderrorw<-unlist(stderror,use.names=FALSE)

M5statsw=cbind(Month,M5w,M5sdw,t(Nobsw),t(Nstarw),stderrorw)

#M8 Cold Year Stats
tstatvals95=c(2.10982, 1.95996, 2.10092, 2.09302,1.95996, 1.95996, 2.10092,
1.95996,2.09302, 2.05954, 2.07961, 1.95996)

stderror<-0
for(i in 1:12){stderror[i]<-
  ((tstatvals95[i]*M8sdc[i])/sqrt(Nstarc8[i]))}
stderrorc8<-unlist(stderror,use.names=FALSE)

M8statsc=cbind(Month,M8c,M8sdc,t(Nobsc8), t(Nstarc8),stderrorc8)

# M8 Warm Year stats
```

```
tstatvals95=c(2.05183, 1.95996, 2.36462, 2.22814, 2.11991, 1.95996,
2.05183,2.16037, 2.13145, 2.30600, 2.57058,2.06866)

stderror<-0
for(i in 1:12){stderror[i]<-
  ((tstatvals95[i]*M8sdw[i])/sqrt(Nstarw8[i]))}
stderrorw8<-unlist(stderror,use.names=FALSE)

#Compile in table
M8statsw=cbind(Month,M8w,M8sdw,t(Nobsw8), t(Nstarw8), stderrorw8)

# Site M5 and M8 monthly climatology with standard error (95% CI)
plot(M5, ylab="Bottom Temperature(dec C)", xlab="
",col='blue',type='o',xaxt='n',lwd=2, ylim=c(-3,3))
axis(1, at=1:12,
labels=c('Sep','Oct','Nov','Dec','Jan','Feb','Mar','Apr',"May",'June','Jul','
Aug'))
par(new = TRUE)
plot(M5+stderror, axes=FALSE,xlab='',ylab='',col='blue', type='l',lty=2,
ylim=c(-3,3))
par(new = TRUE)
plot(M5-stderror, axes=FALSE,xlab='',ylab='',col='blue',type='l',lty=2,
ylim=c(-3,3))
par(new = TRUE)
plot(M8, ylab="Bottom Temperature(dec C)", xlab="
",col='black',type='o',xaxt='n',lwd=2, ylim=c(-3,3))
axis(1, at=1:12,
labels=c('Sep','Oct','Nov','Dec','Jan','Feb','Mar','Apr',"May",'June','Jul','
Aug'))
par(new = TRUE)
plot(M8+stderror8, axes=FALSE,xlab='',ylab='',col='black', type='l',lty=2,
ylim=c(-3,3))
par(new = TRUE)
plot(M8-stderror8, axes=FALSE,xlab='',ylab='',col='black',type='l',lty=2,
ylim=c(-3,3))
legend('topright', legend=c("M5", "M8"),col=c("blue", "black"),
pch=21,cex=0.8,lwd=2)
axis(1, at=1:12,
labels=c('Sep','Oct','Nov','Dec','Jan','Feb','Mar','Apr',"May",'June','Jul','
Aug'))

#Plot climatology with 95% CI across all years standardized
M5norm=M5-mean(M5)
M5norm=M5norm/sd(M5)
M8norm=M8-mean(M8)
M8norm=M8norm/sd(M8)
plot(M5norm, ylab="Bottom Temperature(dec C)", xlab="
",col='blue',type='o',xaxt='n',lwd=2, ylim=c(-3,3))
axis(1, at=1:12,
labels=c('Sep','Oct','Nov','Dec','Jan','Feb','Mar','Apr',"May",'June','Jul','
Aug'))
par(new = TRUE)
plot(M8norm, ylab="Bottom Temperature(dec C)", xlab="
",col='black',type='o',xaxt='n',lwd=2, ylim=c(-3,3))
axis(1, at=1:12,
labels=c('Sep','Oct','Nov','Dec','Jan','Feb','Mar','Apr',"May",'June','Jul','
Aug'))
```

```
legend('topright', legend=c("M5", "M8"),col=c("blue", "black"),
pch=21,cex=0.8,lwd=2)
axis(1, at=1:12,
labels=c('Sep','Oct','Nov','Dec','Jan','Feb','Mar','Apr',"May",'June','Jul','
Aug'))

#Plot Cold years M5 and M8 with standard error
y=t(c(1, 2, 3, 4, 5, 6, 7, 8, 9, 10, 11, 12))
#plot(M5c, ylab="Bottom Temperature (degC)", xlab="Calendar
Month",col='blue',type='o',xaxt='n',lwd=2)
plot(M5c, ylab="Bottom Temperature(dec C)", xlab="
",col='blue',type='o',xaxt='n',lwd=2, ylim=c(-3,5))
axis(1, at=1:12,
labels=c('Sep','Oct','Nov','Dec','Jan','Feb','Mar','Apr',"May",'June','Jul','
Aug'))
par(new = TRUE)
plot(M5c+stderrorc, axes=FALSE,xlab='',ylab='',col='blue', type='l',lty=2,
ylim=c(-3,5))
par(new = TRUE)
plot(M5c-stderrorc, axes=FALSE,xlab='',ylab='',col='blue',type='l',lty=2,
ylim=c(-3,5))
par(new = TRUE)
plot(M8c,col='black',ylab='',xlab='',axes=FALSE,type='o',lwd=2, ylim=c(-3,5))
par(new = TRUE)
plot(M8c+stderrorc8, axes=FALSE,xlab='',ylab='',type='l', lty=2,ylim=c(-3,5))
par(new = TRUE)
plot(M8c-stderrorc8, axes=FALSE,xlab='',ylab='',type='l',lty=2, ylim=c(-3,5))

#Plot Warm years M5 and M8 on same plot as Cold years
par(new = TRUE)
plot(M5w,col='red',ylab='',xlab='',axes=FALSE,type='o',lwd=2, ylim=c(-3,5))
par(new = TRUE)
plot(M5w+stderrorw, axes=FALSE,xlab='',ylab='',col='red',type='l',lty=2,
ylim=c(-3,5))
par(new = TRUE)
plot(M5w-stderrorw, axes=FALSE,xlab='',ylab='',col='red',type='l',lty=2,
ylim=c(-3,5))
par(new=TRUE)
plot(M8w,col='orange',ylab='',xlab='',axes=FALSE,type='o',lwd=2, ylim=c(-
3,5))
par(new = TRUE)
plot(M8w+stderrorw8, axes=FALSE,xlab='',ylab='',col='orange',type='l',lty=2,
ylim=c(-3,5))
par(new = TRUE)
plot(M8w-stderrorw8, axes=FALSE,xlab='',ylab='',col='orange',type='l',lty=2,
ylim=c(-3,5))
legend('topright', legend=c("M5 Cold Years", "M8 Cold Years","M5 Warm
Years","M8 Warm Years"),col=c("blue", "black",'red','orange'),
pch=21,cex=0.8,lty=1,lwd=2)

#Plot Cold and Warm years for Site M5 and M8 standardized
M5cnorm=M5c-mean(M5c)
M5cnorm=M5cnorm/sd(M5c)

M8cnorm=M8c-mean(M8c)
M8cnorm=M8cnorm/sd(M8c)
```

```
M5wnorm=M5w-mean(M5w)
M5wnorm=M5wnorm/sd(M5w)

M8wnorm=M8w-mean(M8w)
M8wnorm=M8wnorm/sd(M8w)

y=t(c(1, 2, 3, 4, 5, 6, 7, 8, 9, 10, 11, 12))
plot(M5cnorm, ylab="Bottom Temperature(dec C)", xlab="
",col='blue',type='o',xaxt='n',lwd=2, ylim=c(-3,5))
axis(1, at=1:12,
labels=c('Sep','Oct','Nov','Dec','Jan','Feb','Mar','Apr',"May",'June','Jul','
Aug'))
par(new = TRUE)
plot(M8cnorm,col='black',ylab='',xlab='',axes=FALSE,type='o',lwd=2, ylim=c(-
3,5))
par(new = TRUE)
plot(M5wnorm,col='red',ylab='',xlab='',axes=FALSE,type='o',lwd=2, ylim=c(-
3,5))
par(new = TRUE)
plot(M8wnorm,col='orange',ylab='',xlab='',axes=FALSE,type='o',lwd=2, ylim=c(-
3,5))
par(new = TRUE)
legend('topright', legend=c("M5 Cold Years", "M8 Cold Years","M5 Warm
Years","M8 Warm Years"), col=c("blue", "black",'red','orange'),
pch=21,cex=0.8,lty=1,lwd=2)

# BT Variance plotted
M5varc=(M5sdc*M5sdc)
M5varw=(M5sdw*M5sdw)
M8varc=(M8sdc*M8sdc)
M8varw=(M8sdw*M8sdw)

plot(M5varc,type='l',col='blue', ylim=c(0,3.5),xaxt='n',xlab=" ",
ylab='Variance ((deg C)^2)',lwd=2)
axis(1, at=1:12,
labels=c('Sep','Oct','Nov','Dec','Jan','Feb','Mar','Apr',"May",'June','Jul','
Aug'))
par(new = TRUE)
plot(M8varc,type='l',ylim=c(0,3.5),xlab='',ylab='',axes=FALSE,lwd=2)
par(new = TRUE)
plot(M5varw,type='l',col='red',ylim=c(0,3.5),xlab='',ylab='',axes=FALSE,lwd=2
)
par(new = TRUE)
plot(M8varw,type='l',col='orange',ylim=c(0,3.5),xlab='',ylab='',axes=FALSE,lw
d=2)
legend('topright', legend=c("M5 Cold Years", "M8 Cold Years","M5 Warm
Years","M8 Warm Years"), col=c("blue", "black",'red','orange'),
cex=0.8,lwd=2)

#BT Variance standardized
M5varc=(M5sdc*M5sdc) #M5 Cold year variance standardized
M5varcnorm=M5varc-mean(M5varc)
M5varcnorm=M5varcnorm/sd(M5varc)

M5varw=(M5sdw*M5sdw) #M5 Warm year variance standardized
M5varwnorm=M5varw-mean(M5varw)
M5varwnorm=M5varwnorm/sd(M5varw)
```

```
M8varc=(M8sdc*M8sdc) #M8 Cold year variance standardized
M8varcnorm=M8varc-mean(M8varc)
M8varcnorm=M8varcnorm/sd(M8varc)

M8varw=(M8sdw*M8sdw) #M8 Warm year variance standardized
M8varwnorm=M8varw-mean(M8varw)
M8varwnorm=M8varwnorm/sd(M8varw)

plot(M5varcnorm,type='l',col='blue', ylim=c(-2.5,2.5),xaxt='n',xlab=" ",
ylab='Variance ((deg C)^2)',lwd=2)
axis(1, at=1:12,
labels=c('Sep','Oct','Nov','Dec','Jan','Feb','Mar','Apr',"May",'June','Jul','
Aug'))
par(new = TRUE)
plot(M8varcnorm,type='l',ylim=c(-2.5,2.5),xlab='',ylab='',axes=FALSE,lwd=2)
par(new = TRUE)
plot(M5varwnorm,type='l',col='red',ylim=c(-
2.5,2.5),xlab='',ylab='',axes=FALSE,lwd=2)
par(new = TRUE)
plot(M8varwnorm,type='l',col='orange',ylim=c(-
2.5,2.5),xlab='',ylab='',axes=FALSE,lwd=2)
legend('topright', legend=c("M5 Cold Years", "M8 Cold Years","M5 Warm
Years","M8 Warm Years"),col=c("blue", "black",'red','orange'), cex=0.8,lwd=2)
```

Cold Pool Variables (Matlab)

```
% Site M5 and M8 Bottom Temperature freezing temperature days 2006-2019
% Time when sea ice at surface and water column is -1.7 degrees (time period:
March 1-April 31)

M5Marc=importdata('M5_Marcoldyear.txt');
M5Aprc=importdata('M5_Aprcoldyear.txt');
M5Marw=importdata('M5_Marwarmyear.txt');
M5Aprw=importdata('M5_Aprwarmyear.txt');

M8Marc=importdata('M8_Marcoldyear.txt');
M8Aprc=importdata('M8_Aprcoldyear.txt');
M8Marw=importdata('M8_Marwarmyear.txt');
M8Aprw=importdata('M8_Aprwarmyear.txt');

M5cold=[M5Marc; M5Aprc];
M5warm=[M5Marw; M5Aprw];
M5=[M5cold M5warm];
M8cold=[M8Marc; M8Aprc];
M8warm=[M8Marw; M8Aprw];
M8=[M8cold M8warm];

close all
%Set vector bin
mint=-2; %minimum temperature
maxt=2; %maximum temperature
dtemp=0.10; %resolution of temperature bins (degree)

tbins=[mint:dtemp:maxt]; %vector bin
%pre-allocate empty dataframe
M5freeze=zeros(1,14);
M8freeze=zeros(1,14);
```

```
site=M8; #designate site M5 or M8
[m,n]=size(site);

%Plot histogram of bottom temperature of days in spring
[t,x]=hist(site(:,:),tbins);
figure
plot(tbins,t);
xlabel('Bottom Temperature (deg C)');
ylabel('No. of Days per Spring Bottom Temp');
tcut=-1.7;
hold on;
dl=line([tcut tcut],[0 20],'color','k');
legend('2006','2007','2008','2009','2010','2011','2012','2013','2014','2015',
'2016','2017','2018','2019')

%Set threshold for -1.7 degrees
for i=1:n;
tcut=-1.7;
df=find(tbins<=tcut);
ndays_less_tcut=sum(t(df,i))
M5freeze(1,i)=ndays_less_tcut;
end

%Plot number of days meeting threshold per year
years=[2006:1:2019];
figure
plot(years,M5freeze)
ylabel('No. of Days Spring Freezing Bottom Temps');

%Cold Pool Presence
% M5 and M8 Bottom Temperature Cold Pool 2006-2019
% Time when bottom temperature is less than 2 degrees (time period: June 1-
August 31)
M5Junec=importdata('M5_Junec.txt');
M5Julyc=importdata('M5_Julyc.txt');
M5Augustc=importdata('M5_Augustc.txt');

M5Junew=importdata('M5_Junew.txt');
M5Julyw=importdata('M5_Julyw.txt');
M5Augustw=importdata('M5_Augustw.txt');

M8Junec=importdata('M8_Junec.txt');
M8Julyc=importdata('M8_Julyc.txt');
M8Augustc=importdata('M8_Augustc.txt');

M8Junew=importdata('M8_Junew.txt');
M8Julyw=importdata('M8_Julyw.txt');
M8Augustw=importdata('M8_Augustw.txt');

M5cold=[M5Junec; M5Julyc; M5Augustc];
M5warm=[M5Junew; M5Julyw; M5Augustw];
M5=[M5cold M5warm];

M8cold=[M8Junec; M8Julyc; M8Augustc];
M8warm=[M8Junew; M8Julyw; M8Augustw];
M8=[M8cold M8warm];
```

```
%set vector bin
mint=-2; %minimum temperature
maxt=4; %maximum temperature
dtemp=0.10; %resolution of temperature bins (degree)

tbins=[mint:dtemp:maxt]; %vector bin
M5coldpool=zeros(1,14);
M8coldpool=zeros(1,14);

site=M8; #designate site M5 or M8
[m,t]=size(site);

 %Plot histogram of bottom temperature during summer days
[y,x]=hist(site,tbins);
figure
plot(tbins,y);
xlabel('Bottom Temperature (deg C)');
ylabel('No. of Days per Summer Bottom Temp');
hold on;
tcut=2;
dl=line([tcut tcut],[0 12],'color','k');
legend('2006','2007','2008','2009','2010','2011','2012','2013','2014','2015',
'2016','2017','2018','2019')

 %Set Cold Pool 2 degree threshold
for i=1:14;
tcut=2;
df=find(tbins<=tcut)';
ndays_less_tcut=sum(y(df,i));
M8coldpool(1,i)=ndays_less_tcut;
end

 %Plot number of days Cold Pool present during Summer
years=[2006:1:2019];
figure
plot(years,M8coldpool)
ylabel('No. of Cold Pool Days');
ylim([0 100])
set(gca, 'XTick', (years) );
legend('Site M5','Site M8')
```

SSI (R)

```
# Load Packages
library(lubridate)
library(tidyr)
library(xts)
library(dplyr)

# NSIDC Ice Area and Extent
#Regional Ice Extent
#.csv files downloaded from (NSIDC.org) containing daily regional extent
calculations with each #column a different year
DailyRegionalE=read.csv(file=paste(datapath,"Sea_Ice_Index_Regional_Daily_Dat
a_JJ_plot_Extent2019.csv", sep="/"), header=TRUE, sep=",")
```

```
Extent<data.frame(Extent=c(DailyRegionalE[,"X2006"],DailyRegionalE[,"X2007"],
DailyRegionalE[,"X2008"], DailyRegionalE[,"X2009"], DailyRegionalE[,"X2010"],
DailyRegionalE[,"X2011"], DailyRegionalE[,"X2012"], DailyRegionalE[,"X2013"],
DailyRegionalE[,"X2014"], DailyRegionalE[,"X2015"], DailyRegionalE[,"X2016"],
DailyRegionalE[,"X2017"], DailyRegionalE[,"X2018"],DailyRegionalE[,"X2019"]))
Extent<-na.omit(Extent)

#Format Date
date=seq(as.Date("2006-01-01"), as.Date("2019-11-14"),by="days")
date<-as.Date(date,format="%d-%b-%Y")

#Compile in data frame
IceTS<-cbind(Extent,date)

#Regional SSI Area
#.csv files downloaded from (NSIDC.org) containing daily regional area
calculations with each #column a different year
DailyRegional=read.csv(file=paste(datapath,"Sea_Ice_Index_Regional_Daily_Data
_JJ_plot_Area2019.csv", sep="/"), header=TRUE, sep=",")
Area<data.frame(Area=c(DailyRegional[,"X2006"],DailyRegional[,"X2007"],DailyR
egional[,"X2008"], DailyRegional[,"X2009"], DailyRegional[,"X2010"],
DailyRegional[,"X2011"], DailyRegional[,"X2012"], DailyRegional[,"X2013"],
DailyRegional[,"X2014"], DailyRegional[,"X2015"], DailyRegional[,"X2016"],
DailyRegional[,"X2017"], DailyRegional[,"X2018"],DailyRegional[,"X2019"]))
Area<-na.omit(Area)

#Format Date
date=seq(as.Date("2006-01-01"), as.Date("2019-11-14"),by="days")
date<-as.Date(date,format="%d-%b-%Y")

#Compile in data frame
IceTS<-cbind(Area,date)

#Plot Bering Sea Ice Area
plot(IceTS$date,(IceTS$Area)/1000, type='l',xaxt="n",ylab="Bering Ice Area
(1000 km^2)", xlab="")
datelabels=seq(as.Date("2005", format="20%y"), tail(date,1), by="1 year")
axis.Date(side=1, date, at=datelabels, format="20%y")

# Local Site M5 Ice
#Local (M5 and M8) % cover and thickness (Time series compiled by K. Seger
completed by Jennifer Johnson)
#.csv files compiled from portal.aoos.org with %cover, thickness, and date in
columns
Localts=read.csv(file=paste(datapath,"2007_2018_NaN_Local1.csv", sep="/"),
header=TRUE, sep=",")
cover<-Localts$Percentcover
thickness<-Localts$thickness_cm

#Format Dates
dates <- with(Localts$Julian.Day,
strptime(paste(Localts$Year,Localts$JulianDay), "%Y %j "))
dates<-as.Date(dates,format="%d-%b-%Y")

#compile dataframe
LocalIceTS<-cbind(cover,dates)
LocalIceTS<-as.data.frame(LocalIceTS)
```

```
#Plot Local % Ice Cover for Site M5
plot(dateslocal,cover,type='l',xaxt="n",ylab="% Ice Cover", xlab='')
par(new=TRUE)
datelabels=seq(as.Date("2008-07-01", format="20%y"), tail(dateslocal,1),
by="1 year")
axis.Date(side=1, dateslocal, at=datelabels, format="20%y")

# Local Ice Site M8 Ice
datapath="Z:/Arctic Back up/Jennifer J/Ice/NSIDC/Local_M8"
datapath=("E:/Jennifer J_AM/Ice/NSIDC/Local_M8")

Localts8=read.csv(file=paste(datapath,"M8_Local_2012-2015_Final.csv",
sep="/"), header=TRUE, sep=",")
cover8<-Localts8$Percentcover
thickness8<-Localts8$thickness_cm

#Format Dates
dates8 <- with(Localts8$JulianDay,
strptime(paste(Localts8$Year,Localts8$JulianDay), "%Y %j "))
dates8<-as.Date(dates8,format="%d-%b-%Y")
dates8<-as.Date(Localts8$Date2,format="%d-%b-%Y")

LocalIceTS8<-cbind(cover8,dates8)
LocalIceTS8<-as.data.frame(LocalIceTS8)

#Plot Site M8 Local Ice cover %
plot(dates8,cover8,type='l',xaxt="n",ylab="% Ice Cover", xlab='')
par(new=TRUE)
datelabels=seq(as.Date("2011-08-22", format="20%y"), tail(dates8,1), by="1
year")
axis.Date(side=1, dates8, at=datelabels, format="%20%y")

#SSI statistics
# Monthly Averages (Local and Regional SSI)
#Monthly averages for all years 2008-2019
Icecover=tapply(Localts$Percent_cover, month(dates), mean,na.rm=TRUE)
RegionalArea=tapply(IceTS$Area, month(IceTS$date), mean,na.rm=TRUE)
RegionalExtent=tapply(IceTS$Extent, month(IceTS$date), mean,na.rm=TRUE)

# Climatologies Cold Years and Warm Years
#Monthly average and standard deviation (sigma) across Cold years Jan 1,
2006-Oct 1, 2013
RegionalAreac=tapply(IceTS$Area[1:2831], month(IceTS$date[1:2831]),
mean,na.rm=TRUE)
RegionalAreac=c(RegionalAreac[9:12], RegionalAreac[1:8])
RegionalAreacsd=tapply(IceTS$Area[1:2831], month(IceTS$date[1:2831]),
sd,na.rm=TRUE)
RegionalAreacsd=c(RegionalAreacsd[9:12], RegionalAreacsd[1:8]) #rearrange
months

#Monthly average across Warm years Oct 2, 2013-Nov 14, 2019
RegionalAreaw=tapply(IceTS$Area[2832:5066], month(IceTS$date[2832:5066]),
mean,na.rm=TRUE)
RegionalAreaw=c(RegionalAreaw[9:12], RegionalAreaw[1:8])
RegionalAreawsd=tapply(IceTS$Area[2832:5066], month(IceTS$date[2832:5066]),
sd,na.rm=TRUE)
```

```
RegionalAreawsd=c(RegionalAreawsd[9:12], RegionalAreawsd[1:8])

#Plot Regional SSI Area climatology by Cold and Warm years
plot((RegionalAreac/1000), type='o',xaxt="n",ylab="Bering Ice Area (1000 sq
km)", xlab="",ylim=c(-90,800),lwd=2)
par(new=TRUE)
plot(RegionalAreac/1000+RegionalAreacsd/1000,
axes=FALSE,xlab='',ylab='',col='black',type='o',lty=2, ylim=c(-90,800))
par(new=TRUE)
plot(RegionalAreac/1000-RegionalAreacsd/1000,
axes=FALSE,xlab='',ylab='',col='black',type='o',lty=2, ylim=c(-90,800))
par(new=TRUE)
plot(abs(RegionalAreaw/1000), type='o',xaxt="n",ylab="",
xlab="",axes=FALSE,col='red',ylim=c(-90,800),lwd=2)
par(new=TRUE)
plot(RegionalAreaw/1000+RegionalAreawsd/1000,
axes=FALSE,xlab='',ylab='',col='red',type='o',lty=2, ylim=c(-90,800))
par(new=TRUE)
plot(RegionalAreaw/1000-RegionalAreawsd/1000,
axes=FALSE,xlab='',ylab='',col='red',type='o',lty=2, ylim=c(-90,800))
par(new=TRUE)
axis(1, at=1:12,
labels=c('Sep','Oct','Nov','Dec','Jan','Feb','Mar','Apr',"May",'June','Jul','
Aug'))
legend("topright", legend=c("Cold Years", "Warm Years"),col=c(
"black",'red'), cex=0.8,lwd=2)

#Standardize SSI climatology values
RegionalAreacnorm=RegionalAreac-mean(RegionalAreac) #Cold years
RegionalAreacnorm=RegionalAreacnorm/sd(RegionalAreac)
RegionalAreawnorm=RegionalAreaw-mean(RegionalAreaw) #Warm years
RegionalAreawnorm=RegionalAreawnorm/sd(RegionalAreaw)

#Plot Standardized climatology values
plot((RegionalAreacnorm), type='o',xaxt="n",ylab="Bering Ice Area (sq km)",
xlab=" ",ylim=c(-3,3),lwd=2)
plot(abs(RegionalAreawnorm), type='o',ylab="",
xlab="",axes=FALSE,col='red',ylim=c(-3,3),lwd=2)
par(new=TRUE)
axis(1, at=1:12,
labels=c('Sep','Oct','Nov','Dec','Jan','Feb','Mar','Apr',"May",'June','Jul','
Aug'))
legend("topright", legend=c("Cold Years", "Warm Years"),col=c(
"black",'red'), cex=0.8,lwd=2)

#Plot 2011-2015 years (Regime Shift) M5 & M8 Local ice, Regional SSI, and
line at beginning of May showing reduction in Ice Cold to Warm years
par(col.axis='blue')
plot(IceTS$date[2060:3554],(IceTS$Area[2060:3554])/1000,
type='l',xaxt='n',ylim=c(0,1000),ylab="Bering Ice Area (1000 km^2)",
xlab="",col='blue')
par(new=TRUE)
Icecrossx=c(IceTS$date[2313],IceTS$date[2678], IceTS$date[3043],
IceTS$date[3408])
Icecrossy=c(IceTS$Area[2313]/1000,IceTS$Area[2678]/1000,
IceTS$Area[3043]/1000, IceTS$Area[3408]/1000)
```

```
plot(Icecrossx,Icecrossy,axes=FALSE,xlab=NA,ylab=NA,col='red',type='o',ylim=c
(0,1000),xaxt='n',xlim=c(IceTS$date[2060],IceTS$date[3554]))
par(new=TRUE)
par(col.axis='orange')
plot(LocalIceTS$dates[1422:2916],cover[1422:2916], type='l',
axes=F,xlab=NA,ylab=NA,col='orange')
par(col.axis='orange')
axis(side = 4)
mtext(side = 4, line = -1, '% Ice Cover')
par(new=TRUE)
par(col.axis='saddlebrown')
plot(dates8,cover8, type='l', axes=F,xlab=NA,ylab=NA,col='saddlebrown')
datelabels=seq(as.Date("2012-01-01", format="20%y"),
tail(LocalIceTS$dates,1), by="1 year")
par(col.axis='black')
axis.Date(side=1, date, at=datelabels, format="20%y", col='black')
legend("topleft",, legend=c("Bering Regional Ice", "Local M5 site Ice
(4km^2)","Local M8 site Ice (4km^2)"),col=c("blue", 'orange','saddlebrown'),
cex=0.65,lwd=2)
```

#Plot Regional SSI and Site M5 local %cover SSI overlaid 2008-11/7/2018 (All years)

```
par(col.axis='blue')
plot(IceTS$date[639:4704],(IceTS$Area[639:4704])/1000,
type='l',xaxt="n",ylab="Bering Ice Area (1000 km^2)", xlab="",col='blue')
par(new=TRUE)
par(col.axis='orange')
plot(LocalIceTS$dates,cover, type='l', axes=F,xlab=NA,ylab=NA,col='orange')
par(col.axis='orange')
axis(side = 4)
mtext(side = 4, line = -1, '% Ice Cover')
datelabels=seq(as.Date("2007-01-01", format="20%y"),
tail(LocalIceTS$dates,1), by="1 year")
par(col.axis='black')
axis.Date(side=1, date, at=datelabels, format="20%y", col='black')
legend("topleft",, legend=c("Bering Regional Ice", "Local M5 site Ice
(4km^2)"),col=c("blue", 'orange'), cex=0.8,lwd=2)
```

Bottom Temperature and SSI (Matlab)

```
%Plot Anomalies between Regimes for all years

%Bottom Temperature
%.xlsx version of bottom temperature .csv file
fname5 = 'M5_2005-2019_NaNs_T.xlsx';
M5in = readtable(fname5);
t5=table2array(M5in(1:5012,1)); %dates
m5=table2array(M5in(1:5012,2)); %values

 %find missing values and interpolate
df = find(isnan(m5)==1);
if numel(df),
    dg = find(isnan(m5)==0);
    m5(df) = interp1(t5(dg), m5(dg), t5(df));
end;

%Regional SSI
%.xlsx version of NSIDC .csv file
```

```
fnameI = 'ICE_AREA_T.xlsx';
Iin = readtable(fnameI);
ti5=table2array(Iin(1:5012,1)); %dates
i5=table2array(Iin(1:5012,2)); %values

%find missing values and interpolate
df = find(isnan(i5)==1);
if numel(df),
    dg = find(isnan(i5)==0);
    i5(df) = interp1(t5(dg), i5(dg), ti5(df));
end;

%Set demarcation for Regime shift
dcut=('10/1/2013');

%Choose Cold, Warm, or All years
coldid = input('use:  0] all data   1] cold years   2] warm years   ');
if coldid > 0
    if coldid == 1, df = find(t5 <= dcut); end;
    if coldid == 2, df = find(t5 >= dcut); end;
    t5 = t5(df);
    m5 = m5(df);
    i5 = i5(df);
    ti5 = ti5(df);
end;
nbands = input('number of freq. bands to average  ');

 %Calculate the monthly climatology (average for all years) and subtract from
each respective month to find anomalies.
[Y,MO,D,H,MI,S] = datevec(t5);
scm = zeros(12, 1);
sci = zeros(12, 1);
m5a = zeros(size(m5));
i5a = zeros(size(i5));
for n=1:12,
    df = find(MO == n);
    scm(n) = nanmean(m5(df));
    sci(n) = nanmean(i5(df));
    m5a(df) = m5(df)-scm(n);
    i5a(df) = i5(df)-sci(n);
end;

 %Designate Cold year BT and SSI
t5cold=t5;
m5cold=m5a;
ti5cold=ti5;
i5cold=i5a;

%Designate Warm year BT and SSI
t5warm=t5;
m5warm=m5a;
ti5warm=ti5;
i5warm=i5a;

%Plot Bottom temperature Cold year anomalies and Warm year anomalies
plot(t5cold, m5cold,'b');
hold on;
```

```
plot(t5warm, m5warm,'r');
datetick
ylabel('Bottom Temperature (deg C)')
x=length(m5cold);
y=length(m5warm);
total=x+y;
plot(repmat(0,1,total),'k');

%Plot SSI Cold year anomalies and Warm year anomalies
plot(t5cold, i5cold/1e5, 'b');
hold on;
plot(t5warm,i5warm/1e5,'r')
datetick
ylabel('Bering Sea Ice Area (1000 sq km)')
x=length(i5cold);
y=length(i5warm);
total=x+y;
plot(repmat(0,1,total),'k');


%% Plot Anomaly Cross-Corrletions with 95% CI

%Cold year Anomalies (BT vs SSI)
nlags0 = 500;
[lags0, corr] = crcor1(m5cold, i5cold, nlags0, 1, 1, 1);
%plot with bootstrap CI
figure(1)
clf;
plot(lags0, corr)
hold on;
dl = line([lags0(1) lags0(end)], [0 0], 'linestyle', '-', 'color', 'k');
set(gca, 'ylim', [-1 1]);
title('Cold Years M5 BT vs. Regional SSI');
xlabel('Lag (days)');
ylabel('Cross-Correlation');

%Warm year Anomalies (BT vs SSI)
[lags0, corr] = crcor1(m5warm, i5warm, nlags0, 1, 1, 1);
figure(2)
clf;
%plot with bootstrap CI
plot(lags0, corr)
hold on;
dl = line([lags0(1) lags0(end)], [0 0], 'linestyle', '-', 'color', 'k');
set(gca, 'ylim', [-1 1]);
title('Warm Years M5 BT vs. Regional SSI');
xlabel('Lag (days)');
ylabel('Cross-Correlation');

ci=0.95;
dt = 1;
nlags = 0;
nloops = 10000;
pid = 101;
fprintf(1, 'm5:\n');
[plags, pcu, pcl, m5nstar] = bootstrap_func(m5cold, m5cold, dt, nlags,
nloops, ci, pid);
```

```
pid = 102;
fprintf(1, 'i5:\n');
[plags, pcu, pcl, itnstar] = bootstrap_func(i5cold, i5cold, dt, nlags,
nloops, ci, pid);
pid = 103;
fprintf(1, 'm5 vs. i5:\n');
[plags, pcu, pcl, cnstar] = bootstrap_func(m5cold, i5cold, dt, nlags, nloops,
ci, pid);
fprintf(1, '\n');

figure(1);
dl = line([lags0(1) lags0(end)], [pcu pcu], 'linestyle', '--');
dl = line([lags0(1) lags0(end)], [pcl pcl], 'linestyle', '--');

ci=0.95;
dt = 1;
nlags = 0;
nloops = 10000;
pid = 101;
fprintf(1, 'm5:\n');

%Bootstrap function
%inputs: time series 1 & 2, each same length and No NaNs, sampling interval,
%number %of lags, number of simulations, confidence level, and figure
%designation
%outputs: lags with cross-correlation function, CI min/max, and number of
%independent observations per lag

[plags, pcu, pcl, m5nstar] = bootstrap_func(m5warm, m5warm, dt, nlags,
nloops, ci, pid);
pid = 102;
fprintf(1, 'i5:\n');
[plags, pcu, pcl, itnstar] = bootstrap_func(i5warm, i5warm, dt, nlags,
nloops, ci, pid);
pid = 103;
fprintf(1, 'm5 vs. i5:\n');
[plags, pcu, pcl, cnstar] = bootstrap_func(m5warm, i5warm, dt, nlags, nloops,
ci, pid);
fprintf(1, '\n');

figure(2);
dl = line([lags0(1) lags0(end)], [pcu pcu], 'linestyle', '--');
dl = line([lags0(1) lags0(end)], [pcl pcl], 'linestyle', '--');
```

% Cold and Warm year Anomalies BT and SSI

```
%% Calculate anomalies=ts(t)-monthly climatology (in Warm years or Cold
years) for BT & SSI

%Cold years (Climatology values calculated in R)
%Climatology month
sequence=('Sep','Oct','Nov','Dec','Jan','Feb','Mar','Apr',"May",'June','Jul',
'Aug')
      M5BTclimatologyc=[-0.7677762 -0.2114998  0.7867226  0.7545501 -
      0.6221264 -1.1791615 -1.5049017 -1.5900717 -1.4822767 -1.3490715 -
      1.1578474 -0.9963186 ];
```

```
      Regionalclimatologyc=[249.49181 2825.61665 25058.88178 154176.84633
      430920.76180 540467.99548 592272.43690 537439.06338 232396.04633
      22079.43996 912.74506 28.06925 ];

%Warm years (Climatology values calculated in R)
      M5BTclimatologyw=[1.66480290 1.67012387 2.93550385 2.78076844
      1.80286329 0.61572651 0.13457838 0.09799319 0.50346313 0.93008422
      1.30572235 1.47903798];
      Regionalclimatologyw=[225.1992 3636.2552 8401.5377 81531.3701
      207325.6181 284319.0242 298092.3168 224960.4935 43429.1268 6455.6897
      1114.4046 263.0777];

%Import Cold and Warm year BT and Ice by Month
      Jan=importdata('JanAnombycoldyearice.txt'); %Regional SSI
      Jan=importdata('JanAnombywarmyearice.txt');
      Jan=importdata('JanAnombycoldyear.txt'); %Bottom Temperature
      Jan=importdata('JanAnombywarmyear.txt');

%Compile all Cold year month (01/01/2008-9/30/2013) data by year
tsc=zeros(365:9);
for i=1:8
      tsc(i,:)=[Jan(:,i)' Feb(:,i)' Mar(:,i)' Apr(:,i)' May(:,i)' June(:,i)'
      July(:,i)' Aug(:,i)' Sept(:,i)' Oct(:,i)' Nov(:,i)' Dec(:,i)'];
end

x=9;
tsc(x,1:273)=[Jan(:,x)' Feb(:,x)' Mar(:,x)' Apr(:,x)' May(:,x)' June(:,x)'
July(:,x)' Aug(:,x)' Sept(:,x)'];
tsc(x,274:365)=NaN; %pad end of year with NANS since 2013 was not complete

%Compile all Warm year (10/1/2014-09/21/2019) data by year
tsc=zeros(365:5);
for i=1:5
  tsc(i,:)=[Jan(:,i)' Feb(:,i)' Mar(:,i)' Apr(:,i)' May(:,i)' June(:,i)'
  July(:,i)' Aug(:,i)' Sept(:,i)' Oct(:,i)' Nov(:,i)' Dec(:,i)'];
end
tsc1=([tsc(1,:), tsc(2,:), tsc(3,:) tsc(4,:) tsc(5,:) tsc(6,:) tsc(7,:)
tsc(8,:) tsc(9,:)]);
tsw1=([tsc(1,:), tsc(2,:), tsc(3,:) tsc(4,:) tsc(5,:)]); %SSI

%Write BT or SSI (Cold or Warm) anomaly for plotting
      csvwrite('WarmyearAnamolytsice.txt',tsw1);

%Import anomaly data
      Anomalyc=importdata('ColdyearAnamolyts.txt');
            Anomalyw=importdata('WarmyearAnamolyts.txt');
      Anomalyc1=importdata('ColdyearAnamolytsice.txt');
      Anomalyw1=importdata('WarmyearAnamolytsice.txt');

%All monthly anomalies by Regime for all years BT
      Anomalytotal=([Anomalyc, Anomalyw]);

%Plot monthly anomalies 2008-2019 BT
figure
plot(dates(1:3193),Anomalyc);
hold on
plot(dates(3194:5018),Anomalyw);
```

```
ylim([-3 3])
hold on;
title('M5 Bottom Temperature Cold and Warm Year Anomalies (2008-2019)')
xlabel('Year')
ylabel('Temperature(deg C)')
plot(repmat(0,1,length(Anomalytotal)));

#All monthly anomalies by regime for all years SSI
Anomalytotal1=([Anomalyc1, Anomalyw1]);

%Plot monthly anomalies 2008-2019 SSI
figure
plot(dates(1:3193),Anomalyc1./(10^5));
hold on
plot(dates(3194:5018),Anomalyw1./(10^5));
hold on;
title('Bering Sea Ice Area Cold and Warm Year Anomalies (2008-2019)')
xlabel('Year')
ylabel('Bering Sea Ice Area (1000 sq km)')
plot(repmat(0,1,length(Anomalytotal)));
```

Environmental Variable Cross-Correlations (Matlab)

```
%Bottom Temperature (Site M5 vs. M8)
M5 = readtable('M5_2005-2019_NaNs.csv');
M8 = readtable('M8_2005-2019_NaNs.csv');
dates=table2array(M5(:,1));
dates1=table2array(M8(:,1));
dates=table2array(M5(243:end,1));
dates=zeros([1,5013:5018]);

      %Cold years (01/01/2006-10/1/2013)
      ts1=table2array(M5(243:3073,2));
      ts2=table2array(M8(170:3000,2));

      %Warm years (10/2/2013-09/21/2019)
      ts1=table2array(M5(3074:5254,2));
      ts2=table2array(M8(3001:5181,2));

%SSI Data (Bering Regional vs. Site M5 local SSI)
RegionalIceArea=readtable('ICE_AREA.csv');
LocalIceCoverPercentage=readtable('M5_Ice_Cover_Final.csv');

      %Cold years 10/1/2007-10/01/2013
      ts1=table2array(RegionalIceArea(639:2831,2));
      ts2=table2array(LocalIceCoverPercentage(1:2193,2));

      %Warm years 10/2/2013-11/7/2018
      ts1=table2array(RegionalIceArea(2832:4694,2));
      ts2=table2array(LocalIceCoverPercentage(2194:4056,2));

%Bering Regional SSI correlation vs. BT (since 2008)
      %Cold years (01/01/2008-10/1/2013)
      ts1=table2array(M5(973:3437,2));
      ts2=table2array(RegionalIceArea(731:3195,2));

      %Warm years (10/2/2013-09/21/2019)
```

```
      ts1=table2array(M5(3438:end,2));
      ts2=table2array(RegionalIceArea(3196:5012,2));

%For autocorrelations send the same t.s. in t.s.2, (don't care about the
%negative lags so only run for positive side)
      Nstar=0;
      lagt=15;
      deltat=1;
      nlags=lagt./deltat;
      [lags,corr]=crcov1(ts1,ts2,nlags,deltat);
```

%Plot cross-correlations: Bottom Temperature site M5 vs. site M8, Bering Regional Ice
vs. site M5 Local Ice, Bering Regional Ice vs. site M5 Bottom Temperature

```
figure
plot(lags,corr);
 ylim([-1 1]);
title('Warm Years Regional SSI vs. Local M5 SSI') %change based on
correlation run
xlabel('Lag(days)')
ylabel('Cross-correlation')
grid on
grid minor
```

Crcov1.m (Matlab function)

```
function [lags,corr]=crcov1(ts1,ts2,nlags,deltat);
%positive lags at highest correlation peak indicate ts1 leading ts2

for j=0:nlags
    ng=0;
    sy=0;
    syy=0;
    sx=0;
    sxx=0;
    sxy=0;

    for n=1:(length(ts1)-j)
        x1=ts1(n);
        y1=ts2(n+j);
        if ~isnan(x1) && ~isnan(y1)
            ng=ng+1;
            sx=sx+x1;
            sy=sy+y1;
            sxy=sxy+x1*y1;
            sxx=sxx+x1*x1;
            syy=syy+y1*y1;
        end
    end

    cort=(sxy/ng)-((sx/ng)*(sy/ng));
    corb=((sxx/ng)-((sx/ng)^2))^0.5;
    corb1=((syy/ng)-((sy/ng)^2))^0.5;
    corr(nlags+1+j)=cort/(corb*corb1);
    lags=j.*deltat;
end

   for j=1:nlags
```

```
    ng=0;
    sy=0;
    syy=0;
    sx=0;
    sxx=0;
    sxy=0;

    for n=1:(length(ts1)-j)
        x1=ts1(n+j);
        y1=ts2(n);
        if ~isnan(x1) && ~isnan(y1)
            ng=ng+1;
            sx=sx+x1;
            sy=sy+y1;
            sxy=sxy+(x1*y1);
            sxx=sxx+(x1*x1);
            syy=syy+(y1*y1);
        end
    end

    cort=(sxy/ng)-((sx/ng)*(sy/ng));
    corb=((sxx/ng)-((sx/ng)^2))^0.5;
    corb1=((syy/ng)-((sy/ng)^2))^0.5;
    corr(nlags+1-j)=cort/(corb*corb1);
    %auto-correlation
    %lags(81-j)=j.*deltat;
    %cross-correlation
   lags=[-nlags:nlags].*deltat;
   end
end
```

Acoustic Backscatter (Matlab)

```
%Acoustic Backscatter time series Plotting

%% Select Directory to read in CSV files
d = uigetdir();
filePattern = fullfile(d, '*.csv');
file = dir(filePattern);
x={};
for k = 1 : numel(file)
      baseFileName = file(k).name;
      fullFileName = fullfile(d, baseFileName);
      x{k} = readtable(fullFileName);
end

%% Append all the files
Total=[];
for i=1:k
      Total= horzcat([Total; x{1,i}]);
end

%Append all months into one table
Totala=table2array(Total(:,4:7));
Totalb=table2array(Total(:,9:11));
Total=[Totala Totalb];
BS=array2table(Total);
```

```
%% Date format and order in chronological time
%Convert the date serial numbers to datetime
date=num2str(Total(:,4));
date=datetime(date,'InputFormat','yyyyMMdd');

%Assort dates in ascending order
BS{:,8}=date(:);
BS=sortrows(BS(:,:),8);

%Plot backscatter time series by day
figure
plot(BS{:,8},BS{:,6})

%loaded time series file
WC1=readtable('19FA_09SP_Backscatter_WC.csv');%final ts for M5
WC1=readtable('15FA_12FA_Backscatter_WCM8.csv');%final ts for M8
BS1=WC1{:,6}; %values
dates=WC1{:,8};%dates

%Plot ABC for site M5 or M8
figure
plot(dates,BS1./(10^-5));
grid on
grid minor
%ylim=[0 35];
%line([dates(1832) dates(1832)], [0 25], 'Color', [1 0 0]); %M5
line([dates(772) dates(772)], [0 35], 'Color', [1 0 0]); %M8
ylabel('Area Backscattering Coefficient/10^-5 (m^2m^-2)')

%Plot Mean Sv for Site M5 or M8
SV=WC1{:,1};
SV=movmean(SV, 7, 'omitnan'); %average for daily
figure
plot(dates,SV);
grid on
ylabel(' Mean Sv (m^2m^3)')

%Plot site M5 and M8 overlaid
M5=readtable('19FA_09SP_Backscatter_WC.csv');
M8=readtable('15FA_12FA_Backscatter_WCM8.csv');

BS1=M5{:,6};
dates=M5{:,8};  %specify range that equals M8
BS2=M8{:,6};
dates2=M8{:,8};

figure
plot(dates,BS1./(10^-5));
hold on
plot(dates2,BS2./(10^-5));
grid on
ylabel('Area Backscattering Coefficient/10^-5 (m^2m^-2)')
legend('M5','M8')

%Delta-Sv TS compilation
 %% Select Directory to read in CSV files
d = uigetdir();
```

```
filePattern = fullfile(d, '*.csv');
file = dir(filePattern);
x={};
for k = 1 : numel(file)
      baseFileName = file(k).name;
      fullFileName = fullfile(d, baseFileName);
      x{k} = readtable(fullFileName);
end

%% Append all the files (if not all months are in one file)
months=k/2 ; %how many months
Total200=[]; %200 kHz
for i=1:months
Total200= horzcat([Total200; x{1,i}]);
end

Total460=[]; %460 kHz
for i=(months+1):k
Total460= horzcat([Total460; x{1,i}]);
end

%If All months are in one files
Total200=x{1,1};
Total460=x{1,2};

%Average rows (Entire WC every 30 minutes)

[m,n]=size(Total200);

for i=1:m
      Total1(i,1)=mean(Total200{i,2:13},'omitnan');
end

for i=1:m
      Total2(i,1)=mean(Total460{i,2:13},'omitnan');
end

%Dates for new exports
dates=Total460{:,5};
dates = datetime(dates, 'ConvertFrom', 'yyyymmdd');
dates=datenum(dates);

%Calculate Delta-Sv or dB differences
dbdiff=((Total460{:,4})-(Total200{:,4})); %for months all in one file
dbdiff(dbdiff <= -30 | dbdiff >= 30) = NaN; %For erroneous data

dbdiff=(Total2-Total1); %for months in separate files

dbdiff1=[dbdiff dates]; %compile data frame
dbdiff1=array2table(dbdiff1);

%export each year Delta-Sv files
writetable(dbdiff1,'19FA_dbdiff.csv','WriteRowNames',true);

%Import all years to compile for Delta-Sv file
dates=datetime(dbdiff{:,2},'ConvertFrom','datenum');
dbdiff{:,3}=dates(:,1);
```

```
dbdiff=sortrows(dbdiff(:,:),3); %sort in chronological order
dbdiff{:,1}=movmean(dbdiff{:,1},1440,'omitnan');

 %Plot Delta-Sv Plots for each site
plot(dbdiff{:,3},dbdiff{:,1});
grid on
grid minor
ylabel('M8 delta SV (460kHz-200kHz)')
line([dbdiff{27911,3} dbdiff{27911,3}], [-20 20], 'Color', [1 0 0]);  %Regime
shift

figure
plot(dbdiff{:,3},dbdiff{:,1})
grid on
grid minor
ylabel('M5 delta SV (460kHz-200kHz)')
ylim([-20 20])
line([dbdiff{85248,3} dbdiff{85248,3}], [-20 20], 'Color', [1 0 0]); %Regime
shift

% Variance BT (demeaned by month)
%Cold years (9/26/2008-10/1/2013)
%Warm yers (10/2/2013-11/7/2018)
%Site M5
fname5 = 'M5_2005-2019_NaNs_T.xlsx';
fname6='M8_2005-2019_NaNs.xlsx';
      M5in = xlsread(fname5);
      M5in = readtable(fname5);
      M8in= xlsread(fname6);
      M8in= readtable(fname6);

 %M5 BT Dates
t5=table2array(M5in(1:5012,1));
t5=t5(1000:2831,1);% M5 Cold years
t5=t5(2832:4694,1); %M5 Warm years

 %M8 BT Dates
t5=table2array(M8in(1:5182,1));
t5=t5(1169:3000,1);% M8 Cold years
t5=t5(3001:4863,1); %M8 Warm years

 %M5 BT values
m5=table2array(M5in(1:5012,2)); %M5
m5=m5(1000:2831,1); %M5 Cold years
m5=m5(2832:4694,1); %M5 Warm years

 %M8 BT values
m5=table2array(M8in(1:5182,2)); %M8
m5=m5(1169:3000,1);% M8 Cold years
m5=m5(3001:4863,1); %M8 Warm years

%Find data gaps and interpolate
df = find(isnan(m5)==1);
if numel(df),
    dg = find(isnan(m5)==0);
    m5(df) = interp1(t5(dg), m5(dg), t5(df));
end;
```

```
[Y,MO,D,H,MI,S] = datevec(t5);
scm = zeros(12, 6);
m5a = zeros(365,6);

%Compute monthly climatology
for n=1:12,
   df = find(MO == n);
   scm(n) = nanmean(m5(df));
   m5a(df) = m5(df)-scm(n);
end;
M5variance=zeros(1,12);
for n=1:12,
    df = find(MO == n);
    M5variance(1,n) = var(m5a(df));
end;

M8variancewarm=[M5variance(9:12), M5variance(1:8)];

%Delta-SV data for computing variance demeaned
fnameI = '19FA_09FAdbdiff.xlsx';
fnameII='12_15FAdbdiffM8_Final.xlsx';
Iin = readtable(fnameI);

%M5 Delta-Sv date
 ti5=table2array(Iin(1:156013,3));
 ti5=ti5(1:85248,1); %M5 Cold
 ti5=ti5(85246:156013,1); %M5 Warm

%M8 Delta-Sv date
Iin=readtable(fnameII); %M8
ti5= table2array(Iin(1:53345,3)); %M8
ti5=ti5(1:27911,1); %M8 Cold
 ti5=ti5(27912:53345,1); %M8 Warm

%M5 Delta-Sv values
 i5=table2array(Iin(1:156013,1)); %M5
i5=i5(1:85248,1); %M5 Cold
 i5=i5(85246:156013,1);%M5 cold

 %M8 Delta-Sv values
i5=table2array(Iin(1:53345,1)); %M8
i5=i5(1:27911,1); %M8 Cold
i5=i5(27912:53345,1); %M8 Warm

%Find repeated dates
[x, index] = unique(ti5);
ti5=ti5(index);
i5=i5(index);

%Find gaps and interpolate in values
df = find(isnan(i5)==1);
if numel(df),
    dg = find(isnan(i5)==0);
    i5(df) = interp1(ti5(dg), i5(dg), ti5(df));
end;
```

```
[Y,MO,D,H,MI,S] = datevec(ti5);
i5a = zeros(size(i5));
sci = zeros(12, 1);
 %calculate Delta-Sv anomalies
for n=1:12,
    df = find(MO == n);
    sci(n) = nanmean(i5(df));
    i5a(df) = i5(df)-sci(n);
end;

M5bsvariance=zeros(1,12);

%Calculate variance
for n=1:12,
    df = find(MO == n);
    M5bsvariance(1,n) = var(i5a(df));
end;

M8bsvariancewarm=[M5bsvariance(9:12), M5bsvariance(1:8)];
```

%Plot Delta-Sv and bottom temperature monthly variance

```
figure
y=1:12;
plot(y,M5variancecold,'--','Color', [0 0 1],'LineWidth',1.5)
hold on
plot(y,M5variancewarm,'--','Color', [1 0 0],'LineWidth',1.5)
hold on
plot(y,M8variancecold,'--', 'Color', [0 0 0],'LineWidth',1.5)
hold on
plot(y,M8variancewarm,'--','Color', [1    0.5   0],'LineWidth',1.5)
hold on
plot(y,M5bsvariancecold./25, 'Color', [0 0 1],'LineWidth',2)
hold on
plot(y,M5bsvariancewarm./25,'Color', [1 0 0],'LineWidth',2)
hold on
plot(y,M8bsvariancecold./25, 'Color', [0 0 0],'LineWidth',2)
hold on
plot(y,M8bsvariancewarm./25,'Color', [1    0.5   0],'LineWidth',2)
legend('M5 BT Cold','M5 BT Warm','M8 BT Cold','M8 BT Warm','M5 BS Cold','M5
BS Warm', 'M8 BS Cold','M8 BS Warm')
ylabel('Variance/25 (db^2)');
xticks([1:12]);
xticklabels({'Sep','Oct','Nov','Dec','Jan','Feb','Mar','Apr','May','Jun','Jul
','Aug'})
xlim([1 12])
ylim([0 4])
```

#Acoustic Backscatter statistics (R)

```
# Site M5 imports
datapath="E:/Jennifer J_AM/M5/AWCP/WC_Exports"
BSCold=read.csv(file=paste(datapath,"13FA_09SP_Backscatter_WC_FINAL.csv",
sep="/"), header=TRUE, sep=",")
BSWarm=read.csv(file=paste(datapath,"19FA_13FA_Backscatter_WC_FINAL.csv",
sep="/"), header=TRUE, sep=",")

#Format Date
datecold=as.character(BSCold$Var8)
```

```
datecold=seq(as.Date("2008-09-26"), as.Date("2013-10-01"),by="days")
datecold<-as.Date(datecold,format="%d-%b-%y")
datewarm=as.character(BSWarm$Var8)
datewarm=seq(as.Date("2013-10-02"), as.Date("2018-11-07"),by="days")
datewarm<-as.Date(datewarm,format="%d-%b-%y")

#Compute Climatology
BSColdClimatology=tapply(BSCold$Total6, month(datecold), mean,na.rm=TRUE)
#Average (mu)
BSColdClimatologysd=tapply(BSCold$Total5, month(datecold), mean,na.rm=TRUE)
#Average (mu)
BSWarmClimatology=tapply(BSWarm$Total6, month(datewarm), mean,na.rm=TRUE)
#Average (mu)
BSWarmClimatologysd=tapply(BSWarm$Total5, month(datewarm), mean,na.rm=TRUE)
#Average (mu)

#Plot ABC Climatology by Warm and Cold years and standard deviation
plot(BSColdClimatology/(10^-05),ylab='Area Backscattering Coefficient/10^-5
(m^2m^-2) ',xlab=" ",col='blue',type='o',xaxt='n',lwd=2,ylim=c(0,4.5))
axis(1, at=1:12,
labels=c('Jan','Feb','Mar','Apr','May','June','July','Aug',"Sept",'Oct','Nov'
,'Dec'))
par(new=TRUE)
plot(BSWarmClimatology/(10^-05),xlab=" ",col='red',type='o',xaxt='n',ylab
='',lwd=2,ylim=c(0,4.5))
par(new=TRUE)
plot((BSColdClimatology+BSColdClimatologysd)/(10^-
05),col='blue',type='l',xaxt='n',ylab ='',xlab='',lty=2,ylim=c(0,4.5))
par(new=TRUE)
plot((BSColdClimatology-BSColdClimatologysd)/(10^-
05),col='blue',type='l',xaxt='n',ylab ='',xlab='',lty=2,ylim=c(0,4.5))
par(new=TRUE)
plot((BSWarmClimatology+BSWarmClimatologysd)/(10^-
05),col='red',type='l',xaxt='n',ylab ='',xlab='',lty=2,ylim=c(0,4.5))
par(new=TRUE)
plot((BSWarmClimatology-BSWarmClimatologysd)/(10^-
05),col='red',type='l',xaxt='n',ylab ='',xlab='',lty=2,ylim=c(0,4.5))
par(new=TRUE)
legend('topright', legend=c("Cold Years", "Warm Years"),col=c("blue", "red"),
pch=21, cex=0.8, lwd=2)

#Site M8 Imports
datapath="E:/Jennifer J_AM/M8/AWCP/WC_Exports"
BSColdM8=read.csv(file=paste(datapath,"M8_Backscatter_Cold_FA11_FA13.csv",
sep="/"), header=TRUE, sep=",")
BSWarmM8=read.csv(file=paste(datapath,"M8_Backscatter_Warm_FA13_FA15.csv",
sep="/"), header=TRUE, sep=",")

#Format Dates
datecoldM8=as.character(BSColdM8$Var8)
datecoldM8=seq(as.Date("2011-08-22"), as.Date("2013-10-01"),by="days")
datecoldM8<-as.Date(datecoldM8,format="%d-%b-%y")
datewarmM8=as.character(BSWarmM8$Var8)
datewarmM8=seq(as.Date("2013-10-02"), as.Date("2015-09-24"),by="days")
datewarmM8<-as.Date(datewarmM8,format="%d-%b-%y")

#Compute Climatologies Average and standard deviation
```

```
BSColdClimatologyM8=tapply(BSColdM8$Total6, month(datecoldM8),
mean,na.rm=TRUE)
BSColdClimatologysdM8=tapply(BSColdM8$Total5, month(datecoldM8),
std,na.rm=TRUE)
BSWarmClimatologyM8=tapply(BSWarmM8$Total6, month(datewarmM8),
mean,na.rm=TRUE)
BSWarmClimatologysdM8=tapply(BSWarmM8$Total5, month(datewarmM8),
std,na.rm=TRUE)
```

#Plot Climatologies by Warm and Cold with standard deviation

```
plot(BSColdClimatologyM8/(10^-05),ylab='Area Backscattering Coefficient/10^-5
(m^2m^-2) ',xlab=" ",col='black',type='o',xaxt='n',lwd=2,ylim=c(0,4.5))
axis(1, at=1:12,
labels=c('Jan','Feb','Mar','Apr','May','June','July','Aug',"Sept",'Oct','Nov'
,'Dec'))
par(new=TRUE)
plot(BSWarmClimatologyM8/(10^-05),xlab="
",col='orange',type='o',xaxt='n',ylab ='', lwd=2, ylim=c(0,4.5))
par(new=TRUE)
plot((BSColdClimatologyM8+BSColdClimatologysdM8)/(10^-05),
col='black',type='l', xaxt='n', ylab ='', xlab='', lty=2,ylim=c(0,4.5))
par(new=TRUE)
plot((BSColdClimatologyM8-BSColdClimatologysdM8)/(10^-
05),col='black',type='l',xaxt='n',ylab ='',xlab='',lty=2,ylim=c(0,4.5))
par(new=TRUE)
plot((BSWarmClimatologyM8+BSWarmClimatologysdM8)/(10^-05), col='orange',
type='l', xaxt='n', ylab ='', xlab='',lty=2,ylim=c(0,4.5))
par(new=TRUE)
plot((BSWarmClimatologyM8-BSWarmClimatologysdM8)/(10^-
05),col='orange',type='l',xaxt='n',ylab ='',xlab='',lty=2,ylim=c(0,4.5))
par(new=TRUE)
legend('topleft', legend=c("M5 Cold Years", "M8 Cold Years",'M5 Warm
Years','M8 Warm Years'),col=c("blue",'black', "red",'orange'),
pch=21,cex=0.8,lwd=2)

#Site M5 and M8 Backscatter Climatology Standardized
#Site M5 Cold
      BSColdClimatologynorm=BSColdClimatology-mean(BSColdClimatology)
      BSColdClimatologynorm=BSColdClimatologynorm/sd(BSColdClimatology)
#Site M5 Warm
      BSWarmClimatologynorm=BSWarmClimatology-mean(BSWarmClimatology)
      BSWarmClimatologynorm=BSWarmClimatologynorm/sd(BSWarmClimatology)
#Site M8 Cold
      BSColdClimatologynormM8=BSColdClimatologyM8-mean(BSColdClimatologyM8)
      BSColdClimatologynormM8=BSColdClimatologynormM8/sd(BSColdClimatologyM8)
#Site M8 Warm
      BSWarmClimatologynormM8=BSWarmClimatologyM8-mean(BSWarmClimatologyM8)
      BSWarmClimatologynormM8=BSWarmClimatologynormM8/sd(BSWarmClimatologyM8)
```

#Plot Site M5 and M8 Backscatter Standardized monthly climatology by Cold and Warm years

```
plot(BSColdClimatologynorm,ylab='Area Backscattering Coefficient (m^2m^-2)
',xlab=" ", col='blue', type='o',xaxt='n',lwd=2,ylim=c(-2,3))
axis(1, at=1:12,
labels=c('Jan','Feb','Mar','Apr','May','June','July','Aug',"Sept",'Oct','Nov'
,'Dec'))
par(new=TRUE)
```

```
plot(BSWarmClimatologynorm,xlab=" ",col='red',type='o',xaxt='n',ylab
='',lwd=2,ylim=c(-2,3))
par(new=TRUE)
plot(BSColdClimatologynormM8,xlab=" ",col='black',type='o',xaxt='n',ylab
='',lwd=2,ylim=c(-2,3))
par(new=TRUE)
plot(BSWarmClimatologynormM8,xlab=" ",col='orange',type='o',xaxt='n',ylab
='', lwd=2, ylim=c(-2,3))
legend('topleft', legend=c("M5 Cold Years", "M8 Cold Years",'M5 Warm
Years','M8 Warm Years'), col=c("blue",'black', "red",'orange'),
pch=21,cex=0.8,lwd=2)
```

Environmental and Acoustic Data (R)

```
# Climatology BT, Ice, and Backscatter Cold Years
#Site M5 Coldyears -> September 26, 2008-Oct 1, 2013
#Site M8 Cold years->August 22, 2011-Oct1, 2013

#Backscatter
#.csv files compiled of ABC , Mean Sv, and dates in columns
BSCold=read.csv(file=paste(datapath,"13FA_09SP_Backscatter_WC_FINAL.csv",
sep="/"), header=TRUE, sep=",")
BSColdClimatology=tapply(BSCold$Total6, month(date), mean,na.rm=TRUE)
#Average (mu)
BSColdClimatology=c(BSColdClimatology[9:12],BSColdClimatology[1:8])

#Site M5 BT
BT=read.csv(file=paste(datapath,"M5_2005-2019_NaNs.csv", sep="/"),
header=TRUE, sep=",")
Temp=BT$Temperature
date=BT$Date
date<-as.Date(date,format="%m/%d/%Y")
M5c=tapply(BT$Temperature[243:3073], month(date[243:3073]), mean,na.rm=TRUE)
M5c=c(M5c[9:12],M5c[1:8])

#Site M8 BT
M8c=tapply(BT1$Temperature[2229:3000], month(date1[2229:3000]),
mean,na.rm=TRUE)
M8c=c(M8c[9:12],M8c[1:8])

#Regional SSI
RegionalAreac=tapply(IceTS$Area[1:2831], month(IceTS$date[1:2831]),
mean,na.rm=TRUE)
RegionalAreac=c(RegionalAreac[9:12], RegionalAreac[1:8])
```

#Plot Site M5 Climatology Backscatter, BT, and Regional SSI Cold Years

```
par(col.axis="green")
plot(BSColdClimatology/(10^-05),ylab='Area Backscattering Coefficient/10^-5
(m^2m^-2) ',xlab="",col='green',type='o',xaxt='n',lwd=2,ylim=c(0,3.5))
par(new=TRUE)
plot(M5c, xlab="",col='black',type='o',xaxt='n',lwd=2, ylim=c(-
2,4.5),ylab='',yaxt='n')
#plot(M8c, xlab="",col='black',type='o',xaxt='n',lwd=2, ylim=c(-
2,4.5),ylab='',yaxt='n')
par(col.axis="black")
axis(side = 4)
mtext(side = 4, line = -1, 'Bottom Temperature (deg C)')
par(new=TRUE)
```

```
plot((RegionalAreac/1000), type='o',xaxt="n", xlab="", yaxt='n', lwd=2,
col='blue', ylab='', ylim=c(0,650), yaxt='n')
par(col.axis="black")
par(new=TRUE)
legend('topright', legend=c("200 kHz Backscatter", "Bottom
Temperature",'Bering Sea Ice'), col=c('green',"black", "blue"), pch=21,
cex=0.8,lwd=2)
axis(1, at=1:12,
labels=c('Sep','Oct','Nov','Dec','Jan','Feb','Mar','Apr',"May",'June','Jul','
Aug'))

#M5 BT Ice and Backscatter Cold Years Climatology Standardized
BSColdClimatologynorm=BSColdClimatology-mean(BSColdClimatology)
BSColdClimatologynorm=BSColdClimatologynorm/sd(BSColdClimatology)
M5cnorm=M5c-mean(M5c)
M5cnorm=M5cnorm/sd(M5c)
RegionalAreacnorm=RegionalAreac-mean(RegionalAreac)
RegionalAreacnorm=RegionalAreacnorm/sd(RegionalAreac)

#Plot Site M5 Standardized Climatology Backscatter, BT, and Regional SSI Cold
Years
par(col.axis="green")
plot(BSColdClimatologynorm,ylab='Area Backscattering Coefficient(m^2m^-2)
',xlab=" ",col='green',type='o',xaxt='n',lwd=2,ylim=c(-3,3))
par(new=TRUE)
plot(M5cnorm, xlab=" ",col='black',type='o',xaxt='n',lwd=2, ylim=c(-
3,3),ylab='',yaxt='n')
#plot(M8cnorm, xlab=" ",col='black',type='o',xaxt='n',lwd=2, ylim=c(-
3,3),ylab='',yaxt='n')
par(col.axis="black")
axis(side = 4)
mtext(side = 4, line = -1, 'Bottom Temperature (deg C)')
par(new=TRUE)
plot((RegionalAreacnorm), type='o',xaxt="n", xlab="
",yaxt='n',lwd=2,col='blue',ylab='',ylim=c(-3,3),yaxt='n')
par(col.axis="black")
par(new=TRUE)
legend('topright', legend=c("200 kHz Backscatter", "Bottom
Temperature",'Bering Sea Ice '), col=c('green',"black", "blue"),
pch=21,cex=0.8, lwd=2)
axis(1, at=1:12,
labels=c('Sep','Oct','Nov','Dec','Jan','Feb','Mar','Apr',"May",'June','Jul','
Aug'))

# BT, Ice, and Backscatter Climatology Warm Years
#Site M5 Warm Years -> Oct 2, 2013- Nov 7, 2018
#Site M8 Warm Years-> OCt 2, 2013-sept 24, 2015
BSWarm=read.csv(file=paste(datapath,"19FA_13FA_Backscatter_WC_FINAL.csv",
sep="/"), header=TRUE, sep=",")
date=BSWarm$Var8
date<-as.Date(date,format="%d-%b-%y")

#Backscatter
BSWarmClimatology=tapply(BSWarm$Total6, month(date), mean,na.rm=TRUE)
#Average (mu)
BSWarmClimatology=c(BSWarmClimatology[9:12],BSWarmClimatology[1:8])
```

```
#Site M5 BT
BT=read.csv(file=paste(datapath,"M5_2005-2019_NaNs.csv", sep="/"),
header=TRUE, sep=",")
Temp=BT$Temperature
date=BT$Date
date<-as.Date(date,format="%m/%d/%Y")
M5w=tapply(BT$Temperature[3074:5254], month(date[3074:5254]),
mean,na.rm=TRUE)
M5w=c(M5w[9:12],M5w[1:8])

#Site M8 BT
M8w=tapply(BT1$Temperature[3001:3723], month(date1[3001:3723]),
mean,na.rm=TRUE)
M8w=c(M8w[9:12],M8w[1:8])

#Regional SSI
RegionalAreaw=tapply(IceTS$Area[2832:5023], month(IceTS$date[2832:5023]),
mean,na.rm=TRUE)
RegionalAreaw=c(RegionalAreaw[9:12], RegionalAreaw[1:8])

#Plot Warm year Backscatter, BT, and SSI Climatology
par(col.axis="green")
plot(BSWarmClimatology/(10^-05),ylab='Area Backscattering Coefficient/10^-5
(m^2m^-2) ',xlab="",col='green',type='o',xaxt='n',lwd=2,ylim=c(0,3))
par(new=TRUE)
plot(M5w, xlab="",col='black',type='o',xaxt='n',lwd=2, ylim=c(-
2,4.5),ylab='',yaxt='n')
#plot(M8w, xlab="",col='black',type='o',xaxt='n',lwd=2, ylim=c(-
2,4.5),ylab='',yaxt='n')
par(col.axis="black")
axis(side = 4)
mtext(side = 4, line = -1, 'Bottom Temperature (deg C)')
par(new=TRUE)
plot((RegionalAreaw/1000), type='o',xaxt="n",
xlab="",yaxt='n',lwd=2,col='blue',ylab='',ylim=c(0,650),yaxt='n')
par(col.axis="black")
par(new=TRUE)
legend('topright', legend=c("200 kHz Backscatter", "Bottom
Temperature",'Bering Sea Ice'), col=c('green',"black", "blue"),
pch=21,cex=0.8,lwd=2)
axis(1, at=1:12,
labels=c('Sep','Oct','Nov','Dec','Jan','Feb','Mar','Apr',"May",'June','Jul','
Aug'))

#M5 Climatology BT, Ice, and Backscatter Warm Years Standardized
BSWarmClimatologynorm=BSWarmClimatology-mean(BSWarmClimatology)
BSWarmClimatologynorm=BSWarmClimatologynorm/sd(BSWarmClimatology)
M5wnorm=M5w-mean(M5w)
M5wnorm=M5wnorm/sd(M5w)
RegionalAreawnorm=RegionalAreaw-mean(RegionalAreaw)
RegionalAreawnorm=RegionalAreawnorm/sd(RegionalAreaw)

#Plot Warm year Backscatter, BT, and SSI Standardized Climatology
par(col.axis="green")
plot(BSWarmClimatologynorm,ylab='Area Backscattering Coefficient(m^2m^-2)
',xlab=" ",col='green',type='o',xaxt='n',lwd=2,ylim=c(-3,3))
par(new=TRUE)
```

```
plot(M5wnorm, xlab=" ",col='black',type='o',xaxt='n',lwd=2, ylim=c(-
3,3),ylab='',yaxt='n')
#plot(M8wnorm, xlab=" ",col='black',type='o',xaxt='n',lwd=2, ylim=c(-
3,3),ylab='',yaxt='n')
par(col.axis="black")
axis(side = 4)
mtext(side = 4, line = -1, 'Bottom Temperature (deg C)')
par(new=TRUE)
plot((RegionalAreawnorm), type='o',xaxt="n", xlab="
",yaxt='n',lwd=2,col='blue',ylab='',ylim=c(-3,3),yaxt='n')
par(col.axis="black")
par(new=TRUE)
legend('topright', legend=c("200 kHz Backscatter", "Bottom
Temperature",'Bering Sea Ice '), col=c('green',"black", "blue"),
pch=21,cex=0.8,lwd=2)
axis(1, at=1:12,
labels=c('Sep','Oct','Nov','Dec','Jan','Feb','Mar','Apr',"May",'June','Jul','
Aug'))

#Overlaid plot Regional & Local SSI, BT, and Backscatter for site M8
07/18/2012-06/17/2013

#Backscatter M8
BS=read.csv(file=paste(datapath,"15FA_12FA_Backscatter_WCM8.csv", sep="/"),
header=TRUE, sep=",")
dateBS=as.character(BS$Var8)
dateBS=seq(as.Date("2011-08-22"), as.Date("2015-09-24"),by="days")
dateBS<-as.Date(dateBS,format="%d-%b-%y")

#BT
BT=read.csv(file=paste(datapath,"M8_2005-2019_NaNs.csv", sep="/"),
header=TRUE, sep=",")
Temp=BT$Temperature
dateBT=BT$Date
dateBT<-as.Date(dateBT,format="%m/%d/%Y")

#Local Ice M8
datapath="Z:/Arctic Back up/Jennifer J/Ice/NSIDC/Local_M8"
datapath=("E:/Jennifer J_AM/Ice/NSIDC/Local_M8")
Localts8=read.csv(file=paste(datapath,"M8_Local_2012-2015_Final.csv",
sep="/"), header=TRUE, sep=",")
cover8<-Localts8$Percentcover
thickness8<-Localts8$thickness_cm
dates8<-as.Date(Localts8$Date2,format="%d-%b-%Y")

LocalIceTS8<-cbind(cover8,dates8)
LocalIceTS8<-as.data.frame(LocalIceTS8)


#Regional Ice Area
DailyRegional=read.csv(file=paste(datapath,"Sea_Ice_Index_Regional_Daily_Data
_JJ_plot_Area2019.csv", sep="/"), header=TRUE, sep=",")
Area<data.frame(Area=c(DailyRegional[,"X2006"],DailyRegional[,"X2007"],DailyR
egional[,"X2008"], DailyRegional[,"X2009"], DailyRegional[,"X2010"],
DailyRegional[,"X2011"], DailyRegional[,"X2012"], DailyRegional[,"X2013"],
DailyRegional[,"X2014"], DailyRegional[,"X2015"], DailyRegional[,"X2016"],
DailyRegional[,"X2017"], DailyRegional[,"X2018"],DailyRegional[,"X2019"]))
```

```
Area<-na.omit(Area)

#Format Date
date=seq(as.Date("2006-01-01"), as.Date("2019-11-14"),by="days")
date<-as.Date(date,format="%d-%b-%Y")

IceTS<-cbind(Area,date)

#Plot Backscatter, BT, and Regional and Local SSI for site M8
par(col.axis="green")
plot(dateBS,BS$Total6/(10^-5),type='l',xaxt='n',xlab='',ylim=c(0,30),
ylab='Area Backscattering Coefficient/10^-5 (m^2m^-2)',col='green')
par(new=TRUE)
par(col.axis="black")
plot(dateBT[2229:3723],Temp[2229:3723],type='l',xaxt='n',xlab='',ylim=c(-
2,6), ylab=NA, axes=F,col='black')
axis(side = 4)
mtext(side = 4, line = -1, 'Bottom Temperature (deg C)')
par(new=TRUE)
par(col.axis="blue")
plot(IceTS$date[2060:3554],(IceTS$Area[2060:3554])/1000, axes=F, xlab=NA,
ylab=NA, type='l',xaxt="n",col='blue')
par(new=TRUE)
par(col.axis="orange")
plot(LocalIceTS8$dates8,LocalIceTS8$cover8, type='l',
axes=F,xlab=NA,ylab=NA,col='orange')
datelabels=seq(as.Date("2011-08-22", format="20%y"), tail(date,1), by="1
year")
par(col.axis="black")
axis.Date(side=1, date, at=datelabels, format="20%y")
legend("topright",, legend=c('200 kHz Backscatter','M8 BT',"Bering Regional
Sea Ice", "Local M8 site Ice (4 km^2)"),col=c('green','black',"blue",
'orange'), cex=0.8,lwd=2)

#Overlaid plot BT, Backscatter, and Regional and Local SSI for M5 07/18/2012-
06/17/2013

#Backscatter M5
BS=read.csv(file=paste(datapath,"19FA_09SP_Backscatter_WC.csv", sep="/"),
header=TRUE, sep=",")
dateBS=as.character(BS$Var8)
dateBS=seq(as.Date("2008-09-26"), as.Date("2018-11-07"),by="days")
dateBS<-as.Date(dateBS,format="%d-%b-%y")

#BT
BT=read.csv(file=paste(datapath,"M5_2005-2019_NaNs.csv", sep="/"),
header=TRUE, sep=",")
Temp=BT$Temperature
dateBT=BT$Date
dateBT<-as.Date(dateBT,format="%m/%d/%Y")

#Local Ice M5
Localts=read.csv(file=paste(datapath,"2007_2015_NaN_Local.csv", sep="/"),
header=TRUE, sep=",")
cover<-Localts$Percentcover

#Format Dates
```

```
dates <- with(Localts$Julian.Day,
strptime(paste(Localts$Year,Localts$JulianDay), "%Y %j "))
dates<-as.Date(dates,format="%d-%b-%Y")

LocalIceTS<-cbind(cover,dates)
LocalIceTS<-as.data.frame(LocalIceTS)
LocalIceTS$dates<-as.Date(dates,format="%d-%b-%Y")
dateslocal<-dates

#Regional Ice Area
DailyRegional=read.csv(file=paste(datapath,"Sea_Ice_Index_Regional_Daily_Data
_JJ_plot_Area2019.csv", sep="/"), header=TRUE, sep=",")
Area<data.frame(Area=c(DailyRegional[,"X2006"],DailyRegional[,"X2007"],DailyR
egional[,"X2008"], DailyRegional[,"X2009"], DailyRegional[,"X2010"],
DailyRegional[,"X2011"], DailyRegional[,"X2012"], DailyRegional[,"X2013"],
DailyRegional[,"X2014"], DailyRegional[,"X2015"], DailyRegional[,"X2016"],
DailyRegional[,"X2017"], DailyRegional[,"X2018"],DailyRegional[,"X2019"]))
Area<-na.omit(Area)

#Format Date
date=seq(as.Date("2006-01-01"), as.Date("2019-11-14"),by="days")
date<-as.Date(date,format="%d-%b-%Y")

IceTS<-cbind(Area,date)

#Plot Backscatter, BT, Regional and Local SSI Site M5
par(col.axis="green")
plot(dateBS[1392:1726],BS$Total6[1392:1726]/(10^-
5),type='l',xaxt='n',xlab='',ylim=c(0,30), ylab='Area Backscattering
Coefficient/10^-5 (m^2m^-2)',col='green')
par(new=TRUE)
par(col.axis="black")
plot(dateBT[2633:2967],Temp[2633:2967],type='l',xaxt='n',xlab='',ylim=c(-
2,6), ylab=NA, axes=F,col='black')
axis(side = 4)
mtext(side = 4, line = -1, 'Bottom Temperature (deg C)')
par(new=TRUE)
par(col.axis="blue")
plot(IceTS$date[2396:2731],(IceTS$Area[2396:2731])/1000, axes=F, xlab=NA,
ylab=NA, type='l',xaxt="n",col='blue')
par(new=TRUE)
par(col.axis="orange")
plot(LocalIceTS$dates[1753:2087],LocalIceTS$cover[1753:2087], type='l',
axes=F,xlab=NA,ylab=NA,col='orange')
datelabels=seq(as.Date("2012-01-01", format="20%y"), tail(date,1), by="2
months")
par(col.axis="black")
axis.Date(side=1, date, at=datelabels, format="%b-20%y")
legend("topleft",, legend=c('200 kHz Backscatter','M5 BT',"Bering Regional
Sea Ice", "Local M5 site Ice (4 km^2)"), col=c('green','black',"blue",
'orange'), cex=0.8,lwd=2)

#Plot M5 Regional Ice, Local Ice, and BT
plot(dateBT[881:4936],Temp[881:4936],type='l',xaxt='n',xlab='',ylim=c(-2,6),
ylab='Bottom Temperature (deg C)')
par(new=TRUE)
```

```
plot(IceTS$date[639:4694],(IceTS$Area[639:4694])/1000, axes=F, xlab=NA,
ylab=NA, type='l',xaxt="n",col='blue')
par(new=TRUE)
par(col.axis='orange')
plot(LocalIceTS$dates,cover, type='l', axes=F,xlab=NA,ylab=NA,col='orange')
axis(side = 4)
mtext(side = 4, line = -1, '% Ice Cover')
par(col.axis="black")
datelabels=seq(as.Date("2005-01-01", format="20%y"), tail(date,1), by="1
year")
axis.Date(side=1, date, at=datelabels, format="20%y")
legend("topleft",, legend=c('M5 BT',"Bering Regional Sea Ice", "Local M5 site
Ice (4 km^2)"),
col=c('black',"blue", 'orange'), cex=0.8,lwd=2)
abline(h=47.5, col="black")

#Plot Regional Ice, Local Ice, BT, and Backscatter for Site M5 Cold Years
par(col.axis="green")
plot(dateBS,BS$Total6/(10^-5),type='l',xaxt='n',xlab='',ylim=c(0,30),
ylab='Area Backscattering Coefficient/10^-5 (m^2m^-2)',col='green')
par(new=TRUE)
par(col.axis="black")
plot(dateBT[1242:3073],Temp[1242:3073],type='l',xaxt='n',xlab='',ylim=c(-
2,6), ylab=NA, axes=F,col='black')
axis(side = 4)
mtext(side = 4, line = -1, 'Bottom Temperature (deg C)')
par(new=TRUE)
plot(IceTS$date[1002:2831],(IceTS$Area[1002:2831])/1000, axes=F, xlab=NA,
ylab=NA, type='l',xaxt="n",col='blue')
par(new=TRUE)
plot(LocalIceTS$dates[362:2193],LocalIceTS$cover[362:2193], type='l',
axes=F,xlab=NA,ylab=NA,col='orange')
datelabels=seq(as.Date("2008-01-01", format="20%y"), tail(date,1), by="1
year")
axis.Date(side=1, date, at=datelabels, format="20%y")
legend("topleft",inset=c(0,0),legend=c('200 kHz Backscatter','M5 BT',"Bering
Regional Sea Ice", "Local M5 site Ice (4 km^2)"),
pch=c(1,3),col=c('green','black',"blue", 'orange'), cex=0.6,lwd=2)

#Plot Regional Ice, Local Ice, BT, and Backscatter for Site M5 Warm years
par(col.axis="green")
plot(dateBS,BS$Total6/(10^-5),type='l',xaxt='n',xlab='',ylim=c(0,30),
ylab='Area Backscattering Coefficient/10^-5 (m^2m^-2)',col='green')
par(new=TRUE)
par(col.axis="black")
plot(dateBT[3074:4936],Temp[3074:4936],type='l',xaxt='n',xlab='',ylim=c(-
2,6), ylab=NA, axes=F,col='black')
axis(side = 4)
mtext(side = 4, line = -1, 'Bottom Temperature (deg C)')
par(new=TRUE)
plot(IceTS$date[2832:4694],(IceTS$Area[2832:4694])/1000, axes=F, xlab=NA,
ylab=NA, type='l',xaxt="n",col='blue')
par(new=TRUE)
plot(LocalIceTS$dates[2194:4056],LocalIceTS$cover[2194:4056], type='l',
axes=F,xlab=NA,ylab=NA,col='orange')
datelabels=seq(as.Date("2008-01-01", format="20%y"), tail(date,1), by="1
year")
```

```
axis.Date(side=1, date, at=datelabels, format="20%y")
legend("topright",inset=c(0,0), legend=c('200 kHz Backscatter','M5
BT',"Bering Regional Sea Ice", "Local M5 site Ice (4
km^2)"),pch=c(1,3),col=c('green','black',"blue", 'orange'), cex=0.6,lwd=2)
```

Acoustic and Environmental Signal Filtering (Matlab)

```
% High and Low Frequency variability Plots
%import files
fname5 = 'M5_2005-2019_NaNs_T.xlsx'; %Bottom Temperature
M5in = xlsread(fname5);
M5in = readtable(fname5);
t5=table2array(M5in(1:5012,1)); %Dates
m5=table2array(M5in(1:5012,2)); %BT values

%Find missing data and interpolate
vector=(1:length(m5));
m5interp = interp1( vector(~isnan(m5)), m5(~isnan(m5)) , vector, 'linear')';

%Set sampling interval
 delt = 86400; %Seconds in a day for a sampling interval once per day
fs=1;

%Fourier transform to frequency domain
% function inputs time series and gives one and 2 sided
% spectrums (fourier transforms) P1 and P2 a time vector, and a frequency
vector

[P1, P2, f] = my_fft_6(m5interp,fs);
p1temp=P1;
ftemp=f;
figure
plot(f,P1)
figure
loglog(f,P1)

%Filter out high frequencies for bottom temperature
% function inputs time series and low or high cut off frequency, outputs
%filtered time series
[tsfilt] = my_filter(m5interp, fs, 0.01, 0.5);
tsfilt1=tsfilt;

 %Delta-Sv import
dbdiff=readtable('19FA_09FAdbdiff.csv');
dbdiff{:,1}(dbdiff{:,1} >= 30) = NaN; %erroneous data
n = 48; % average every n values for daily sample interval
dbdiffavg = arrayfun(@(i) mean(dbdiff{:,1}(i:i+n-1)),1:n:length(dbdiff{:,1})-
n+1)'; % the averaged vector

%find missing data and interpolate
vector1=(1:length(dbdiffavg));
dbdiffavg = interp1( vector1(~isnan(dbdiffavg)), dbdiffavg(~isnan(dbdiffavg))
, vector1, 'linear')';

%Compensate for missing data values for time vector
time = arrayfun(@(i) mean(dbdiff{:,3}(i:i+n-1)),1:n:length(dbdiff{:,3})-
n+1)'; % the averaged vector
```

```
%Fourier transform to see where to cut off frequencies
 [P1, P2, f] = my_fft_6(dbdiffavg,fs);
p1db=P1;
fdb=f;
figure
plot(fdb,p1db)
figure
loglog(fdb,p1db)

%Plot log transformed frequencies
figure
loglog(ftemp,p1temp)
hold on
loglog(fdb,p1db)

%Filter Delta-Sv frequencies
 [tsfilt] = my_filter(dbdiffavg, fs, 0.005, 0.5);% high band pass (make all
low freqs=0)
tsfilt2=tsfilt;

[tsfilt] = my_filter(dbdiffavg, fs, 0, 0.05);% low band pass (make all high
freqs=0)
tsfilt2=tsfilt;

#Plot filtered Delta-Sv or Bottom Temperature data
figure
plot(time,tsfilt2)
line([dbdiff{85248,3} dbdiff{85248,3}], [-10 15], 'Color', [1 0 0]); %M5
ylabel('Low frequency Amplitude')
```

Environmental Modelling (R)

```
#Site M5 Cold year ABC Modelling
library(mgcv) #GAM package
library(stringr)  # character string manipulations

# Reading the Data
#.csv with all model variables (ABC, Date, BT, Regional SSI, Local SSI, Cold
Pool Presence, Freezing #Temperature Presence
MMcold=read.csv(file="Model_Master_Cold1.csv", header=TRUE) #without 2013
Regime shift year

# creating continuous time (fractional year)
(yr.rows <- as.vector(table(MMcold$Year)) )
(leaps <- as.vector(tapply(MMcold$DOY,MMcold$Year,max) )  )  # last yr should
be 365
leaps[length(leaps)] <- 365

# create variable maxdoy and repeat it over entire data frame
maxdoy <- NULL
for (i in 1:length(leaps)) maxdoy <- c(maxdoy,rep(leaps[i],yr.rows[i]))

# create continuous time in units of years (note leap year days are slightly
shrunk)
# This is mainly for plotting and numerical calculations
MMcold$fracyear <- MMcold$DOY/maxdoy
```

```
MMcold$ctime <- MMcold$Year + MMcold$fracyear


mm <- min(MMcold$Regional_SSI[MMcold$Regional_SSI > 0])
hist(log(MMcold$Regional_SSI+(mm-1)),nclass = 50)

MMcold$logReg_SSI <- log(MMcold$Regional_SSI+(mm-1))

#Full Model
mod1 <- formula(log(ABC*10^06) ~ s(fracyear,bs="cc") + s(Bottom_Temp) +
s(Regional_SSI)
                + s(Bottom_Temp,by = Pres_Cold_Pool) + s(Regional_SSI, by =
Freezing_Temp)
                + ti(fracyear,Bottom_Temp) + ti(fracyear,logReg_SSI) +
ti(Bottom_Temp, Regional_SSI))

MMgam1 <- gam(mod1,data = MMcold)
summary(MMgam1)
par(mfrow = c(2,2))
gam.check(MMgam1)
coef(MMgam1)

#Plot Cold Regime Residuals
par(mfrow=c(3,1),mar=c(3,4,1,1))
for (i in 1:3) plot(MMgam1, residuals= T, select = i,scale=0)

#Site M5 Warm Year ABC Modelling
rm(list=ls(all=TRUE))
library(mgcv)
library(stringr)  #character string manipulations

MMwarm=read.csv(file="Model_Master_Warm.csv",  header=TRUE)

# creating continuous time (fractional year)
 (yr.rows <- as.vector(table(MMwarm$Year)) )
(leaps <- as.vector(tapply(MMwarm$DOY,MMwarm$Year,max) )  )  # last year
should be 365
leaps[length(leaps)] <- 365

# create variable maxdoy and repeat it over entire data frame
maxdoy <- NULL
for (i in 1:length(leaps)) maxdoy <- c(maxdoy,rep(leaps[i],yr.rows[i]))

# create continuous time in units of years (note leap year days are slightly
shrunk)
# This is mainly for plotting and numerical calculations
MMwarm$fracyear <- MMwarm$DOY/maxdoy
MMwarm$ctime <- MMwarm$Year + MMwarm$fracyear

#Full Model
mod1 <- formula(log(ABC*10^06) ~ s(fracyear,bs="cc") + s(Bottom_Temp) +
s(Regional_SSI)
                + s(Bottom_Temp,by = Pres_Cold_Pool) + s(Regional_SSI, by =
Freezing_Temp)
                + ti(fracyear,Bottom_Temp) + ti(fracyear,Regional_SSI) +
ti(Bottom_Temp, Regional_SSI))
```

```
MMgam1 <- gam(mod1,data = MMwarm)
summary(MMgam1)
par(mfrow = c(2,2))
gam.check(MMgam1)

#Plot Warm Regime Residuals
par(mfrow=c(3,1),mar=c(3,4,1,1))
for (i in 1:3) plot(MMgam1, residuals= T, select = i,scale=0)
```